Effects of a food contaminant on cell cycle

Glycidamide induced S-phase arrest followed by apoptosis in a lymphoblastoid cell line.

by Elin Bakken Ansok

Master thesis in Toxicology

Department of Toxicology

Institute of Biology

University of Oslo

June 2009

1. Acknowledgments

Denne masteroppgaven ble utført ved avdeling for kjemikalietoksikologi (MIKT), divisjon for miljømedisin ved Nasjonalt follkehelseinstitutt (FHI). Hovedveileder har vært Kristine Bjerve Gutzkow, biveileder Gunnar Brunborg, og Steinar Øvrebø som internveileder ved Universitet i Oslo.

For å gjøre det kort: takk til alle gærninger ved MIKT for en artig tid og meget sosial avdeling! For det første veileder Kristine B. Gutzkow! Christine, Silja og Håvard, mine kjære medstudenter som har bidratt til en livlig lab til alle døgnets tider! Siri, nå skal jeg slutte å mase om statistikk og akrylamid! Elisabeth, uten deg hadde jeg vel blitt litt smågal! Silje, våre mange diskusjoner! Ikke minst korrekturlesere!

Nå skal jeg gjøre andre ting! :-)

Contents

2. Abbrevations

8-oxo-G	7,8-dihydro-8-oxoguanine
β-ME	β-Mercaptoethanol
AA	Acrylamide
Ab	Anti-body
AP site	(Abasic) apurinic/apyrimidinic site
ALS	Alkali Labile Sites
Ape1/APEX1	Mammalian AP Endonuclease 1
ATM	Ataxia Teleangesica Mutated
BER	Base Excision Repair
bp	base pair
BPB	Bromo Phenol Blue
BrdU	Bromodeoxyuridine (5-bromo-2-deoxyuridine)
BSA	Bovine Serum Albumin
DNA	Deoxyribonucleic acid
DSB	DNA Double Strand Break
Fapy	2,6-diamino-4-hydroxy-5N-formamidopyrimidine
Fpg	Formamidopyrimidine-DNA-glycolase
FITC	fluorescein isothiocyanate

GA	Glycidamide
GAPDH	Glyceraldehyde-3-Phosphate Dehydrogenase
GGR	Global Genome Repair
GO	Gene Ontology
GSH	Glutathione
GST	Gluthathione S-transferase
HRP	Horseradish Peroxidase
IARC	International Agency for Research on Cancer
ROS	Reactive oxygen species
RNA	Ribonucleid acid
MMR	Mismatch Repair
N1-GA-Ade	N1-(2-carboxy-2-hydroxyethyl)-2'-deoxyadenosine
N3-GA-Ade	N3-(2-carbamoyl-2-hydroxyethyl)-adenine
N7-GA-Gua	N-7-(2-carbamoyl-2-hydroxyethyl)guanine
NER	Nucleotide Excision Repair
PCNA	Proliferating Cell Nuclear Antigen
PI	Propidium Iodide
PKC	Protein Kinase C
Pol β	Polymerase β
SDS	Sodium Dodecyl Sulphate

SPR	Short-Patch Repair
SSBs	DNA Single Strand Breaks
WHO	World Health Organisation
3MeA	3-methyladenine
7MeG	7-methylguanine
AP1	AP endonuclease 1
MMR	Mismatch repair
NHEJ	nonhomologous end joining
HR	homologous recombination
dRP	deoxyribose phosphate
GG-NER	global genomic NER
TCNER	transcription coupled NER
XPA	Xeroderma pigmentosum group A
XPC	Xeroderma pigmentosum group C
TCNER	transcription coupled NER
XPA	Xeroderma pigmentosum group A
XPC	Xeroderma pigmentosum group C

3. Aims of the study

Cooking and food processing at high temperatures generate various kinds of toxic substances. Acrylamide has been traced in many different types of processed food and beverages and there is a risk for human exposure. Acrylamide is metabolized to the genotoxic mutagen glycidamide. To contribute to a better estimation of the health risk associated with acrylamide intake, its biological effects must be understood at a cellular and molecular level. We therefore wanted to explore the genotoxic effect and the molecular impact of exposing human peripheral lymphocytes (PBL) and the lymphoblastoid cell line GM00130 to glycidamide *in vitro*. PBL and the cell line were both used for the genotoxic studies, while only the cell line was exploited in all other mechanistic experiments.

Specific goals:

1. **Determine the genotoxic effect of GA on human lymphoid cells.** We wanted to use the comet assay to determine the genotoxic effect of the metabolite glycidamide, and to study the type of DNA lesions caused by glycidamide. By introducing a specific repair enzyme to the comet assay, more specific types of lesions induced by glycidamide could be detected. In addition we wanted to explore the repair capability in lymphoid cells.

2. **Analyse GA-induced changes in the cell cycle.** By using flow cytometry and DNA-staining, together with BrdU-incorporation, we were able to determine changes in the cell cycle distribution, in GM00130, after GA-exposure.

3. **Analyse the molecular mechanism of DNA damage responses of glycidamide.** With the use of western blotting we wanted to study GA-induced altered expression of selected proteins involved in cell cycle regulation, DNA repair or markers for genotoxic stress and apoptosis in GM00130.

4. **Analyse effects on cell viability.** By using a cell viability assay such as PI/Hoechst, we wanted to detect cytotoxic effects of GA in GM00130, discriminating between the levels of apoptotic or necrotic cells induced by GA.

4. Summary

Exposure to environmental toxicants is a contributing factor to health disorders such as cancer, asthma and allergy. A toxicant which has been studied more in depth the last years is the well known neurotoxicant acrylamide (AA) and its metabolite, glycidamide (GA). The reason for this is that AA have been traced in many different types of processed food and beverages. Although the genotoxic effect of AA has been widely studied, the molecular function remains mostly unclear. We therefore wanted to explore the molecular impact of the genotoxic effect of glycidamide, and to look more carefully into the mechanisms involved. In large biomonitoring studies, lymphocytes are an invaluable and often the only source of medium for such genotoxic analysis, and, therefore human lymphocytes and a lymphoblastoid cell line were used for the in vitro exposure studies.

In correspondence with results from ongoing studies in our laboratory, we found that very low exposure of the GA, but not AA alone, induced high levels of DNA damage recognised by the repair enzyme, Formamidopyrimidine glycosylase (Fpg). Further, when relatively high concentrations of GA (1 mM and 0.5 mM) was used, together with long exposure duration, a marked increase in DNA damage without the Fpg-enzyme was apparent. Thus, since GA is found to be highly genotoxic we wanted to study GAs effect on lymphoid cell cycle and survival when relatively low GA(0.1 mM) concentrations were used. No cell cycle arrest of the lymphoblastoid cell line, GM00130, was seen with low GA concentrations. Instead, by increasing the GA dose, starting from 0.5 mM, an accumulation of cells in early S-phase became apparent after 24 hours exposure time. Preliminary results also indicated a reduction in the incorporation of bromodeoxyuridine (5-bromo-2-deoxyuridine, BrdU) following GA-exposure, indicating a halt in DNA-replication and an S-phase arrest. At the same GA-concentration used, the tumor suppressor protein p53 was highly phosphorylated at ser15, followed by a total p53 increase. An increase in the CDK inhibitor $p21^{CIP1}$ was also notable at 0.5 mM GA concentration, while no significant changes were observed in the case of $p27^{Kip1}$. Further, the expression of cyclin A that drives S-phase did not decrease as expected. When increasing the concentration of GA to 1 mM and also the time of exposure, an increased level of cells arresting in S-phase was observed together with an elevation of cell undergoing

apoptosis. Additionally, since the transcription of the NER-enzymes, XPA and XPC, was previously found to be regulated by GA in other cell systems, we analysed the expression of these proteins after GA-exposure. However, in a preliminary experiment, no notable GA-induced increase in the protein level of these enzymes was noted.

Thus, unexpectedly, we found that the high number of Fpg-sensitive sites induced by low levels of GA did not lead to any cell cycle arrest or cell death or any changes in protein expression of important cell cycle parameters tested in the lymphoblastoma cell line. This may indicate that lymphoid cells are able to overcome or ignore these lesions at low levels of GA. However, continuous exposure may eventually lead to an accumulation of GA-induced lesions leading to mutations and cancerous development over time. When increasing the concentration and the exposure duration of GA, DNA-replication was markedly slowed down and cells were arrested in S-phase followed by a significant progression of apoptosis. This may be due to the observed GA-induced activation of p53 and the induction $p21^{CIP1}$. All in all it shows that GA is genotoxic and affects the lymphoid cell cycle in a dose and time dependent matter.

5. Introduction

5.1 Acrylamide

Acrylamide (AA) (2-propenamid) is an important industrial monomer, and has been commercially available since the mid-1950s and is manufactured on a large scale world wide. In addition of being a well known neurotoxicant (Deng et al., 1993; He et al., 1989), AA has shown to induce the development of various tumors in several animal studies published in the 1980s (Friedman et al., 1995; Johnson et al., 1986). Therefore, epidemiologic evaluations of cancer risk in workers who were exposed occupationally to AA were also undertaken in the 1980s (Sobel et al., 1986). However, no consistent effect of AA exposure on cancer incidence was identified. Additional subsequent studies concluded the same (Collins et al., 1989; Marsh et al., 1999).

AA is generated, predominantly, from the precursor aspargine (Stadler et al., 2002; Tareke et al., 2000) in a Maillard reaction involving asparagine and reducing sugars during the heating of carbohydrate-rich food with temperatures above 120˚C (Mottram et al., 2002; Stadler et al., 2002) and is therefore found in baked and fried starchy foods, such as French fries and chips (Svensson et al., 2003). Since AA surprisingly was found in measurable significant quantities in many common human foods in addition to its presence in coffee and smoke, it introduced a new dimension to carcinogenic risk assessment of AA. Therefore, based on its effect in animals and that AA is biotransformed in mammalian tissue to a genotoxic metabolite; the International Agency for Research on Cancer (IARC) classifies AA as a 2A, a probable human carcinogen (IARC, 1994).

5.1.1 Toxic effects of Acrylamide

Acrylamide can be conjugated with gluthation (GSH) for excretion (Sumner et al., 1992) or oxidized to the reactive epoxide glycidamide (GA) by cytochrome P450 2E1 (Cyp 2E1) (Ghanayem et al., 2005a; Settels et al., 2008; Sumner et al., 1992). GA can also be conjugated by gluthation or oxidated to glyceramide (Fennell et al., 2005).

Figure 1 Metabolism of acrylamide to its epoxide glycidamide *(Martins et al., 2007)*

Acrylamide is metabolized via two competing pathways. Direct conjugation of AA with reduced glutathione results in a glutathione adducts, and the degradation results in the formation and urinary excretion of a mercapturic acid (Sumner et al., 1992). The second pathway involves oxidation of AA, leading to the formation of its epoxide, GA, mediated by cytochrome P450 2E1 (CYP2E1) (Ghanayem et al., 2005a; Sumner et al., 1992). When conversion of AA to GA is inhibited as in CYP2E1 knockout mice, the genotoxicity of AA is inhibited (Ghanayem et al., 2005b). This supports the conclusion that GA is the genotoxic form of AA and that the enzyme CYP2E1 is the primary enzyme responsible for the epoxidation of AA to GA, which further leads to DNA and hemoglobin adducts (Ghanayem et al., 2000; Ghanayem et al., 2005a).

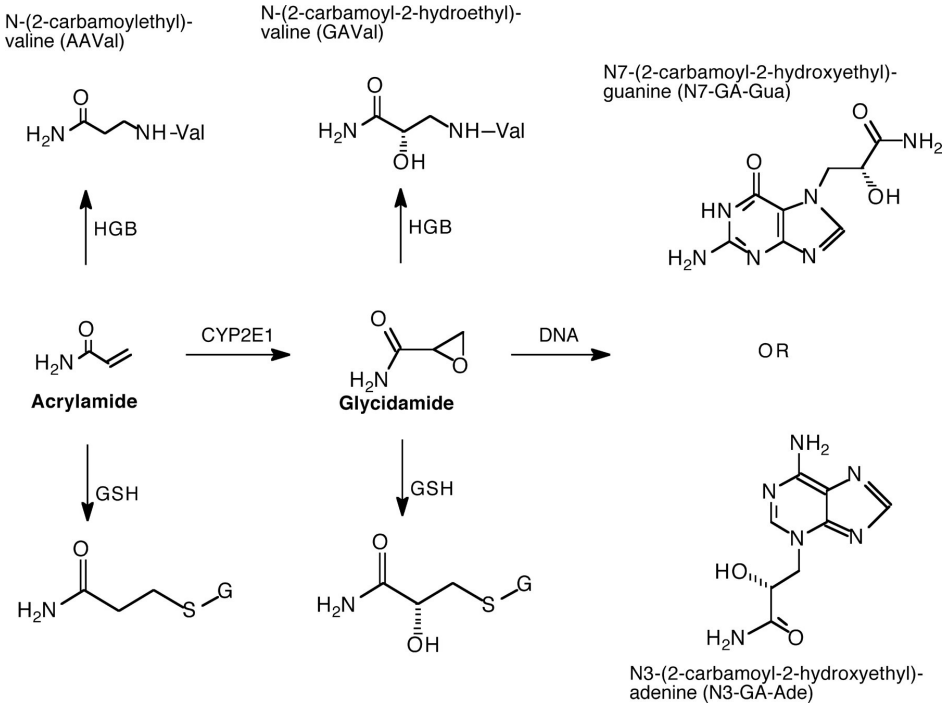

Figure 2 Acrylamide metabolism showing the formation of glycidamide, glutathione conjugates, and hemoglobin and DNA adducts *(Ghanayem et al., 2005a).*

GA forms adducts directly with DNA and protein and it is presumed that the GA induced adducts play a role in cytotoxicity, mutagenicity, reproductive toxicity and carcinogenicity by AA (Gamboa da Costa et al., 2003; Ghanayem et al., 2005a; Segerback et al., 1995). The relative contributions of AA and GA in the mode of action of AA are the subject of current research. Differences between species, exposure route and dose are important factors in risk assessment of the effects of AA exposure (Fennell et al., 2005).

5.1.2 Genotoxicity of Acrylamide and Glycidamide

AA has shown to be weakly genotoxic at high concentrations (>10mM) in micronucleus and *TK* gene mutation assays, causing chromosomal aberration and sister chromatid exchange in vivo and in vitro (Koyama et al., 2006; Martins et al., 2007; Tsuda et al., 1993). Further, since AA has been proven negative in bacterial gene mutation assays (Knaap et al., 1988; Tsuda et al., 1993) it seems that AA is weakly clastogenic without damaging DNA directly, acting through protein binding rather than DNA binding. In addition, AA have been reported to generate reactive oxygen species (ROS) that can attack cellular constituents such as proteins, nucleic acids, and lipids (Yousef and El-Demerdash, 2006).

Reactivity:

Apparently, AA will react very slowly with DNA (Friedman et al., 1995; Solomon et al., 1985), forming adduct only under forced chemical conditions and after extended reaction time (>40 days) (Solomon et al., 1985). Although AA is a weak mutagen, the DNA adducts is a possible mechanism for the production of mutations and/or subsequent carcinogenicity (Gamboa da Costa et al., 2003; Segerback et al., 1995). GA is much more reactive and gives rise to a number of DNA adducts including the two alkylating adducts N7-GA-Gua (N-7-(2-carbamoyl-2-hydroxyethyl)guanine), and to a lesser extent N3-GA-Ade (N3-(2-carbamoyl-2-hydroxyethyl)-adenine) (depurinating) *in vivo and in vitro*, and N1-GA-Ade (N1-(2-carboxy-2-hydroxyethyl)-2'-deoxyadenosine) (stable) *in vitro* (Figure 3) (Gamboa da Costa et al., 2003; Segerback et al., 1995).

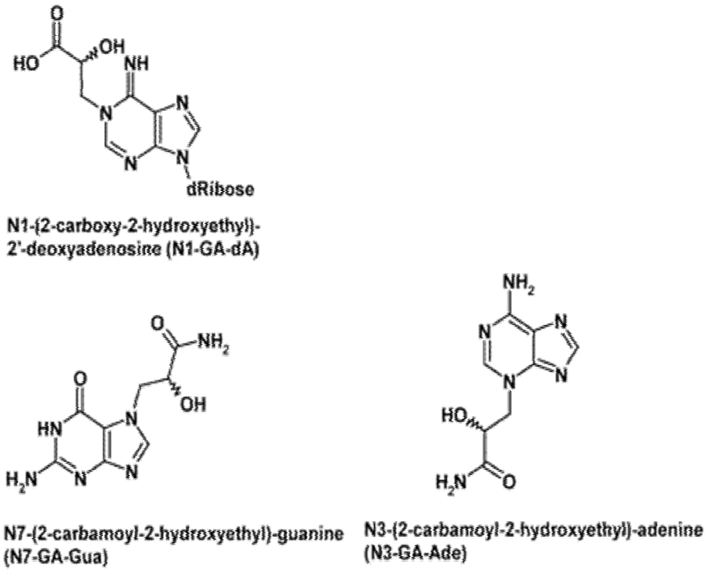

Figure 3. Structures of GA derived adducts. *Modified from (Gamboa da Costa et al., 2003)*

The in vitro reaction of GA with DNA forms adduct in the following order: N7-GA-Gua > N1-GA-dA > N3-GA-dA (Gamboa da Costa et al., 2003), a pattern which also have been seen with other epoxides (Koskinen and Plna, 2000). Thus, N7-GA-Gua is the predominant adduct induced by GA and the predominant reaction of many alkylating chemicals (Gamboa da Costa et al., 2003; Maniere et al., 2005; Mei et al., 2008).

5.1.3 Acrylamid on vital proteins of the mitotic spindle

The neurotoxicity of AA is, among other effects, caused by interference with the kinesin-related motor proteins in nerve cells (as reviewed in LoPachin, 2004). Effects on kinesin proteins could also explain some of the indirect genotoxic effects of AA. These proteins form the spindle fibers in the nucleus that function in the separation of chromosomes during cell division.

Studies on the effects of AA on microtubules have shown very little effect. However, microtubule-associated motor proteins are also essential components of the spindle, therefore kinesin motors are logical targets due to their critical involvement in cell division and previous observations of AA-induced neuronal kinesin inhibition (Sickles et al., 1996; Sickles et al., 2007) Kinesins have shown AA-induced neuronal kinesin inhibition (Sickles et al., 2007) and AA and GA specifically inhibit a type of kinesin motor proteins associated with the mitotic/meiotic spindle, in a similar concentration range as the neuronal kinesins (Sickles et al., 1996). So there seems to be a similar dose-response effect on dividing cells and neurotoxicity caused by AA. This inhibition is relevant in relation to mutagenicity, cell cycle effects and potential carcinogenicity of AA/GA. KRP2, a kinesin motor protein responsible for spindle assembly and disassembly of kinetochore microtubuli, have shown to be significantly inhibited by concentrations of GA of 5- to 10-fold less than AA. GA may therefore act on multiple kinesin family members and produce toxicities in organs highly dependent on microtubule-based functions (Sickles et al., 2007). This may also explain some of the clastogen effects of AA and GA.

Overall, Since epidemiological studies presume that 20-50% of all human cancers are due to dietary causes (Strickland and Groopman, 1995) food is likely to have an important impact on cancer development. In addition, since AA is found as a by-product in different popular food products, such as French fries and chips, and the carcinogenicity of AA in mice and rats is well documented, there should be room for concerns.

The mode of action still remains unclear for AA-induced carcinogenicity. However, both AA and GA show clastogenic effects. Additionally, GA and have been positive for mutagenicity and DNA reactivity in a number of *in vitro* and *in vivo* assays. Thus, the potential for altered

cell cycle regulation and genotoxicity is highly likely. Lastly, since neurotoxicity of AA is, related to actions on proteins also important in cell division further research is still needed to investigate the relationship between AA, GA and the effects at the molecular level leading to carcinogenicity. For this reason, we have studied the affect of GA on DNA damage and cell cycle regulation.

5.2 DNA damage

Cellular DNA is susceptible to damage every day from different carcinogenic compounds in the environment or food, UV light, spontaneous hydrolytic events or normal reactive metabolites. DNA damage can be divided into two major classes, endogenous and exogenous, which may be partly overlapping although their cause is different. Endogenous DNA damage includes mainly hydrolytic and oxidative reactions. Exogenous factors include physical and chemical agents, especially electrophilic molecules and substances producing reactive oxygen species.

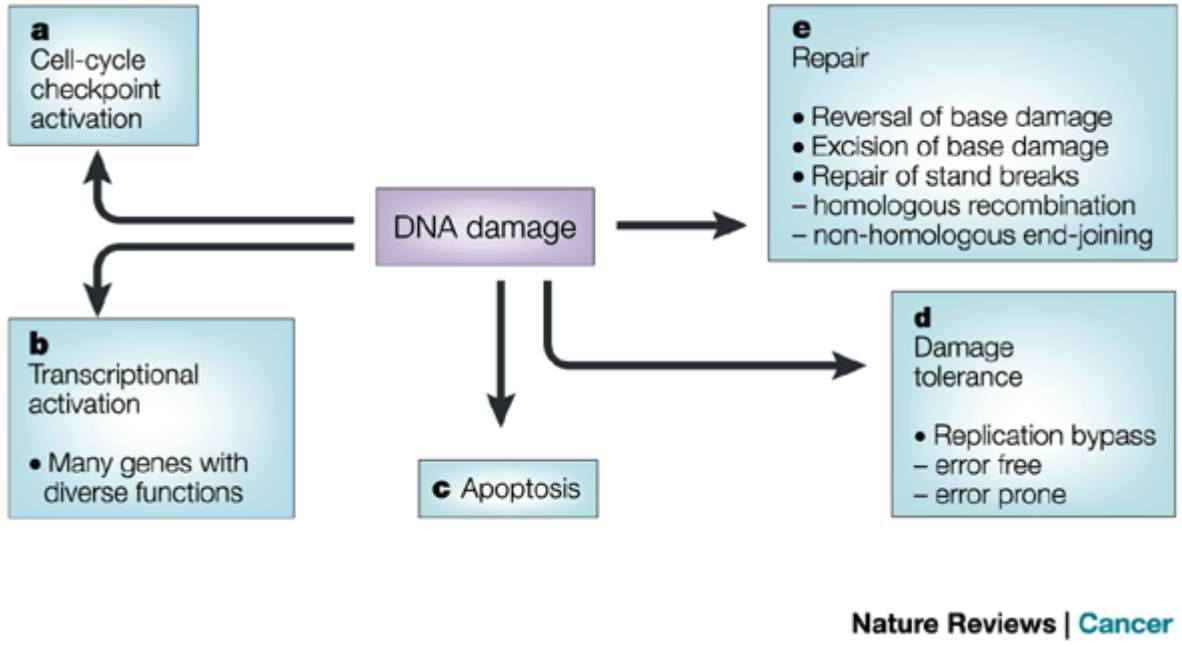

Figure 4. Cellular responses to DNA damage *(Friedberg, 2001).*

5.2.1 DNA adducts

Electrophilic compounds can interact with the ring nitrogens, exocyclic amino groups, carbonyl oxygens, and the phosphodiester backbone. This results in alkylation products that are covalent derivatives of reactive chemical species with DNA. Direct-alkylating agents induce preferential binding to highly nucleophilic centers such as the N7 guanine (Loeb and Preston, 1986).

DNA adducts are mostly connected to the nucleophilic groups of adenine and guanine. The adduct can be stable or unstable (depurinating) depending on the position on the base at which the adduct is formed (Loeb and Preston, 1986). Stable adducts remain covalently bonded to DNA unless removed during repair, while depurinating adducts are spontaneously released from DNA by destabilization of the glycosidic bond (as reviewed in Cavalieri et al., 2000). Depurination of adenine most often leads to A → T mutations, while depurination of guanine leads to G → T mutations (Cavalieri et al., 2000).

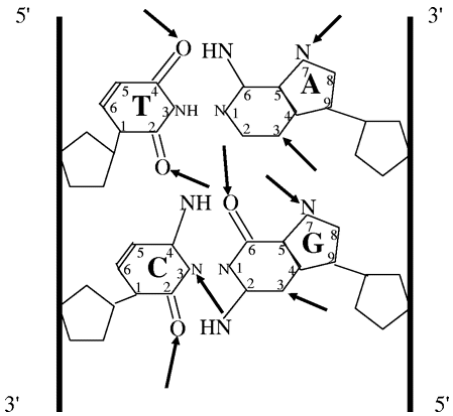

Figure 5 Double-stranded DNA showing the sites of DNA adduct formation including important targets for alkylators (N7G, N3A etc.) *(Jenkins et al., 2005).*

Depurination can occur spontaneously or following the formation of an unstable adduct (Loeb and Preston, 1986). Cleavage of the N-glycosyl bond results in loss of bases from nucleic acids leaving the sugar-phosphate behind as an abasic site (AP site). An AP site is denoted ”apurinic” with the loss of a purine, or ”apyrimidinic” with the loss of pyrimidine; these are the most common DNA lesions generated by both spontaneous and induced base loss (Loeb and Preston, 1986). During replication, a random nucleotide is incorporated opposite to the

AP site, usually adenine, producing mispairing and hence a mutation after DNA replication. The glycosyl bond at an AP site is susceptible to hydrolysis, which results in a single strand break. The biological consequences of unrepaired AP sites are numerous. AP sites can block progression of RNA and DNA polymerase, resulting in impairment of gene transcription and DNA replication. If polymerases manage to bypass these lesions during transcription or replication, the effect may be deleterious for genome stability since there is a high probability that a wrong base will be inserted opposite an AP site leading to gene mutations (Frosina et al., 1996).

Alkylating agents comprise one of the broadest classes of DNA-damaging agents. Of particular interest are methylated bases, such as 3-methyladenine (3MeA) and 7-methylguanine (7MeG) (Figure 6), that are formed i.e. by cancer chemotherapeutics, agents in the environment, and also by endogenous cellular processes (Sedgwick, 1997).

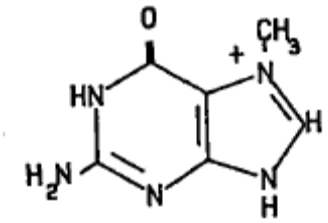

Figure 6 N7-Methyleguanine *(O'Connor et al., 1988)*

Each of these lesions, if not properly repaired, may have detrimental effects. Of these, 7MeG is considered to be the most harmless, since it does not appear to interfere directly with DNA replication in vivo or in vitro. However, 7MeG lesions may spontaneously depurinate to form potentially mutagenic abasic sites or the ring-opening formamidopyrimidines (Fapy) derivative Fapy-7MeG with DNA inhibition potential in vitro (O'Connor et al., 1988; Wyatt and Pittman, 2006).

N1-MeA and N3-MeA could serve as a block to DNA synthesis since N3-MeA can slow S-phase progression in the absence of its repair (Engelward et al., 1998; Smith and Engelward, 2000) and has been shown to be a lethal lesion in vitro (Boiteux et al., 1984), while the N1 lesion disrupts basepairing (Singer, 1975). N7-alkylated guanines can depurinate or be attacked by a hydroxyl group at the C-8 position leading to an opening of the imidazol ring

giving an alkyl-FaPy-G lesion (Figure 7). Unsubstituted FapyA and FapyG caused by DNA oxidation cause moderate inhibition of DNA synthesis, which is DNA polymerase and sequence dependent. Fapy-7MeG, the methylated version of FapyG, efficiently inhibits DNA replication in vitro, but is not mutagenic. FapyA and Fapy-7MeA on the other hand, possess miscoding potential. Though, Fapy lesions are actively eliminated by repair glycosylases specific for oxidized purines and pyrimidines (Tudek, 2003).

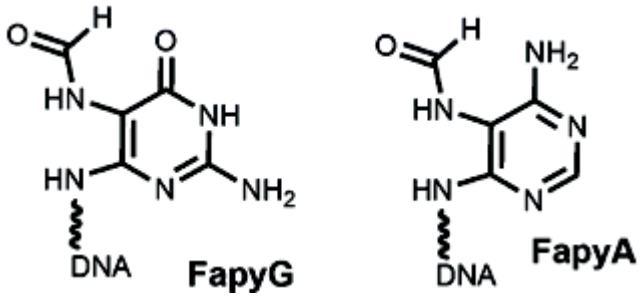

Figure 7 FapyA and FapyG *(Krishnamurthy et al., 2008)*

5.2.2 Single- and double-strand breaks

Radiation, oxidative damage and depurination can lead to single- and double-strand breaks. Of the different types of DNA damage that occur in cells, single-strand breaks (SSBs) are the most common, arising at a frequency of tens of thousands per cell per day from direct attack, by intracellular metabolites and from spontaneous DNA decay. SSBs occur in three orders of magnitude more frequently than double-strand breaks (DSBs). SSBs can occur directly by disintegration of the oxidized sugar or indirectly during DNA base-excision repair (BER) of oxidized bases, abasic sites, or bases that are damaged.(as reviewed in Hegde et al., 2008). During BER, incision occurs at an AP site by the AP endonuclease 1 (AP1) or by the lyase activity of a bifunctional DNA glycosylase occurs (Hegde et al., 2008). Chromosomal SSBs can, if not repaired rapidly, block DNA replication forks during the S-phase of the cell cycle, possibly leading to the formation of DSB (Kuzminov, 2001). Even though this type of DSB is rapidly repaired by homologous recombination (HR), an acute increase in cellular SSB levels might saturate this pathway, leading to genetic instability and/or cell death (Kuzminov, 2001).

5.3 DNA repair

Since the genome suffer from various kinds of damage every day a multitude of different mechanisms have evolved by which either damaged DNA is removed, or the potential dangerous or lethal effects are mitigated. There are two fundamental DNA repair mechanisms that involve either reversal of DNA damage or the excision of damaged elements (excision repair). In excision repair the damaged bases can be excised as free bases in base excision repair (BER), or as nucleotides in nucleotide excision repair (NER). Mismatch repair (MMR) is another version of excision repair and involves the removal of mismatched bases in DNA. Cells also acquire fracture in the sugar-phosphate backbone that results in either single- or double-strand breaks. While strand breaks do not directly alter coding information in the genome, fracture of the covalent integrity of the genome can interfere with normal DNA transactions and lead to altered coding information.

DNA damage resulting in modified bases and sugars, DNA-protein adducts, base-free sites and tandem lesions, can if unrepaired, impede DNA replication in dividing cells and provoke DSB formation. The repair of DBSs is primarily divided into two types of pathway: nonhomologous end joining (NHEJ) and homologous recombination (HR).Three different mechanisms can be distinguished within excision repair: BER, NER and MMR. Mismatch repair eliminated falsely paired bases or small DNA loops that occur during DNA slippage at microsatellites during replication (Cann and Hicks, 2007; Frosina et al., 1996; Hegde et al., 2008).

5.3.1 Base excision repair (BER)

Base excision repair (BER) is the predominant pathway for copying with a broad range of small lesions resulting from oxidative, methylating, alkylating, deaminating and depurination/depyrimidation damage. Typically, only a small region (1 to 13 nucleotides), around the damaged base is removed and replaced during BER. It requires four to five enzymes to carry out repair of DNA containing AP sites or base damage. These include a specific DNA glycosylase that recognizes specific damaged bases and cleave the N-glycosidic bond, and creating an AP site. An AP endonuclease cleaves the phosphodiester bond and generates 3'OH and 5'deoxyribose phosphate (dRP) terminus. Then a DNA polymerase (Pol

b) adds a new nucleotide and the nick is sealed by a DNA ligase. In addition to catalyzing the cleavage of N-glycosidic bonds, some glycosylases have an additional AP lyase activity. The gap filling and rejoining can continue by either of two sub-pathways: short-patch or long-patch BER, whereby only one or 2-13 nucleotides are replaced, respectively. The decision to proceed via the long-patch or short patch BER is not completely clear (Matsumoto et al., 1994; Petermann et al., 2003). "Short-patch" repair represents approximately 80-90% of BER activity. Long-patch requires many of the same factors as are involved in short-patch repair, but unlike short-patch repair, long-patch is a PCNA dependent pathway (Frosina et al., 1996).

5.3.2 Nucleotide excision repair (NER)

NER is one of the most flexible DNA repair pathways, considering the diversity of DNA lesion it may act upon. The most significant of the lesions are pyrimidine dimers caused by UV. Other NER substrates include bulky chemical adducts, DNA intrastrand crosslinks, and some form of oxidative damage. The common features of these lesions that are recognized by NER are that they cause both helical distortion of the DNA duplex and a modification of the DNA chemistry.

The NER process requires the action of more than 30 proteins in successive steps of damage recognition, local opening of the DNA double helix around the injury, and incision of the damaged strand on either side of the lesion. After excision of the damage-containing oligonucleotide the resulting gap is filled by DNA repair synthesis, followed by strand ligation (as reviewed in Fousteri and Mullenders, 2008).

There are two distinct forms of NER; global genomic NER (GG-NER) and transcription coupled NER (TCNER). In both cases, the Xeroderma pigmentosum group C (XPC) protein acts as the damage sensor and recruiter, and initiates the NER process (Leibeling et al., 2006). Xeroderma pigmentosum group A (XPA) binds to the DNA and verifies the damage and recruit further NER proteins. GG-NER corrects damage in trancriptionally silent areas throughout the genome, and its repair efficiency varies across the genome most likely influenced by the chromatin environment. TC-NER repairs lesions on the actively transcribed strand of the DNA (as reviewed in Fousteri and Mullenders, 2008). The pathways are identical except in mechanism of damage detection. (as reviewed in Fousteri and Mullenders,

2008). The ability of certain proteins in the NER pathway to identify bulky DNA lesions that have undergone helical distortions enables NER proteins to discriminate between damaged and undamaged DNA. Three factors involved in the recognition step; XPC-RAD23B, XPA and RPA, all show a binding preference to damaged duplex DNA compared to undamaged (as reviewed in Shuck et al., 2008).

5.4 DNA damage and cell cycle response

Cell-cycle progression is a highly organized and tightly regulated process that controls cell growth and cell proliferation and is tightly coupled with the regulation of DNA damage repair. Changes in cell cycle regulators may lead to aberrant cell proliferation and development of cancer. In order to better understand the mechanisms involved in response to DNA damage it is essential to have a good knowledge of normal cell cycle regulation.

5.4.1 Regulation of the cell cycle machinery

The cell cycle is divided into four non-overlapping phases; G_1, S, G_2 and M. G_1 and G_2 are gap phases that allow the cells to grow and prepare for transition to the next phase. In addition, the cells may enter non-proliferative resting phase after mitosis (quiescent or terminally differentiated cells) referred to as G_0-phase. During G_1 the biosynthetic activities of the cell increases and the diploid cell has 2n chromosomes. Integration of proliferative and anti-proliferative signals may lead to progression, pause or exit of the cell cycle. The S-phase consists of DNA synthesis with doubling of the DNA content to 4n. Subsequently, cells enter the G. phase where it prepares for mitosis in the M phase. Mitosis involves segregation of the replicated genomes into separate nuclei and the division of the cell into two daughter cells (Guttinger et al., 2009). Several control mechanisms exist to avoid inappropriate cell proliferation.

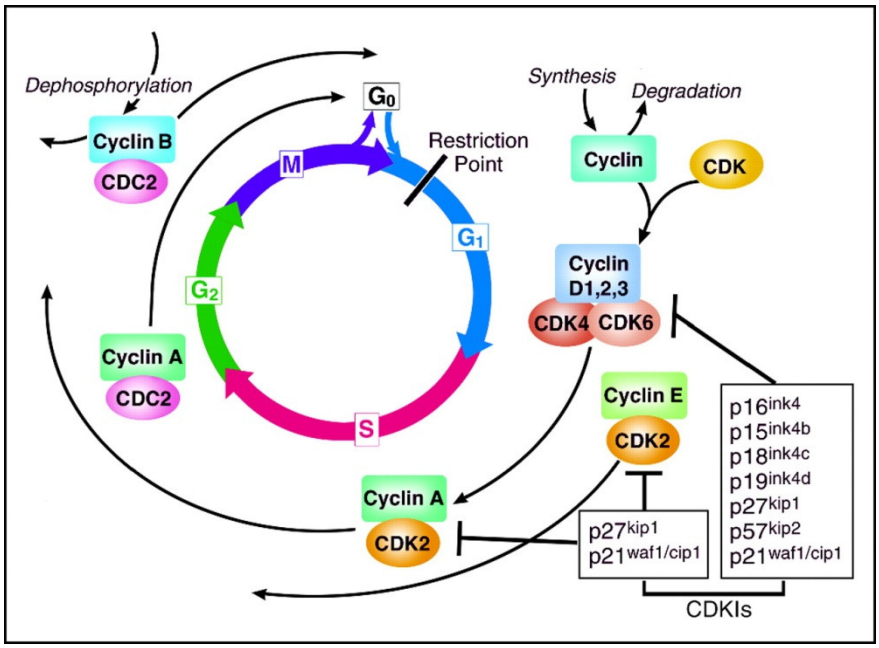

Figure 8. The cell cycle with its four phases (G1, S, G2, and M).
Progression through the cell cycle is promoted by CDKs, which are regulated positively by cyclins and negatively by CDKIs. (Schwartz and Shah, 2005)

Progression through the different phases of the cell cycle is a highly regulated process mediated by cyclin-dependent kinases (CDKs), a group of serine-threonine kinases. Activation of CDKs is determined by their post-translational modification consisting of phosphorylation/dephosphorylation events, and by the association of their respective cyclin, the regulatory subunit of the CDK complex. Inhibition of CDK-cyclin complexes is determined by the increased association of the cdk inhibitors (CKI's) which will negatively regulate the cell cycle (Jeffrey et al., 2000) (see Figure 8).

Cyclins

Cyclins are, as the name indicates, cycling proteins. They oscillate through the cell cycle and form a complex with their CDK partners, which have stable protein levels. The first cyclins to be expressed in G_0/G_1 are the D-type cyclins. Cyclin Ds complex with CDK4/6 and the resulting active kinase-complex phosphorylates pRB initially in G_1 and promotes the pRb-dependent exit from the quiescent state of the cell cycle (as reviewed in Maddika et al., 2007). Cyclin E is expressed in late G_1-phase, with a peak in abundance at the G_1/S boundary of the cell cycle (Dulic et al., 1994). E-type cyclins are thought to be required to activate Cdk2 for proper completion of the G_1-phase and its activity is required for the G_1-S transition and the

initiation of DNA replication. Cyclin A is the second partner of CDK2 and its activity is necessary for the passage through S-phase (as reviewed in Maddika et al., 2007).

Cyclin-dependent kinase inhibitors, CKI's

CDKs, which in connection with their positive regulators, cyclins, allow the transition from one cell cycle to the other. They are, in addition, tightly regulated by inhibitory phosphorylation and by inhibitory molecules such as cdk inhibitors (CKI). Based on their sequence homology and specificity of action, CKIs are divided into two distinct families: INK4 and Cip/Kip. The INK4 family of CDKIs ($p16^{INK4A}$, $p15^{INK4B}$, $p18^{INK4C}$, $p19^{INK4D}$) interact specifically with cdk4 and cdk6 kinase subunit (cyclin D-associated kinases), and are specific for early G_1 phase regulation and prevent entry into S phase (Jeffrey et al., 2000). The second family, the Cip/Kip (CDK interacting protein/kinase inhibitory protein) family inlclude $p21^{CIP1}$, $p27^{KIP1}$ and $p57^{KIP2}$ and inhibit a broader spectrum of cyclin-CDK complexes during all phases of the cell cycle (Denicourt and Dowdy, 2004), and are therefore not specific for a particular cell cycle phase.

$p21^{CIP1}$ and $p27^{KIP1}$

Due to a high level of homology, $p21^{CIP1}$ and $p27^{KIP1}$ are believed to inhibit their targets through similar mechanisms (as reviewed in Coqueret, 2003). Following anti-mitogenic signals or DNA damage, $p21^{CIP1}$ and $p27^{KIP1}$ bind to cyclin-CDK complexes to inhibit their catalytic activity and induces cell cycle arrest (Denicourt and Dowdy, 2004; Sanchez-Beato et al., 1997; Vervoorts and Luscher, 2008). $p27^{KIP1}$ protein levels significantly decrease once cyclinE/CDK2 is activated in late G_1 as a result of decreased $p27^{KIP1}$ protein stability. The main role of $p21^{CIP1}$ in cell cycle regulation is to inhibit the activity of CDK4 and especially CDK2, required for G_1/S transition and may therefore lead to G_1 arrest (Zhang et al., 1993). Induction and activation of the tumour suppressor p53 in response to DNA damage may in many cases lead to the induction of $p21^{CIP}$, owing to the strong p53 binding element in the $p21^{CIP1}$ gene promoter (Dulic et al., 1994). Further, may this lead to a G_1 arrest, and in combination with other events, may lead to apoptosis (Deng et al., 1995). In addition, $p21^{CIP1}$ is able to bind and inhibit the proliferating cell nuclear antigen (PCNA) (Zhang et al., 1993), a subunit of the DNA-polymerase. This enables $p21^{CIP1}$ to regulate DNA synthesis and thereby contributing to the p53-dependent checkpoint of cell cycle progression by impeding DNA-

replication. Additionally, $p21^{CIP1}$ can be regulated via p53 independent pathways as well (Somasundaram et al., 1997) (Coller et al., 2000). This may occur for example by post translational modification, such as phosphorylation leading to cytoplasmic localization and thereby inactivation of $p21^{CIP1}$ (Zhou et al., 2001).

5.4.2 Cell cycle checkpoints

In conclusion, each phase of the cell cycle contains checkpoints that provide an opportunity to put the cells on halt in order to repair damaged DNA and complete replication before attempting further cell-cycle progression and entry into mitosis. After passing these checkpoints cells are irreversibly committed to the next phase. DNA damage and/or malfunction of the critical organelles or structures (e.g. faulty mitotic spindle) can activate cell cycle arrest and even apoptotic cascades, leading to cell death which allows selective removal of unwanted or damaged cells (Jeggo and Lobrich, 2006; Lukas et al., 2004; Su, 2006).

5.4.3 G_1/S checkpoint

The activation of the G_1/S checkpoint leads to cell cycle arrest before the onset of DNA synthesis, giving time to repair the lesions in the DNA template. An important protein in this step is p53 which is rapidly activated following DNA damage. In general, cell cycle arrest before or during S phase (G_1-S and intra-S chekpoints, respectively) occurs via inhibition of cyclin-dependent kinase 2 (CDK2) activity, which is needed for S phase, either by binding of a Cdk inhibitor or by reduction of Cdc25 phosphatase activity an activator of Cdk2. ATM, Chk1- and Chk2-mediated phosphorylation, and subsequent degradation of Cdc25A, contribute to both G_1-S and intra S checkpoints (Su, 2006).

5.4.4 S-phase checkpoints

Given the complexity of the DNA replication, there are several errors and lesions that occur spontaneously during the S-phase process of every cell. Protecting the integrity of the genome during this critical phase is more significant than in G_1 or G_2 via checkpoints of these phases, or the mitotic spindle checkpoint (Lukas et al., 2004). The S-phase checkpoints can be divided

into three categories. 1) The replication checkpoint is initiated when the progression of replication forks becomes stalled in response to stress. This checkpoint has two functions; first to inhibit the initiation of DNA replication from hitherto unfired origins through targeting cyclin-CDK complexes, and secondly to protect the integrity of the replication forks and allowing the recovery of cell-cycle progression after DNA repair and/or restoration of the dNTP pool. 2) The intra-S-phase checkpoint is activated by DSBs that are generated in the genomic loci outside the active replicons. This is in contrast to the other checkpoints independent of replication forks. 3) The S-M checkpoint ensures that cells do not attempt to divide before their entire genome becomes fully duplicated. Failure results in mitotic catastrophy of cells that have incompletely replicated DNA. None of these three S-phase checkpoints has p53 as an absolute requirement, which is the key target of sustained G_1 arrest, but may contribute (Lukas et al., 2004).

5.4.5 G_2/M checkpoint

The role of the G_2/M checkpoint is to ensure that the chromosomes are intact and ready for separation before cells enter mitosis. This is important for the genomic stability, since the segregation of partially replicated or damaged chromosomes can result in DNA breakage and lead to chromosomal aberrations and aneuploidy. However, the control mechanisms are not absolute and cells with low levels of damage or incompletely separated/replicated DNA may in fact enter mitosis (Shimada and Nakanishi, 2006). If cells enter S-phase after an aberrant sister chromatide segregation during mitosis, known as mitotic slippage, this may result in endoreduplication of the DNA, thus the DNA is duplicated without mitosis. p53 was found to be activated during spindle checkpoint-mediated mitotic arrest thereby leading to a crucial postmitotic G_1-checkpoint. Thus, p53 activation together with an intact spindle checkpoint is required to prevent endreduplication upon mitotic failure and therefore protects normal cells from polyploidisation (Tsuiki et al., 2001; Vogel et al., 2004).

5.5 Tumor supressor protein, p53

The p53 tumour suppressor protein is a short-lived transcription factor that becomes stabilised in response to a wide range of cellular stresses. Ubiquitination and the targeting of p53 for

degradation by the proteasome is mediated by Mdm2 (mouse double minute clone 2), a negative regulatory partner of p53. Serine 15 phosphorylation of p53 leads to a stabilization of p53 by reducing its interaction with Mdm2. p53 regulates various cellular events, such as the cell cycle, apoptosis and DNA repair in response to DNA damage, and plays an important role in maintenance of genomic stability (Hoeijmakers, 2001). Therefore, p53-mediated DNA repair may play an essential role in the maintenance of genomic stability. Moreover, p53 has been shown to be involved in various types of DNA repair, including NER, BER and repair DSBs (Smith and Seo, 2002; Zurer et al., 2004).

Once activated, p53 transcribes a number of genes. There are three primary responses to a stress input signal by the p53 pathway; cell cycle arrest, apoptosis or cellular senescence. For instance, $p21^{CIP1}$ is a target gene of p53 that mediates G_1 arrest, and is phosphorylated and activated by p53 in response to cellular stress. This further inhibits CDK4/Cyclin D that normally phosphorylates pRB which ultimately leads to inhibition of transcription of S-phase genes required for G_1 transition (Lavin and Gueven, 2006).

5.6 Cell death

Dying cells are engaged in a process that is reversible until an irreversible phase of "point-of-no-return" is trespassed. This is not yet a clearly defines biochemical event, but the Nomenclature committee on Cell Death (NCDD) proposes that a cell should be considered dead when one of the following morphological criteria is met: (1) The cell integrity of the plasmamembrane is lost, as defined by the incorporation of vital dyes (eg., PI) in vitro; (2) complete fragmentation into discrete bodies (apoptotic bodies) of the cell and its nucleus; and/or (3) its corpse (or its fragments) has been engulfed by an adjacent cell *in vivo* (as reviewed in Kroemer et al., 2009). Thus, cell death can be classified according to its morphological appearance (apoptotic, necrotic, autophagic or associated with mitosis), enzymologial criteria (with or without the involvement of nucleases or proteases), functional aspects (programmed or accidental, physiological or pathological) or immunological characteristics (immunogenic and non-immunogenic) (Gorczyca, 1999).

5.7 Apoptosis

Apoptosis is generally referred to as “programmed cell death” and is one of the main types of programmed cell death which involves a series of biochemical events leading to specific cell morphology characteristics and ultimately death of cells.

The apoptotic process commence with specific signals that initiates a number of distinctive biochemical and morphological changes in the cell. A family of caspases and proteases are activated early in the process and they cleave cellular substrates necessary for normal cellular function, and activate other degradation enzymes which cleave the DNA. This results in the appearance of morphological changes in the cells and extensive DNA cleavage (Riccardi and Nicoletti, 2006). The morphological features of apoptosis include rounding up of the cell, retraction of pseudopodes, reduction of cellular and nuclear volume (pykonosis), modification of cytploasmic organelles, plasma membrane blebbing and engulfment of resident phagocytes in vivo (Kroemer et al., 2009). Because DNA fragments are lost from apoptotic cells, nuclear DNA content can be easily measured by flow cytometry, as they eventually end up in the sub-G_1 population. In contrast to apoptosis, the morphological features of necrosis include cytplasmic swelling (oncosis), rupture of the plasma membrane, swelling of cytplasmic organelles and moderate chromatin condensation, and is caused by a passive degenerative process (Kroemer et al., 2009).

5.7.1 DNA-damage induced apoptosis

A DNA-damaging agent not only targets DNA but also causes damage to other cellular components. Therefore targets other than DNA must also be taken into account when studying DNA-damage and apoptosis. However, apoptosis provoked by genotoxins is largely due to DNA damage (Roos and Kaina, 2006a). Apoptosis can be triggered by many different types of DNA damage induced by for instance UV light or different types of carcinogens, such as methylating agents found in tobacco smoke or food causing the killing lesion, O-6-methyl-guanine. N-methylated bases that are induced by alkylating agents such as N3-methyl adenine or N7-methylguanine are cytotoxic and at high levels such lesions can trigger apoptosis(O'Connor et al., 1988). Chemical genotoxins like benzo(a)pyrene (BaP) from

combustion reactions or smoke cause bulky adducts in the DNA and can trigger apoptosis. One important pathway linking DNA damage to apoptosis is the ATM/ATR-triggered pathway involving the checkpoint kinases, CHK1 and CHK2, and p53. p53 induces transcriptional activation of pro-apoptotic factors such as FAS, PUMA and BAX leading to mitochondria dysfunction and thereby apoptosis (Roos and Kaina, 2006b).

6. Methods

6.1 Cell cultures

6.1.1 Lymphocytes versus lymphoid cell culture

Circulating human peripheral blood lymphocytes (PBL) will only survive for a short period of time without undergoing morphological alterations, extensive synthesis of macromolecules or mitosis, when cultured *in vitro*. The resting peripheral blood lymphocytes normally remain in a quiescent state, described as G0, containing a diploid DNA content (2C). When stimulated, they will increase their RNA, protein and DNA synthesis. The stimulation can be brought about by several agents; in this case in this case phytohemagglutinin (PHA) was used. PHA stimulation triggers a set of metabolic events resulting in entering of the G_1-phase, after approximately 12 hours, and RNA synthesis, which will continue to increase during the S-phase, beginning about 30 hours after stimulation, in which DNA synthesis occurs.

As a model system for studying the effect of AA/GA on human lymphoid cells, we used a continuously growing Epstein-Barr Virus (EBV) transformed B-lymphoid cell line already available in our laboratory (GM00130C). The advantages of using a cell line are: 1) access to a practically unlimited number of cells, 2) they can be grown for an extended time period and 3) easier handling and less time consuming cell isolation, than required for PBL. However, there are also disadvantages using cell lines, especially when studying cell cycle control and responses to DNA-damage. Obviously the cell cycle is altered in these cells and therefore should be taken into consideration when interpreting the data.

6.1.2 EBV transformed B-lymphocytes

In this project, the GM00130C cell line was utilized as a model system resembling stimulated normal lymphocytes. GM00130C is derived from B-lymphocytes immortalized by the Epstein-Barr virus (EBV) and was obtained from Coriell Cell Repositories (Coriell Institute for Medical Research, Camden, New Jersey). These cell lines are usually polyclonal in derivation. The lymphoblasts were grown as a suspension culture in RPMI with 10% heat

inactivated calf serum and 1% penicillin and streptomycin with 5% CO_2 in air under saturated humidity at 37^0C. Their morphology is small (7-9 micron) round cells that grow as loose aggregates in suspension. The cells were cultured at a density between 0.2 x 10^6 – 1 x 10^6 cells/ml.

Cell culture treatment.

The cells were seeded out in Costar cell culture dishes at a concentration of 0.2 x 10^6 cells/ml. Cells were exposed to AA or its metabolite GA at concentrations varying from 20 µM to 1 mM. GA or AA was always prepared in fresh solutions the same day (diluted in PBS). All cell treatment was performed under sterile conditions.

6.1.3 Isolation of primary lymphocytes from whole blood

Blood samples were obtained by venepuncture from healthy volunteers. Lymphocytes were isolated by Ficoll-Hypaque density gradient as follows:

1. Whole blood was diluted 1:1 with PBS and transferred to pre-made lymphoprep™ tube (Axis-Shield PoC AS). The tubes was centrifuged for 20 min 500 x G at room temperature.
2. The layer of mononuclear cells was transferred to a new falcon tube and washed with medium and centrifuged at 500 x G at room temperature for 5 minutes.
3. The pellet was resuspended in medium, counted and diluted in prewarmed RPMI-medium containing 10% FCS and 1% PS to the desired cell concentration, preferably 2x10^6/ml.

6.1.4 Stimulation of resting peripheral blood lymphocytes (PBL) into late G_1

In order to obtain good control lysates for the Western procedure when detecting the cell cycle parameters such as $p21^{CIP1}$, p27, cyclin A and cyclin E, we stimulated PBL into late G_1. In resting cells, G_0, the protein content of $p21^{CIP/KIP}$ is low and the content of $p27^{KIP}$ is high due to $p27^{KIP}$ contribution to maintain lymphocytes in a quiescent state (Vervoorts and Luscher, 2008).When PBL are stimulated by PHA into late G_1, around 30 hours post

stimulation, the cyclins and $p21^{KIP}$ are upregulated while $p27^{KIP}$ is down regulated (Vervoorts and Luscher, 2008).

1. The cells were seeded out at a concentration of 2 x 10^6 cells/ml and phytohemagglutinin (PHA) added to a final concentration of 1µg/ml.
2. The cells were incubated at 37°C with 5% CO_2 for 31 hours until cells had reached late G_1. For western procedure, cells were pelleted by centrifugation at 500 x G for 5 minutes and lysed according to the protocol in section 6.9.5.

6.2 Metabolism of acrylamide to glycidamide using liver S9 fractions

In order to metabolize AA to GA in cell cultures we used liver S9 fractions which are subcellular fractions that contain several drug-metabolizing enzymes, including the cytochromes P450, flavin monooxygenases and UDP gluronyl transferases, and are therefore expected to metabolize AA. Pooled human liver S9 obtained from In Vitro Technologies was prepared form several donors with mixed sexes.

Procedure:

1. The final culture medium should contain 10% of S9-mix.
2. The NADPH Regenerating System (NRS) was prepared fresh every time and kept on ice.
3. All ingredients were mixed except the G-6-P dehydrogenase and the S9-fraction.
4. Immediately before exposure to AA the S9-fraction and the G-6-P dehydrogenase was added to the mixture.

From the stock solutions, the amount of S9-mix needed was prepared according to the volumes (µl) in the Table 1:

Table 1: Ingredients used in S9 mix

Total S9-mix volume		**Stock solutions**	**100 µl**	**End conc. (mM)**
S9 fraction			**30**	
NRS (stored stock solutions at at 4˚C)	**1 M KCl**	1.118 g/15ml	3.3	33
	0,25 M $MgCl_2$*6H_20	0.762 g/15ml	3.2	8
	0,2 M G-6-P	0.913 g/15ml	2.5	5
	G-6-P DH (140 U/ml)		2.7	263.75 U/ml
	0,04 M NADP	0.473 g/15ml	10	4
	RO water		21.0	
	PBS x		30.0	0.3x

6.3 Methods to detect DNA damage and repair

6.3.1 The comet assay

The comet assay (single cell gel electrophoresis or SCGE) is a simple and sensitive technique for measuring DNA strand breaks in single cells (Olive et al. 259-67;Ostling and Johanson 291-98;Singh et al. 184-91). The comet assay can be performed under neutral or alkaline conditions. The neutral version is generally less sensitive. It was thought that the DNA of the head and tail primarily was double-stranded and that only double strand breaks was measured, whereas under alkaline conditions ssDNA appears in the tail while the head largely consist of dsDNA (Collins et al., 1997), but this is still debated. However, the alkaline version detects both DNA double strand breaks (DSB), DNA single strand breaks (SSB) and alkali-labile sites (ALS) leading to an increased DNA migration (Collins et al., 1997). In our studies we have only used the alkaline version.

The method is based on embedding exposed cells in agarose and lysing the cells with detergents and high salinity. After lysing, we are left with the 'nucleoids' in the gel. Nucleoids are protein depleted nuclei containing intact supercoiled DNA loops. After incubating the gel and running electrophoresis at high pH (13.2) the DNA unwinds and if

damaged, migrates out of the nucleoid resulting in structures resembling comets. This alkaline comet assay detects both ss- and dsDNA breaks. The ssDNA breaks, which dominate largely in numbers, are generally quickly repaired and maybe not the most interesting type of lesions since they are not regarded as a significant lethal or mutagenic lesion. When exposing cells to genotoxic compounds the DNA may encounter AP (Apurinic or Apyrimidinic) sites and not strand breaks directly. The high pH of the electrophoresisbuffer causes the transformation of these alkali-labile AP sites to single strand breaks by introducing breaks in the phosphodiester backbone. Thus, the supercoiled DNA becomes relaxed and can be pulled out of the nucleoide towards the anode (Collins et al., 1993). Additionally, to make the comet assay more sensitive and more specific, the DNA can be incubated with lesion-specific endonucleases that detect and digest specific base lesions and thereby produce single strand breaks. The more strand breaks that exist in the DNA the more loops can be pulled out and therefore, the percentage of DNA in the tail is a direct measurement of the amount of damage the DNA possess. The net damage obtained by the specific enzyme can be calculated by subtracting the damage obtained without adding the enzyme, giving an estimate of the percentage of a specific lesion the DNA has attained.

Lesion specific endonucleases

By introducing lesion-specific repair endonucleases any lesion for which a repair endonuclease exist can be detected. This is a necessary step to allow detection of lesions that are not frank breaks.

Formamido pyrimidine *N*-glycosylase (FPG)

The bacterial enzyme from *Escherichia coli*, formamido pyrimidine *N*-glycosylase (FPG) protein is widely used and is recommended for the detection of oxidative DNA base damage and frequently used in our laboratory. The Fpg-enzyme function is part of the BER-pathway and it preferentially recognises 8-oxo guanine, but also ring-opened Fapy lesions. The ring-opened Fpg-substrates include for instance Fapy-Gua (2,6-diamino-4-hydroxy-5-formamidopyrimidine) and Fapy-Ade (4,6-diamino-5-formamidopyrimidine) (Boiteux et al. 106-10;Chetsanga and Lindahl 3673-84). The ring-opened purines of guanin will be excised at the N-7 and C-8 position (Boiteux et al., 1987). Since the glycosylases in general have an associated AP lyase or AP endonuclease activity, they cleave the DNA at the AP-sites and

baseless sugars are left as BER intermediates. Since there might be other AP-sites not related to oxidation, these too will be detected and cleaved by FPG. So, the enzyme specificity is not absolute (Azqueta et al., 2008; Collins et al., 1993).

The comet assay protocol

DNA strand breaks and alkali labile sites were measured using the comet assay which was performed using the method described by Singh et al. 1998 and Tice et al. 2000 with some modifications.

1. After cell exposure, harvesting and washing the pellet, the cells were resuspended carefully in PBS at a concentration of approximately 1 million cells per ml and kept on ice.
2. The cells were then mixed 1:10 with 0,75% low melting agarose and dissolved in 10 mM EDTA in PBS at 37˚C. The cell suspension was mixed carefully and immediately moulded out in the wells on a cold GelBond film with the use of a casting frame, producing 12 gels on one film. Three technical replicates per sample were added each time.
3. The GelBond films were then placed in cold lysis buffer at 4˚C for minimum 2 hours, or overnight. Furthermore, the films were rinsed quickly in cold, distilled water before equilibrating the gels in enzyme reaction buffer for 10 minutes followed by 50 minutes prior to enzyme treatment.
4. The enzyme, Fpg, was added to a final concentration of 1 µg/ml to the preheated enzyme reaction buffer, including 0.2 mg/ml bovine serum albumin (BSA) and incubated at 37˚C for one hour.
5. The films were placed in electrophoresis buffer (pH 13.2) at 4˚C for 5 minutes + 35 minutes. This will stop the enzyme reaction and unwind the DNA.
6. Gel electrophoresis was performed in electrophoresis buffer (pH 13.2) at 8˚C for 20 minutes at 20 V and approximately 300mA, with an approximately voltage drop of 0.74 V/cm across the platform.
7. The films were neutralized in neutralizing buffer 2 x 5 min, to prevent further unwinding. The gels were then fixed in absolute ethanol, dried and stored dark until scoring.

6.3.2 Scoring of comets

The DNA was stained with SYBR®Gold in TE-buffer for 20 minutes. The comets were scored using the image analysis software "Comet assay IV" from Perceptive Instruments and using a Leica DMLB with an Osram Mercury Short ARC HBO® 50W/2 light bulb or or an Olympus BX51 microscope with an Osram Mercury Short ARC HBO 100® W/2 light bulb. The comets were selected by the operator. For each comet, the software calculates the total intensity (amount of DNA) of the comet, the intensity of the tail (from the middle of the head and to the end of the tail) and of the head, and then calculates per cent DNA in the tail versus that of the total comet. This "per cent tail intensity" was used as a measure of damage. It increases linearly with break frequency. In each gel 50 comets were scored, overlapping comets were avoided since the software cannot discriminate between them and this would lead to an incorrect per cent tail DNA. Importantly, the cell density is critical when moulding the cells in order to avoid overlapping cells or comet tails.

6.3.3 Determination of repair capacity

To determine the repair capacity of GA-induced lesions in GM00130C, suspension cells were exposed to 0.1 mM and 0.5 mM GA in a cell incubator under standard conditions at 37˚C with 5% CO_2. The cells were exposed to different concentrations of GA for 2 or 4 hours, washed twice with medium and incubated further in medium for 2 and 20 hours, respectively. The DNA damage and repair was then analyzed by the Comet assay procedure.

6.4 Flow cytometric analysis of cell cycle distribution

Flow cytometric analysis is a widely used method that allows simultaneous multi-parameter analysis of single cells, and is predominantly used to measure fluorescence intensity produced by fluorescent-labelled antibodies detecting proteins or ligands that bind to specific cell-associated molecules, such as DNA binding by Propidium Iodide. All analysis was performed on BD LSRII ™ flow cytometer from BD Biosiences.

Two of the most popular flow cytometric applications are the measurement of cellular DNA content and determining the stages of the cell cycle within a population of cells. This can be carried out on fixed or live cells using different fluorescent DNA binding dyes in conjunction with antibodies to analyse antigen expression.

Cellular DNA content:

By adding a fluorescent dye that binds stoichiometrically to the DNA, the nuclear DNA content can be quantitatively measured. The principle is based on that the stained material has incorporated an amount of dye proportional to the amount of DNA. When measured in the flow cytometer the emitted fluorescent signal yields an electronic pulse with a height (amplitude) proportional to the total fluorescence emission from the cell. These data are considered as a measurement of the cellular DNA content (Shapiro, 2003).

Cell cycle analysis:

The determination of the relative DNA content enables discrimination between the various phases of the cell cycle. There are four distinct phases G1- S-, G2 and M-phase in a proliferating cell cycle, However since both G2- and M-phase contain the same amount of DNA they cannot be discriminated based on differing DNA contents.

One important aspect of DNA analysis by flow cytometry is the ability of the cytometer to exclude cell doublets. A doublet is formed when two cells with a G_1-phase DNA content are recorded by the flow cytometer as one event with a cellular DNA content similar to a G_2/M-phase cell. If the sample analyzed contains many doublets this would yield an overestimation of the G_2/M-phase population. By looking at pulse width (i.e duration) versus pulse area one can exclude cell doublets since a true G_2 cell will have a smaller width compared to a pair of G_1 cells passing through the laser beam simultaneously. Since the width of the fluorescence from the DNA dye increases with the diameter of the doublet particle, while both the G_1doublet and the G_2/M single produce the same fluorescence area signal, one can discriminate the G_1-doublet from a single G_2-cell (Figure 9). Therefore, in a dot plot histogram it is possible to isolate or "gate" the population of singlet G_1, S and G_2/M cells in order to study the population of interest (Nunez, 2001). Once the single cell population is

identified, the percentage of cells in G_1-, S- and G_2/M-phase can be estimated either by subjectively setting gates or by using a program that will mathematically deconvolute the DNA histogram and thus give a more accurate measurement of the percentage of cells in each phase (Shapiro, 2003).

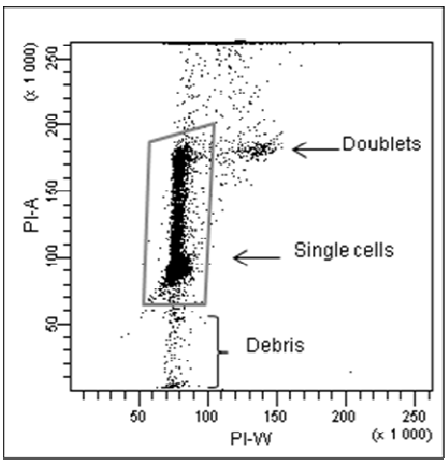

Figure 9 Gating of single cells in flow cytometry

Cell cycle analysis software

Several manufacturers have developed software for cell cycle analysis. These provide several mathematical models for fitting the DNA histogram. We used MultiCycle AV for Windows from Phoenix flow systems and BD FACSDiva^{TM} Software. These software programs provide mathematical models for fitting the DNA histogram. However in most cases a subtraction of the background is required in order to remove events caused by debris, which will produce a better fit with the models given by the software. Before the calculation of the phases, two main regions at the left of G_1 and the right part of G_2/M of the histogram are excluded. The lower left region consists of debris and is excluded from the analysis by defining it as background in the software. The upper left region is set by the position of G_1, and marks the starting point of the phase analysis. The lower right region marks the end of G_2/M –phase and the upper right region is gated out and excluded (Figure 10).

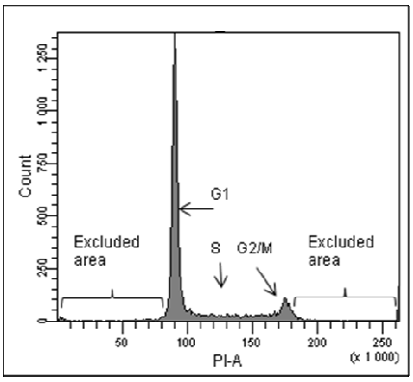

Figure 10: Gating of cell cycle population.

6.5 Cell Cycle Analysis by Propidium Iodide (PI) Staining

Propidium iodide (PI) form complexes with double stranded DNA and RNA by intercalating between the bases with a stoichiometry of one dye per 4–5 base pairs of DNA. Since PI stains both double-stranded DNA (dsDNA) and double-stranded RNA (dsRNA), cells must be treated with RNAse to ensure that the PI staining is DNA specific. Otherwise one would get artificial broadening of the DNA content distribution due to fluorescence dye bound to double stranded RNA. When excited by 488nm of laser light, the PI staining can be detected with 562-588nm band pass filter using flow cytometry (Riccardi and Nicoletti, 2006).

6.5.1 Fixation of cells:

1. After exposure, the cells were harvested by centrifugation at 310 x G at 4˚C and washed twice in ice cold Dulbecco's PBS without Ca^{2+} or Mg^{2+}.
2. The pellet was resuspended in PBS and added ice cold 100% ethanol, to give a final concentration of 70% ethanol, and stored at -20˚C until analysis.

*Propidium Iodide (**PI**) Staining procedure:*

1. To facilitate the pelleting of ethanol fixated cells, the ethanol concentration of the fixated cells were diluted to 50% or below with Dulbeccos PBS without Ca^{2+} or Mg^{2+}, and added 1% FCS to avoid clumping.

2. The pellet was resuspended in 0.5 ml PBS with 40 µg/ml RNase, to remove any residual RNA, and 20 µg/ml PI to stain the DNA, and incubated for 10 minutes at 37˚C.

The samples were then analyzed on a BD LSR II flow cytometry (BD Biosience) to determine PI (red) staining and cell count.

6.6 Cell Cycle Analysis by Bromodeoxyuridine

The limitation of using only a single fluorochrome, such as PI, is that we do not get any kinetic information. It is difficult to tell if cells that have an S-phase amount of DNA actually are cycling. To assess this problem we can use bromodeoxyuridine (BrdU) which is an analogue of thymidine that will be incorporated into the DNA of cycling cells. The BrdU incorporation can be detected by unwinding the DNA and then using a FITC (fluorescein isothiocyanate)-labelled antibody against BrdU. The result is a better separation of the S-phase population from the G_1 and G_2 cells (Shapiro, 2003). Therefore, we can get a bivariate analysis of total DNA content using propidium iodide staining along the X-axis, plotted against BrdU incorporation detected by the FITC-labelled antibodies against BrdU on the Y-axis. In addition, the rate of cell division can be monitored by puls labelling the cells with BrdU and harvesting at different time points. In our experiments BrdU was added 1 hour prior to harvesting the exposed cells. The cells were then fixed according to the protocol. After labelling the cells with FITC-anti-BrdU and resuspending in RNAse/PI solution, cells that synthesize DNA during the BrdU pulse labelling will be positive for FITC and thereby easily detected. The benefit of using BrdU incorporation is that we are able to distinguish cells in early S-phase from cells in G_1- and late S-phase from those in G_2-phase without the need of mathematical software to deconvolute DNA histograms.

BrdU-FITC procedure:

Cells were exposed and harvested the same way as for PI-staining and flowcytometry.

1. To facilitate the pelleting of ethanol fixated cells, the ethanol concentration of the fixated cells was diluted to 50% or below with Dulbeccos PBS (without Ca^{2+} or Mg^{2+}), and added 1% FCS to avoid clumping. Centrifugation for 20 minutes 250 x G.

2. Pellet was resuspended in 1ml 2M HCl with 0.3 mg/ml pepsin, slowly while vortexing carefully, and left for 30 minutes at room temperature to denature the DNA.
3. The HCl was neutralized by adding 3ml 0.1M sodium tetraborate.
4. Cells were pelleted by centrifugation at 250 x G for 10 minutes, then washed in IFA buffer (10 mM HEPES [pH 7.4], 25 mM NaCl, 4% FCS) and pelleted again.
5. Pellet was resuspended in 1ml IFA with 0.5% tween for 10 minutes at room temperature, then pelleted by centrifugation at 250 x G for 10 minutes.
6. The pellet was subsequently resuspended in 100 µl IFA together with the FITC conjugated anti-BrdU antibody diluted 1:10 and incubated for 30 minutes at room temperature.
7. After the final IFA wash and centrifugation, the pellet was resuspended in 0.5 ml PBS with 40 µg/ml RNase to remove any residual DNA, and 20 µg/ml PI was added to stain the DNA.

6.7 Methods for detection of cell death

6.7.1 Flow cytometric analysis for identification and quantification of apoptotic or necrotic cells

Apoptotic cells show reduced DNA stainability following staining with a variety of fluorochromes such as propidium iodide (PI), DAPI (4',6-diamidino-2-phenylindole), acridine orange or Hoechst dyes. Therefore, the appearance of cells with lower DNA stainability than that of G1 cells, sub-G1 peak, is considered to be a marker of cell death by apoptosis. This reduced stainability is a consequence of partial loss of DNA due to activation of an endogenous endonuclease and subsequent diffusion of the low molecular weight DNA products from the apoptotic cell(Darzynkiewicz et al., 1992). A necrotic cell, on the other hand, does generally not show an immediate reduction in DNA stainability. Thus the discrimination by live- and necrotic- cells is not recommended based on single-parameter DNA content analysis alone (Darzynkiewicz et al., 1992).

Due to chromatin condensation and nuclear fragmentation during the process of apoptosis, the apoptotic cells and bodies arising from G_1 emit fluorescent signals that are lower than those of G_1 cells. The fluorescent signals can be much smaller than expected in non-apoptotic G_1 cells and thus represent only a fraction of the original amount of DNA in a whole nucleus. Therefore, if the treatment causes a great increase in the percentage of apoptotic bodies, it must be remembered that one G_1 nucleus can fragment into many smaller condensed chromatin units. As apoptosis progresses, the size of the fluorescent signal become progressively smaller and at some point will be gated out together with the background fluorescence. In this way, apoptotic G_2/M- and S-phase nuclei progress backwards through S-, G_1- and eventually sub G_1-phase as the apoptotic process progress.

6.7.2 Fluorescence microscopy

1. The integrity of the plasma membrane of cells undergoing apoptosis is preserved and most functions of the membrane remain unchanged. Thus, apoptotic cells exclude dyes such as PI or trypan blue, often used as "viability assays" dyes. This is in contrast to necrotic cells where one of the earliest changes is loss of membrane function and its structural integrity. By using PI and Hoechst 33342 staining simultaneously one can discriminate between live versus apoptotic versus necrotic cells. In this method PI is not excluded by necrotic cells, and after entering the cell PI intercalates with DNA, causing red fluorescence of the necrotic nucleus. Vital cells actively take up Hoechst 33324 and show blue fluorescence of the cellular DNA. When applied to apoptotic cells, Hoechst 33342 emits a more intense blue fluorescence than live cells due to the condensation of the cell and nucleus. For a period of 4-6 hours the apoptotic cells are still able to exclude PI. Thus, this method offers differentiation between viable (blue fluorescence), apoptotic (intense blue fluorescence, unstained or only faintly red fluorescence) and necrotic cells (red fluorescence), as well as the feasibility to discriminate between early and late phases of apoptosis, apoptotic/necrotic cells, based on the difference in membrane permeability to PI.

6.8 Determining the vitality of cells by staining with propidium iodide and Hoechst 33342

A cell that is undergoing apoptosis demonstrates nuclear condensation and DNA fragmentation, which can be detected by staining with the DNA stain, Hoechst 33342 (H342) and by using a fluorescence microscope.

Hoechst 33342 (H342) is a rather large molecule (MW 616) but readily crosses intact cell membranes, and specifically stains DNA (bluish-grey fluorescence). It binds both specifically and quantitatively to DNA, preferably to AT-rich regions in the small grove of DNA and fluoresces blue when excited by UV light (Shapiro, 2003). Thus, all nuclei stain blue.

Propidium iodide (PI) is a rather large molecule (MW 668.4) that does not cross intact cell membranes. However, it is able to pass through compromised plasma membranes. Thus, a red or pink-stained cell indicates damage to the plasma membrane.

A) Normal, healthy cells (H342 positive) with normal heterochromatic nuclei are stained blue.
B) Cells with compromised plasma membranes are normally reddish or pinkish blue.
C) Dead cells with compromised plasma membranes are PI positive and the nucleus is red. Cells are typically swollen.
D) Apoptotic cells that are either PI+ or PI-, are characterized by condensed chromatin which may appear as small, round homogeneously-stained nuclear fragments.

Procedure:

1. An eppendorf tube with 1 ml of cell suspension (0.5 to 1.0 x 10^6 cells/ml medium) was added 10 µl PI and 10 µl H342 (both stock solutions: 0.5 mg/ml distilled water) and incubated for 15 minutes in the dark at room temperature.

2. Cells were pelleted at 300 x G for 5 minutes and washed once with culture medium.

3. Supernatant was removed and pellet was resuspended in 5 µl FCS. Suspending the cells in serum helps to eliminate salt crystals and helps to maintain cell shape.

4. Two 2 µl drops of the cell suspension were placed on a microscope slide and smeared out with another slide, drawn behind the leading slide.

5. The slides were left to dry and stored in a dark slide box.

6. Using an oil immersion objective (magnification x400), approximately 400 cells were counted using Leica DMLB with an Osram Mercury Short ARC HBO® 50W/2 light source and with an UV-2A excitation filter 330-380 nm, each cell was placed into one of the four categories defined above.

6.9 Protein detection methods

SDS Polyacrylamide Gel Electrophoresis (SDS-PAGE)

Polyacrylamide Gel Electrophoresis (PAGE) is used to separate macromolecules on the basis of their molecular weight. The mobility of a molecule in an electric field is inversely proportional to molecular friction which is the result of its molecular size and shape, and is directly proportional to the voltage and the charge of the molecule

In PAGE, proteins charged negatively by the binding of the anionic detergent SDS (sodium dodecyl sulfate) are separated within a matrix of polyacrylamide gel in an electric field according to their molecular weights. Prior to this process, denaturation of proteins is performed by heating them in a buffer containing a soluble thiol reducing agent (mercaptoethanol) and SDS. Mercaptoethanol reduces all disulfide bonds of cysteine residues to free sulfhydryl groups. SDS is an anionic detergent, and heating in SDS disrupts all intra- and intermolecular protein interactions and all protein aquire a high negative charge. Sampled proteins therefore move to the positively charged electrode through the acrylamide mesh of the gel. Smaller proteins migrate faster through this mesh and the proteins are thus separated according to size

6.9.2 Western Blot

Western blotting is a technique used to identify and locate proteins based on their ability to bind to specific antibodies. By using gel electrophoresis one can separate proteins by their size. The most common type of gel electrophoresis is the SDS-PAGE as described above.

In order to make the proteins accessible to antibody detection, they are transferred from the gel onto a membrane while maintaining their relative position and resolution. This step is called blotting, and can be done in different ways. Electroblotting uses an electric current to pull proteins from the gel onto the membrane. This protein binding is based upon hydrophobic interactions, as well as charged interactions between the membrane and protein. After the blotting procedure the proteins can be detected on the membrane by adding specific antibodies after the remaining membrane has been blocked by milk proteins to avoid unspecific binding of antibodies. During the detection process the membrane is probed with a primary antibody specific for the protein of interest. The primary (antibody) Ab is then recognised by a secondary antibody which is conjugated to a reporter enzyme, such as horseradish peroxidase (HRP). HRP and the reporter enzyme causes a chemiluminescent reaction is based on the catalyzed oxidation of luminol by peroxide. Oxidized luminol emits light as it decays to its ground state. The resulting light is detected using an x-ray film which is developed manually by standard procedures.

6.9.3 Preparation, separation and detection of proteins:

Preparation of cell extract:

Cell extract was prepared in order to run and separate proteins through a polyacrylamide gel. Treated cells were harvested at different time points, washed in PBS and lysed in SDS buffer according to the following procedure:

1. The cells were washed twice in ice cold PBS and centrifuged at 500 x G for 10 minutes.
2. Protein extracts were prepared by resuspending the pellet on ice in 200-400 µl (depending on cell density) of lysis buffer (Table 2) containing freshly added phosphatase inhibitors such as, 1 mM sodium orthovanadate, 50 mM sodium fluoride

(tyrosinphosphate inhibitor), 10 mM β-glycerol 2-phosphate disodium salt, a stock of Complete Mini pill (Roche) was added as a cocktail of protease inhibitors. The lysates were transferred to eppendorf tubes and incubated further on ice for 10 min.

3. The cell lysate was sonicated on ice (one pulse per second, 40 amplitude, 3 x 10 sec with 5 sec intervals). Sonication breaks DNA strands thereby reducing the to solution's viscosity, and membrane bound proteins are released.
4. The lysates was boiled for 5 minutes, centrifuged at 16100 x G and the supernatant was frozen in liquid nitrogen and stored at -70^{o}C until use.

Table 2: Lysis buffer with inhibitors

2 ml lysis buffer	**2ml**
SDS-buffer	1.790 ml
NaF 20x	100 µl
NaVO 200x	10 µl
Complete 25x	80 µl
B-glyc 100x	20 µl

6.9.4 Protein concentration:

Protein concentration was determined using Bio-Rad *DC* (detergent compatible) protein assay which is a colorimetric assay for protein concentration. The assay is based on the reaction of protein with an alkaline copper tartrate solution and Folin reagent. The reaction takes place in two steps which leads to colour development: The reaction between protein and copper in an alkaline medium and the subsequent reduction of Folin reagent by the copper-treated protein. The colour development is primarily due to the amino acids tyrosine and tryptophan. The proteins causes a reduction of the Folin reagent by loss of one to three oxygen atoms, thereby

producing several possible reduced species which have a characteristic blue colour with maximum absorbance at 750 nm and minimum absorbance at 405 nm ref.

BSA diluted in lysis buffer with concentrations ranging from 0 - 10 µg/µl in was prepared to make a standard curve. Basically, the procedure according to the manufactures (Bio Rad) protocol was followed:

1. Three replicates of each sample (5 µl) were added to a microtiterplate.
2. 25 µl of reagent A containing 2% of reagent S was added.
3. 200 µl of reagent S was added.
4. After 15 minutes of colour development, absorption was measured in a plate-reader (Sunrise) at 750 nmd and analyzed with the software Magellan V.1.11.

6.9.5 Seperation of proteins and Western Blot Procedure:

Polyacrylamide gels:

Polyacrylamide is formed by the polymerization of the monomer molecule acrylamide crosslinked by N,N'-methylene-bis-acrylamide (BIS). Free radicals generated by ammonium persulfate (APS) and a catalyst acting as an oxygen scavenger (-N,N,N',N'-tetramethylethylene diamine [TEMED]) are required to start the polymerization since acrylamide and BIS are nonreactive by themselves or when mixed together.

The concentration of acrylamide and BIS controls the hardness and degree of cross linking of the gel. This subsequently controls the friction that macromolecules encounter as they move through the gel in an electric field, and therefore affects the resolution of the components to be separated. Hard gels (12-20% acrylamide) retard the migration of large molecules more than they do with the small ones. In loose gels (4-8% acrylamide), high molecular weight molecules migrate much further down the gel due to less friction caused by acrylamide and BIS.

A separation gel was made by first adding the ingredients listed below in Table 3, in the exact order to avoid premature polymerization. Water was added on top of the gel to even out the

top layer of the gel. The gel was left to polymerize for approx. 30 minutes. Then the stacking gel was made the same way (Table 4), and added on top of the separation gel.

Table 3: Separation gel ingredients

Separation gel	**2 gels, 6 %**	**2 gels, 8 %**	**2 gels, 10 %**	**2 gels, 12 %**	**2 gels, 15 %**
dH_20	7,9 ml	6,9 ml	5,9 ml	4,9 ml	3,4 ml
Acrylamide mix – 30%	3,0 ml	4,0 ml	5,0 ml	6,0 ml	7,5 ml
1,5 M Tris (pH 8,8)	3,8 ml	3,8 ml	3,8 ml	3,8 ml	3,8 ml
10 % SDS	150 µl	150 µl	150 µl	150 µl	150 µl
10% APS	150 µl	150 µl	150 µl	150 µl	150 µl
TEMED	12 µl	9 µl	6 µl	6 µl	6 µl

Table 4: Stacking gel ingredients

4 % stacking gel	**2 gels**
dH_20	4,05 ml
Acrylamide mix – 30%	0,85 ml
0,5 M Tris (pH 6,8)	1,65 ml
10 % SDS	67 µl
10% APS	34 µl
TEMED	7 µl

1. All the samples were diluted in lysis buffer in order to obtain equal amounts of protein loaded to each lane. Bromophenol blue (2.5%) and β-mercaptoethanol (5%) were added to the samples, and heated at 95-98^{o}C for 5 min to sustain inactivation of proteases and denaturation of proteins.

2. Proteins were separated by SDS-Polyacrylamide gel electrophoresis (PAGE) by using 8-16% precise™ Protein Gels (Thermo Fischer Scientific) or self made gels with the appropriate acrylamide concentration ranging from 10-12% acrylamide in the separation gel and a 4% stacking gel. 10µl Precision Plus Protein™ Standard, Kaleidoscope™ were applied to the first well in order to allow direct visualization of protein mobility during electrophoresis and for precise sizing of proteins. 25-50 µg of proteins of each sample was applied to the different wells.
3. Electrophoresis was run at 30-40 mA and 120 V in electrophoresis buffer until the Brophenol blue stain had reached the bottom of the gel. Then the gels were equilibrated in transferbuffer before blotting.
4. Proteins were transferred onto nitrocellulose membrane using Protran BA 85 nitrocellulose membrane from Whatman®. The Blotting was carried out in transferbuffer for 1 hour at 100 V, with ice blocks to keep the temperature low.
5. Further, the membrane was blocked for 30 minutes using Starting Block (TBS) Blocking Buffer at room temperature, in order to cover the remaining membrane with proteins to avoid unspecific binding of primary or secondary antibodies and to avoid background noise. Blocking Solution contains milk proteins that bind to the membrane.
6. Incubation with primary antibody (Ab) was performed over night at 4˚C with shaking. Subsequently, the membrane was washed 3 x 10 minutes with TBST
7. Next day, the membrane was incubated with an HRP-conjugated secondary Ab for 1.5 hour at room temperature prior to washing for 3 x 10 minutes with TBST and 1x 10 minutes with TBS.
8. Detection of protein was performed by using Supersignal® West Dura Extended Duration substrate (Bio Rad). By incubating the membrane with a chemiluminescent substrate that emits light in a reaction with horse radish peroxidase (HRP), the HRP-conjugated secondary Ab attached to the primary Ab will emit light at the spot where the protein of interest is positioned on the membrane.
9. Equal amounts of SuperSignal® West Dura Luminol/Enhancer Solution and SuperSignal® West Dura Stable Peroxide buffer were added to the membrane and incubated for 5 minutes.

10. The development of the proteins was carried out by placing the membrane in a photo development cassette and placing an X-ray film on top. The X-ray film is exposed by the light from the chemiluminiscent reaction and after developing and fixation of the film, dark spots or bands can be seen on the film. These dark bands may in turn be quantified since their intensity is proportional to the amount of fluorescence and hence to the protein content.

6.10 Statistical analysis

All statistical analysis of DNA damage, cell cycle distribution was done with the software programme SPSS v.14.0.

To perform statistical analysis, one would in general want at least three independent experiments, but due to time limitations, this was not possible for all analyses in this thesis, e.g. the comet data. The data was analysed statistically to show possible trends and should not be thought of as conclusive statements. The data from the comet assay were analyzed in a hierarchical model using univariate nested ANOVA with experimental number as random factors, and exposure as the fixed factor for the dependent variable %-tail DNA. The nesting was done by specifying exposure as fixed factor and the nested factor, experiment, as random factor. The SPSS syntax was altered to allow nesting by applying: /DESIGN = Exposure experiment(exposure). In the resulting ANOVA table, a significant "nestedfactor(main factor)" effect means that the dependent variable varies by the nested factor event within the same level of (controlling for) the main factor.

The normality of the data was evaluated using the Kolmogorov-Smirnov test, and the homogeneity of variances was evaluated with Levene's test. Violation of homogeneity will increase type I errors in the F test (wrongly rejecting the null hypothesis). However the failure to meet the assumption of homogeneity of variances is not fatal to ANOVA, which is relatively robust, particularly when groups are of equal sample size as in the comet assay.

Pairwise comparison, with Bonferroni confidence interval adjustment, was used to determine significant differences among the various exposures. This was applied to determine whether there are significant differences among the groups, as *post-hoc* comparisons can not be done with nested ANOVA. A *P* value of 0.05 was considered significant.

Parametric tests such as ANOVA rely on the assumption of independence, equal variance and normality (Lovell and Omori, 2008). Comet data usually fail the normality test, which also applies to Log transformation of the data due to some left skewed data in highly damaged samples. Less damaged samples skew to the right, which can be taken care of by the Log transformation. A further limitation of the Log transformation is that it may result in heterogeneity of variances (Lovell and Omori, 2008). One might use non-parametric test when the data violate the assumptions of parametric tests, however they are slightly less powerful than their parametric equivalents. Non-parametric tests such as Kruskal-Wallis and Mann Whitney tests have a tendency to be oversensitive in detecting small differences between samples, and is therefore not suitable when detecting genotoxic effects(Duez et al., 2003).

A univariate ANOVA was also conducted to explore the impact of GA on the different cell cycle phases, which were analysed separately. Experimental number was used as random factors, and exposure as the fixed factor for the particular cell cycle.

7. Results

In the results to follow, we first report on the ability of AA and GA to induce DNA damage; this damage was partly characterised by employing the Fpg enzyme which recognises and cleaves certain types of base alterations. Subsequently, we show cellular repair of such damage in cultured cells. These experiments were carried out using the comet assay. Specific effects of GA on cell cycle progression were then investigated using flow cytometry, followed by changes in the expression of specific and relevant gene products.

7.1 Glycidamide, but not acrylamide, induces DNA damage recognised by the Fpg-enzyme in lymphoid cells in vitro.

DNA damage induced by AA and its metabolite, GA, was measured by the alkaline comet assay. This assay detects single strand breaks and alkali labile sites in the DNA. In addition, when introducing an exogenous repair enzyme, some other lesions not leading to direct strand breaks are detected; with Fpg these lesions are preferentially oxidized purines (i.e.8-oxo guanine) but also ring-opened formamidopyrimidine lesions (both denoted as Fpg sensitive sites) (Krokan et al., 1997).

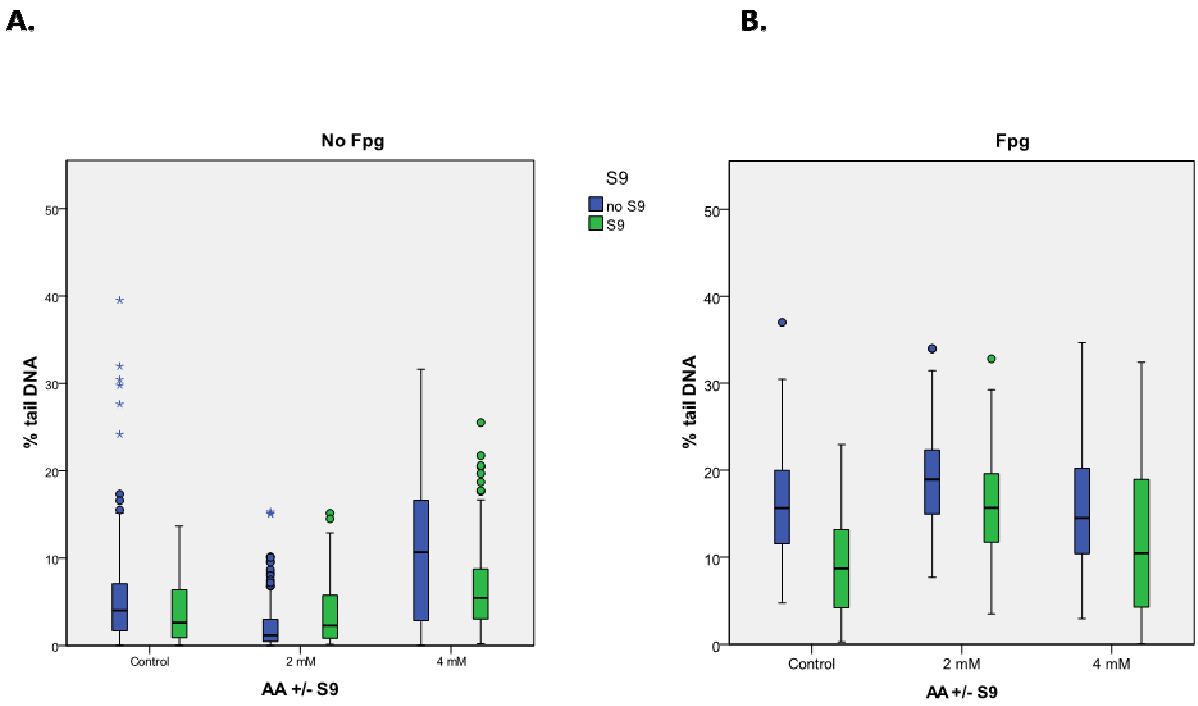

Figure 11. Acrylamide exposure of normal human lymphocytes.
Normal human lymphocytes (PBL) were exposed to different AA concentration for 2 hours with (green) or without (blue) S9 fraction. The level of DNA damage was measured by the comet assay (see method section). The lysed cells were incubated in enzyme buffer alone (A), or together with the Fpg -enzyme (B). The level of DNA damage is presented as % tail DNA intensity. One experiment is performed (n=1). 150 comets are scored for each exposure. The line across the box marks the median value (50th percentile), the length of the box is the interquartile range (IQR) (25th and 75th percentile, 50% of the cases), the circles represent outliers (> 1.5 x IQR) and asterisk (*) represent extreme points (> x IQR).

The DNA damaging effect of AA exposure of resting human lymphocytes (PBL) with or without human S9 fractions is shown in Figure 11. Human liver S9 fractions contain several drug-metabolizing enzymes, i.e. CYP2E1 (see methods) and are therefore expected to contribute to the metabolism of AA to GA. As shown in Figure 11A, AA did not induce any significant increase in DNA damage even at high concentrations of AA (4mM). In addition, the S9 fraction did not facilitate the DNA damaging effect of AA, instead it lead to a small decrease both in the control and in the exposed samples. When including the one-hour Fpg enzyme treatment step in the comet assay, a general increase in Fpg-sensitive sites where detected (Figure 11), however AA did not induce any increased Fpg-sensitive sites.

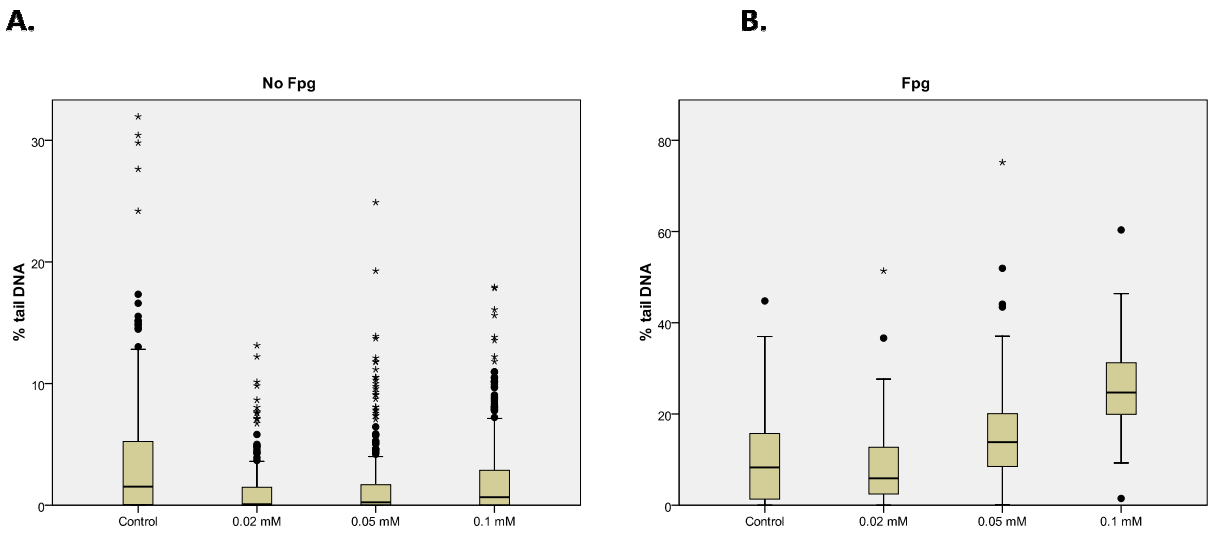

Figure 12: Glycidamide-induced DNA damage in PBL
Normal human lymphocytes (PBL) were exposed to different concentrations of GA for 2 h. The level of DNA damage was measured by the comet assay (see Methods section). The agarose embedded and lysed cells were incubated in enzyme buffer alone (A), or together with the Fpg -enzyme (B). The level of DNA damage is presented as % tail DNA intensity. GA induced a significantly increased level of DNA damage compared to the control $p < 0.001$, $F = 179.407$). *The figure shows two independent experiments combined (n= 2). The line across the box marks the median value (50th percentile), the length of the box is the interquartile range (IQR) (25th and 75th percentile, 50% of the cases), the circles represent outliers (> 1.5 x IQR) and asterisk (*) represent extreme points (> x IQR).*

Due to the lack of DNA damaging effect of AA, which reflects a limited activation of AA into GA during short exposure times, even in the presence of S9, we decided to perform subsequent studies only with its directly genotoxic metabolite GA. PBL was exposed to different concentrations of GA for two hours and the resulting DNA damage was analyzed by the comet assay (Figure 12). As Figure 12A shows, no GA-induced DNA-stand breaks or alkali labile sites were seen at relatively low concentrations of GA (up to 0.1 mM). However, when including Fpg, an increase in the DNA-damaging effect of GA was noticed. Already at 0.05 mM GA exposure, with Fpg the tail DNA intensity had increased compared to the control. At a concentration of GA of 0.1 mM, the tail DNA intensity had increased significantly. A nested one-way ANOVA was performed to show that there was a significant increase in GA-induced DNA with Fpg ($p < 0.001$, $F = 179.407$). Pairwise comparison indicated that both 50 µM and 100 µM GA (both $F = 273.645$, $p < 0.001$) ($n = 2$) had significantly more DNA damage than the control, but not at 20 µM of GA ($n = 1$).

However, the experiments performed in Figure 12 showed unexpectedly low levels of DNA damage after GA exposure and Fpg treatment, when compared with previous experiments performed by others in our laboratory (Hansen, 2007). To test the overall response of the cell cultures and the methodologies used in the present thesis, an additional experiment was performed using X-rays as a positive control (Figure 13). This time a higher DNA damage level was observed. At 0.1mM GA concentration and Fpg treatment, the tail DNA intensity increased from 7% (control) to 50% DNA, i.e. nearly the double of what was observed in Figure 10. The low DNA damage observed in the two first experiments may be due to an old GA stock that may have lost reactivity or perhaps individual differences in DNA damage susceptibility between the different blood donors.

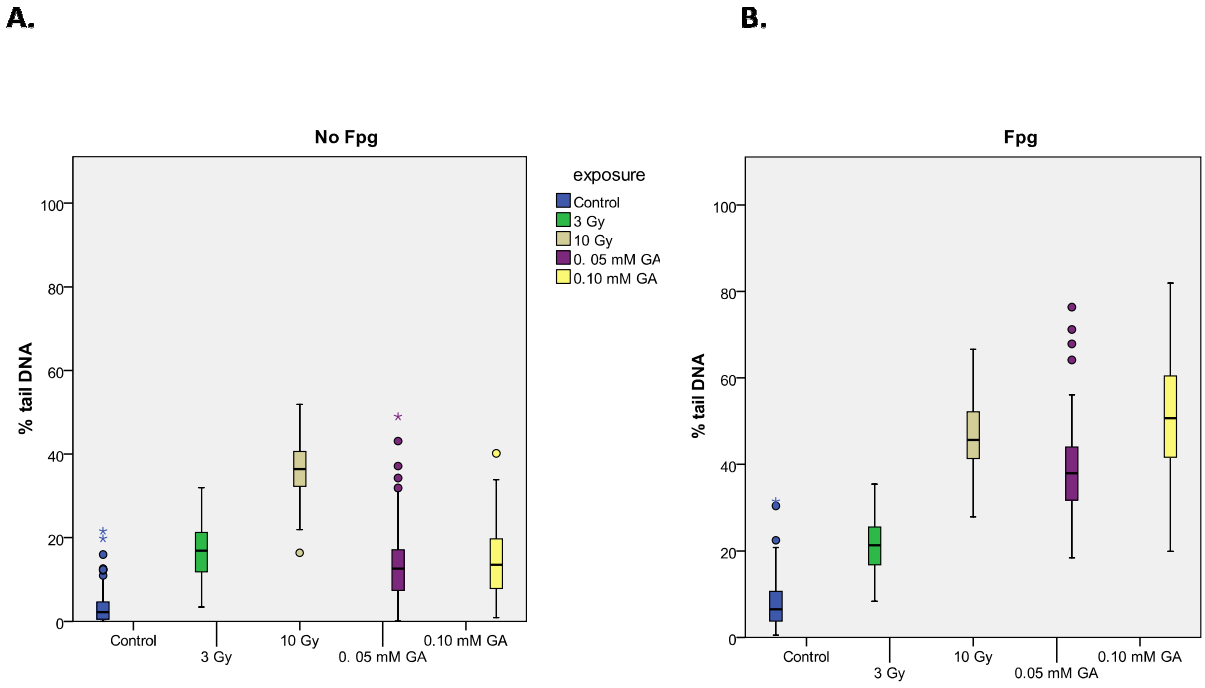

Figure 13: GA compared to x-ray- induced DNA damage
Normal human lymphocytes (PBL) were exposed to different concentrations of GA for 2 hours with different concentrations; 0.05mM GA (purple box) and 0.1mM (yellow box). The level of DNA damage was measured by the comet assay (see method section). The lysed cells were incubated in enzyme buffer alone (A), or together with the Fpg -enzyme (B). PBL X-ray irradiated with 3 Gy (green box) and 10 Gy (grey box) were included as a positive control. The level of DNA damage is presented as % tail DNA intensity.. The line across the box marks the median value (50th percentile), the length of the box is the interquartile range (IQR) (25th and 75th percentile, 50% of the cases), the circles represent outliers (> 1.5 x IQR) and asterisk (*) represent extreme points (> x IQR).

A lymphoblastoid cell line, GM00130, was introduced to study more in depth the mechanisms of GA-induced DNA damaging effect on lymphoid cells. In particular, unlike lymphocytes

these cells can be incubated for long periods of time, allowing a study of DNA repair. The cells were exposed to various concentrations of GA over time and the DNA-damaging effect was analysed with the comet assay with and without Fpg treatment. Firstly, the results show that GA exposure for 2 hours with 0.1mM GA exposure gave no significant increase in DNA damage, and only a minor increase in DNA damage with 0.5mM GA exposure without Fpg was seen (Figure 14A). However, a dramatic induction of Fpg-sensitive sites at both 0.1 mM and 0.5 mM GA concentration was seen in Figure 14B. Secondly, GA exposure over a time period of 24 hours gave a small increase in DNA damage, without Fpg, at low GA (0.1 mM) concentrations but much higher with a GA concentration of 0.5 mM. The Fpg sensitive sites induced after long-time GA-exposure (after 6 hours) increased dramatically and apparently saturated the assay as the dose response with 0.1 mM GA levelled off (Figure 14B)

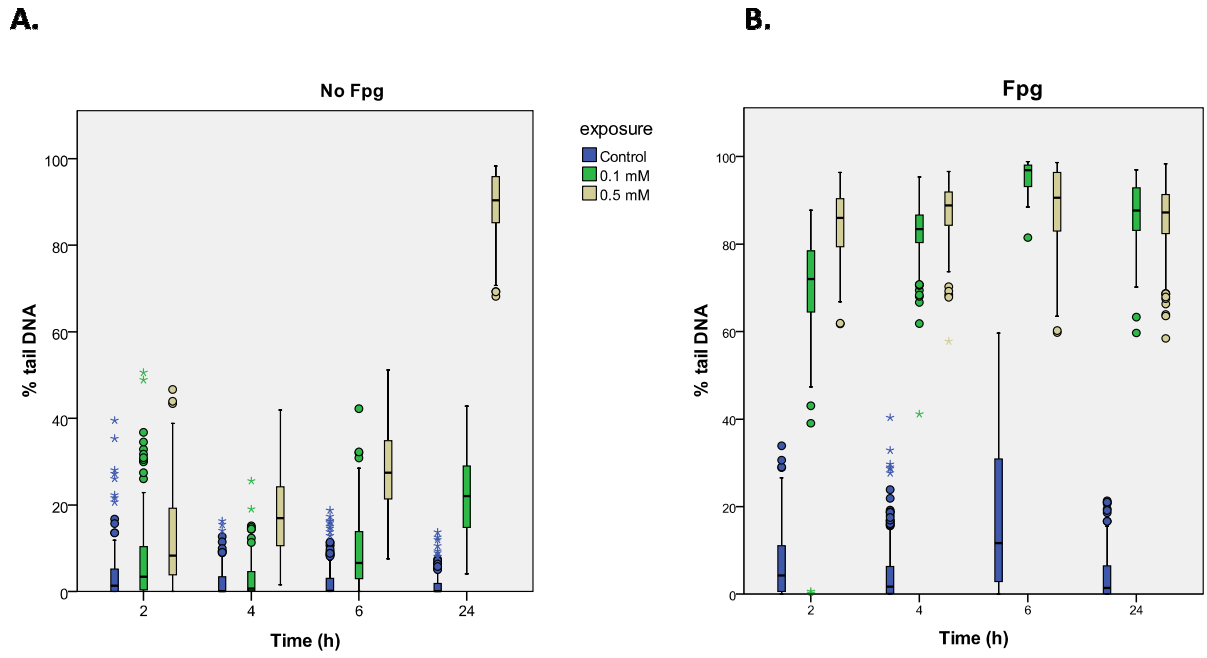

Figure 14: DNA-damage measured in GM00130 cells after GA exposure over time
GM00130 cells were exposed to 0.1mM (green box) and 0.5 mM GA (yellow box) for several time periods and analyzed by the comet assay (see method section) to measure DNA damage expressed as % tail DNA intensity. After lysis, cells were incubated in enzyme buffer alone (A), or together with the Fpg -enzyme (B). The line across the box marks the median (50th percentile), the length of the box is the interquartile range (IQR) (25th and 75th percentile, 50% of the cases), the circles represent outliers (> 1.5 x IQR) and asterisk (*) represent extreme points (> x IQR). The figure show two independent experiments combined (n= 2),

A nested univariate ANOVA of the comet data without Fpg treatment showed at all time points that the GA exposure led to a statistically significant higher %tail DNA intensity than the control at a $p < 0.001$ level. *F*-values at 2 hours is $F = 179.407$, at 4 hours is $F = 643.214$, at 6 hours is $F = 1152.049$ and at 24 hours $F = 680.331$. Pairwise comparisons indicated $p \leq 0.001$ at all concentrations and time points. The Fpg treated cells have all significantly higher DNA damage than the control, without the need for statistical analysis.

7.2 Repair of GA-induced DNA damage in lymphoid cells.

The repair of GA-induced DNA breaks was evaluated using the alkaline comet assay. GA-exposed GM00130 cells for 2 or 4 hours were harvested and rinsed prior to seeding the cells in fresh growth medium. These cells were then incubated at 37^0C for 2 or 20 hours in order allow repair of any induced DNA-damage (Figure 15 and Figure 16). The most prominent result shown in Figure 15 and Figure 16 was the reduction in Fpg-sensitive sites. After 2 hours incubation at 37^0C, some reduction in DNA damage indicates that the cells are repairing the Fpg sensitive sites. After 4 hours GA exposure and 20 hours incubation time, at 37^0C, a marked reduction in Fpg-sensitive sites was seen (Figure 16). There was also an indication of repair of SSB or AP sites as seen in Figure 14 without Fpg treatment.

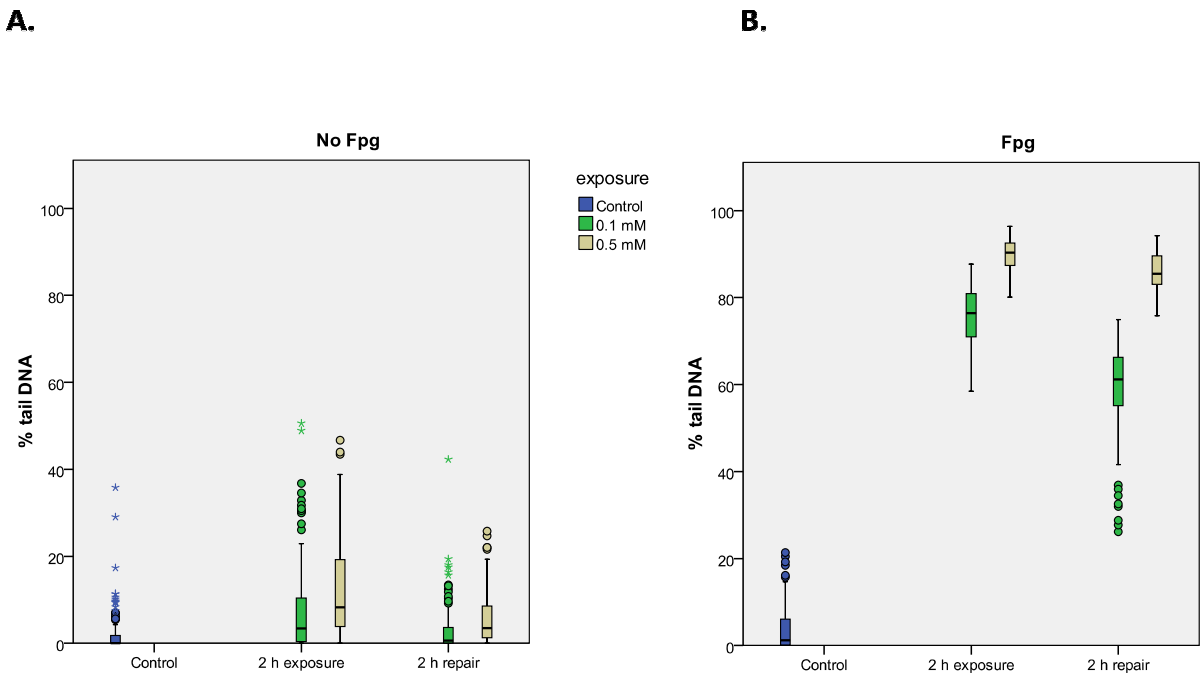

Figure 15: The repair of GA-induced DNA damage in GM00130 cells.
The DNA repair capacity of GM00130 cells after 2 hours of 0.1 mM GA (green box) or 0.5 mM GA (grey box) exposure was measured with the comet assay after 2 hours incubation in fresh medium, followed by comet analysis with (B) or without (A) Fpg-treatment (n = 1). The line across the box marks the median (50th percentile), the length of the box is the interquartile range (IQR) (25th and 75th percentile, 50% of the cases), the circles represent outliers (> 1.5 x IQR) and asterix (*) represent extreme points (> x IQR).

This experiment is only performed once, but the results of the various exposures and repair incubations are consistent. Taken together, the data show that, both with and without Fpg treatment, a reduction in tail DNA intensity was observed during a post-exposure incubation period, implying repair of both Fpg-sensitive sites, and also of strand breaks and alkali labile sites.

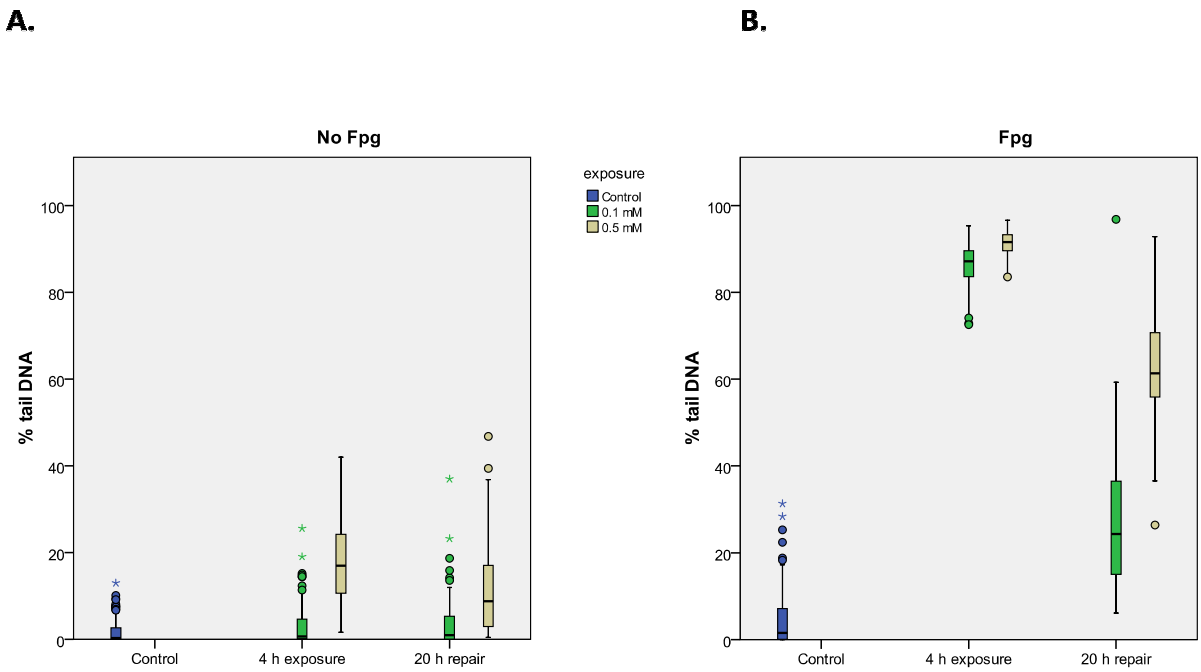

Figure 16. The repair of GA-induced DNA damage in GM00130 cells
The DNA repair capacity of GM00130 cells after 4 hours of 0.1 mM GA (green box) or 0.5 mM GA (grey box) exposure was measured with the comet assay after 20 hours incubation in fresh medium , with (B) or without (A) Fpg treatment, (n=1). The line across the box marks the median (50th percentile), the length of the box is the interquartile range (IQR) (25th and 75th percentile, 50% of the cases), the circles represent outliers (> 1.5 x IQR) and asterisk (*) represent extreme points (> x IQR).

7.3 Cell cycle analysis by PI staining and flow cytometry

The comet assay revealed high levels of DNA damage recognised by Fpg. We were therefore interested in analysing the cell cycle distribution of GA-exposed cells after prolonged exposure and thus comparing the cell cycle distribution with the level of DNA damage after a 24 hour exposure period. To test whether long time GA exposure had an effect on cell cycle progression, flow cytometric analysis with PI staining of asynchronously proliferating GA exposed GM00130C cells was performed.

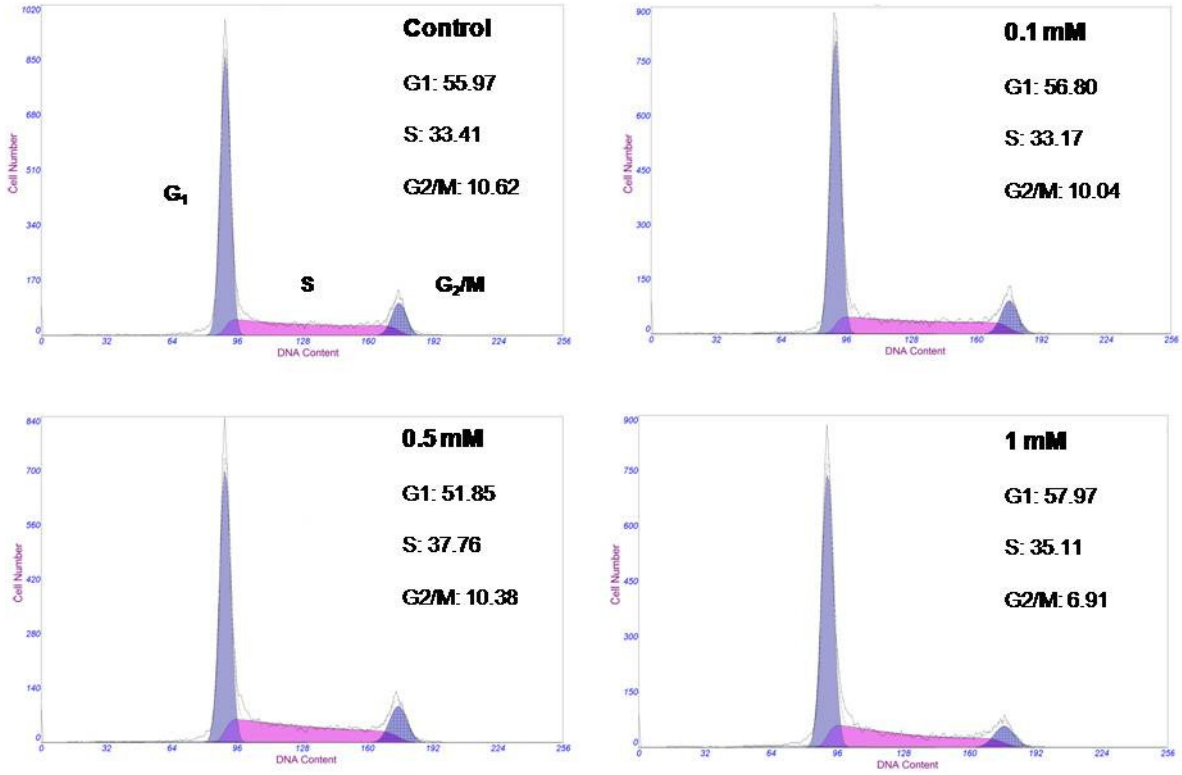

Figure 17. Cell cycle distribution following GA-exposure for 8 h.
GM00130C cells were treated with 0.1, 0.5, and 1 mM GA, harvested at the respective time points and analysed for cell cycle distribution by PI staining and flow cytometric analysis. The x axis represents the DNA content (PI staining) and the y axis represents number of cells analysed (cell count). The figure shows one representative experiment of three independent (n=3).

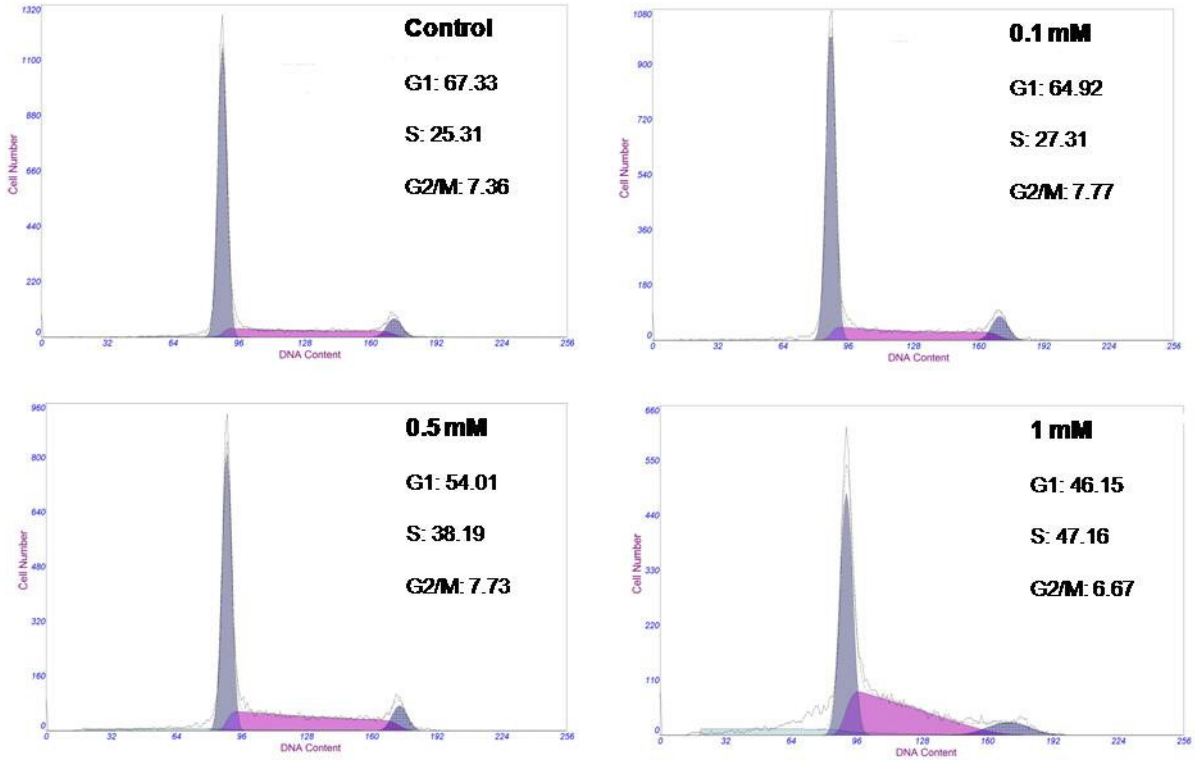

Figure 18: Cell cycle distribution following GA-exposure for 24 h.
GM00130C cells were treated with 0.1, 0.5, and 1 mM GA, and harvested at the respective time points for cell cycle distribution analysis by PI staining and flow cytometry. The x axis represents the DNA content (PI staining) and the y axis represents number of cells (cell count). The figure shows one representative experiment of three independent (n=3).

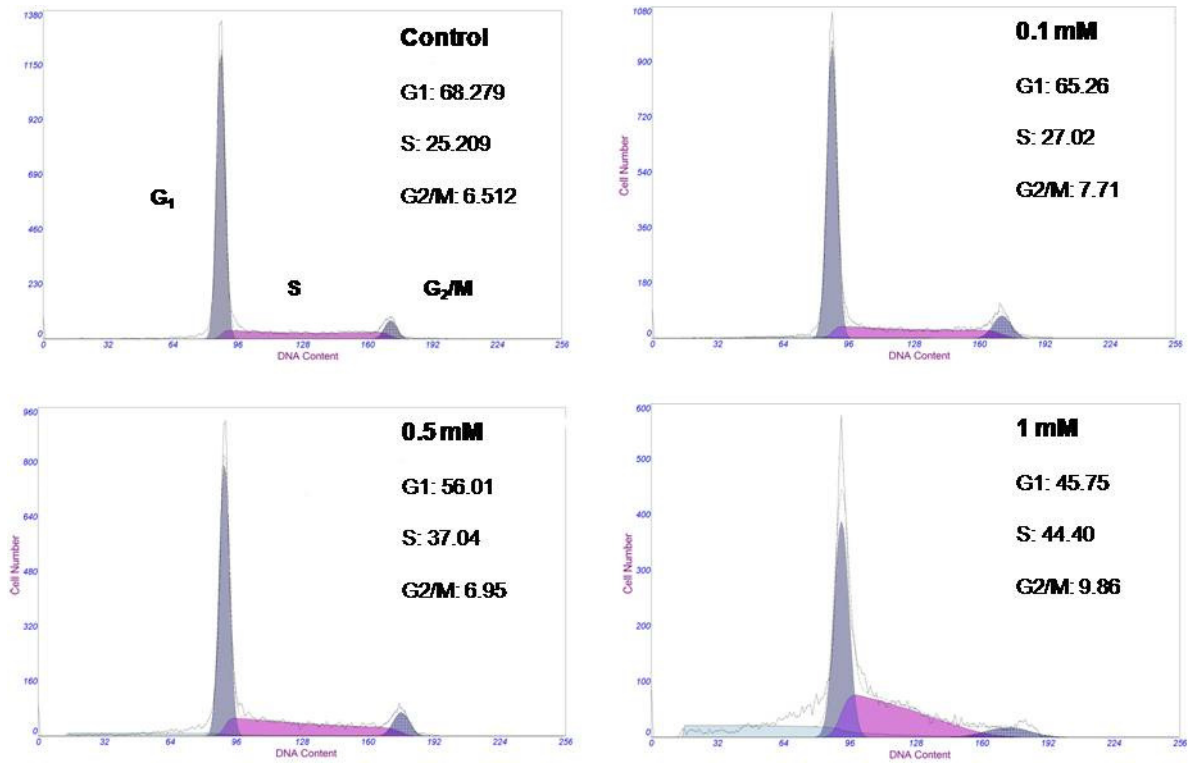

Figure 19: Cell cycle distribution following GA-exposure for 31 h.
GM00130C were treated with 0.1, 0.5, and 1 mM GA and harvested at the respective time points and analysed for cell cycle distribution by flow cytometry by PI staining The x axis represents the DNA content (PI staining) and the y axis represents number of cells (cell count). The figure shows one experiment (n=1).

The cell cycle distribution was apparently not affected by GA at 0.1 mM even after long exposure times, up to 31 hours. However, when exposing the cells to 0.5 mM and 1mM GA the cells clearly accumulated in S-phase together with a reduction of cells in G1 noted after 24 hours exposure as seen with PI-staining and flow cytometric analysis (Figure 18 and Figure 19)

After 24 hours exposure with 1 mM GA there was an increase in apoptotic/necrotic cells seen as increased cell debris accumulating to the left of the G1 peak (Figure 18). Also with GA exposure for up to 31 hours (performed only once), there was an increase in apoptotic/necrotic cells which was notable at 0.5 mM GA and even more prominent at 1 mM GA (Figure 19). The percentage of cells in each cell cycle phase indicated in Figure 18 and Figure 19 include only live cells. Accumulation of apoptotic cells/debris is seen to the left of the G1 population.

Figure 20 show a combined histogram of three independent flow cytometry experiments with PI staining of GM00310C exposed to various concentrations of GA up to 24 hours (Similar to Figure 17 and Figure 18). A univariate one-way ANOVA was conducted to explore the impact of GA on the different cell cycle phases. There was a statistically significant change in G1 and S phase (relative to control, $p < 0.05$) at 24 hours only, of GA exposure at all concentrations tested.

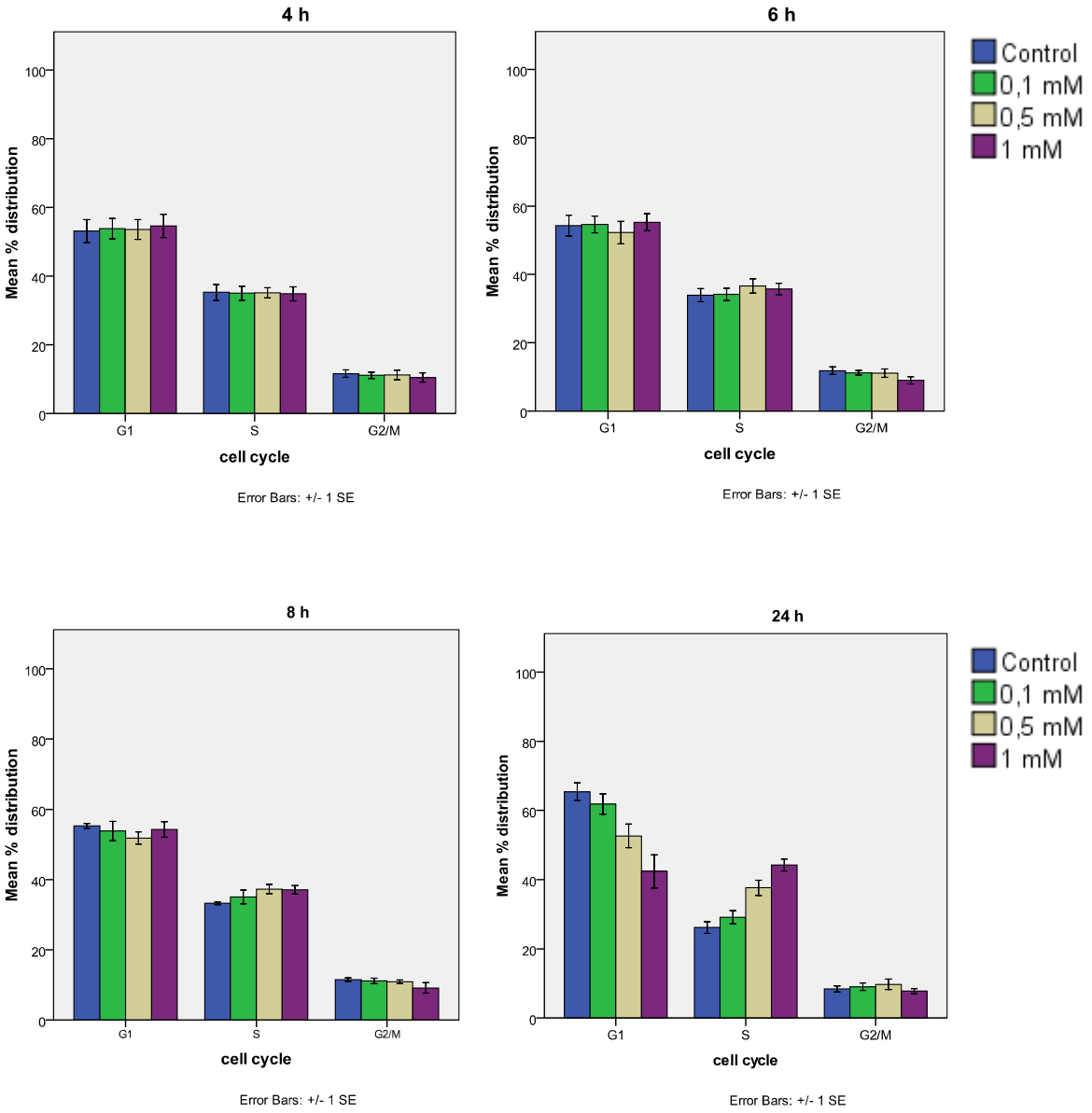

Figure 20: Cell cycle distribution following GA exposure of GM00130C.
GM00130C was treated with 0.1mM (green bar), 0.5mM (grey bar), and 1mM GA (purple bar) and harvested at the respective time points. Cell cycle distribution was analysed by PI staining and flow cytometry as described in the method section. The figure represents three independent experiments (n=3)

The G_1 phase: $F(3, 8) = 8.577$, $p = 0.007$. The actual difference in mean scores between the groups is considerably different. The effects size, calculated using partial eta squared, was 0.763. Post -hoc comparison using the Tukey HSD test indicated that the mean score for the control ($M = 65.42$, $SD = 4.43$) was significantly different from 1 mM GA ($M = 42.40$, $SD =$

8.27), p = 0.007. And that the mean score for 0.1 mM GA (M = 61.82, SD = 5.10) was significantly different from 1 mM GA (M = 42.40, SD = 8.27), p = 0.019.

The S phase: F(3, 8) = 18.828 , p = 0.001. The actual difference in mean scores between the groups is considerably different. The effects size, calculated using partial eta squared, was 0.876. Post -hoc comparison using the Tukey HSD test indicated that the mean score for the control (M = 26.15, SD = 2.99) was significantly different from 1 mM GA (M = 44.22, SD =3.01), p = 0.001, and 0.5 mM GA (M =37.66, SD =3.80), p = 0.011, but not 0.1 mM. The mean score for 0.1 mM GA (M = 29.14, SD = 3.27) was also significantly different from 1 mM GA (M = 29.14, SD = 3.27), p = 0.002, and borderline significant from 0.5 mM GA (M =37.66, SD = 3.80), p = 0.052.

Thus, the results show a statistical significantly change in the cell cycle distribution after GA-exposure with a prominent S-phase accumulation following 0.5 mM and 1 mM GA-exposure for 24 hours.

7.3.1 Cell cycle analysis with BrdU incorporation

Asynchronously proliferating GM00130C cells were cultured in the absence or presence of 0.5 mM GA, for 2, 4, 12 or 24 hours. Cells were pulse-labeled with BrdU during the last 60 min of treatment before being harvested at the indicated time points. Cells were stained with FITC-coupled anti-BrdU antibody and PI prior to flow cytometric analysis to determine BrdU incorporation and cell cycle distribution. The figure shows scatter plots with the log FITC anti-BrdU staining (FITC-A) versus PI staining (PI-A). From Figure 21, a GA-induced reduction in BrdU-incorporation was seen as a reduced FITC-staining of S-phase cells (measured at the y-axis), after 24 hours exposure time only. However, we did not observe a prominent accumulation of cells in S-phase as expected from the previous PI and flow cytometry analysis (Figure 18). Due to a low population of single cells detected in the 4 hours control, it is not an optimal representative figure of untreated cells at that time point. Unfortunately, due to methodological difficulties, the BrdU experiment could only be carried out successfully once.

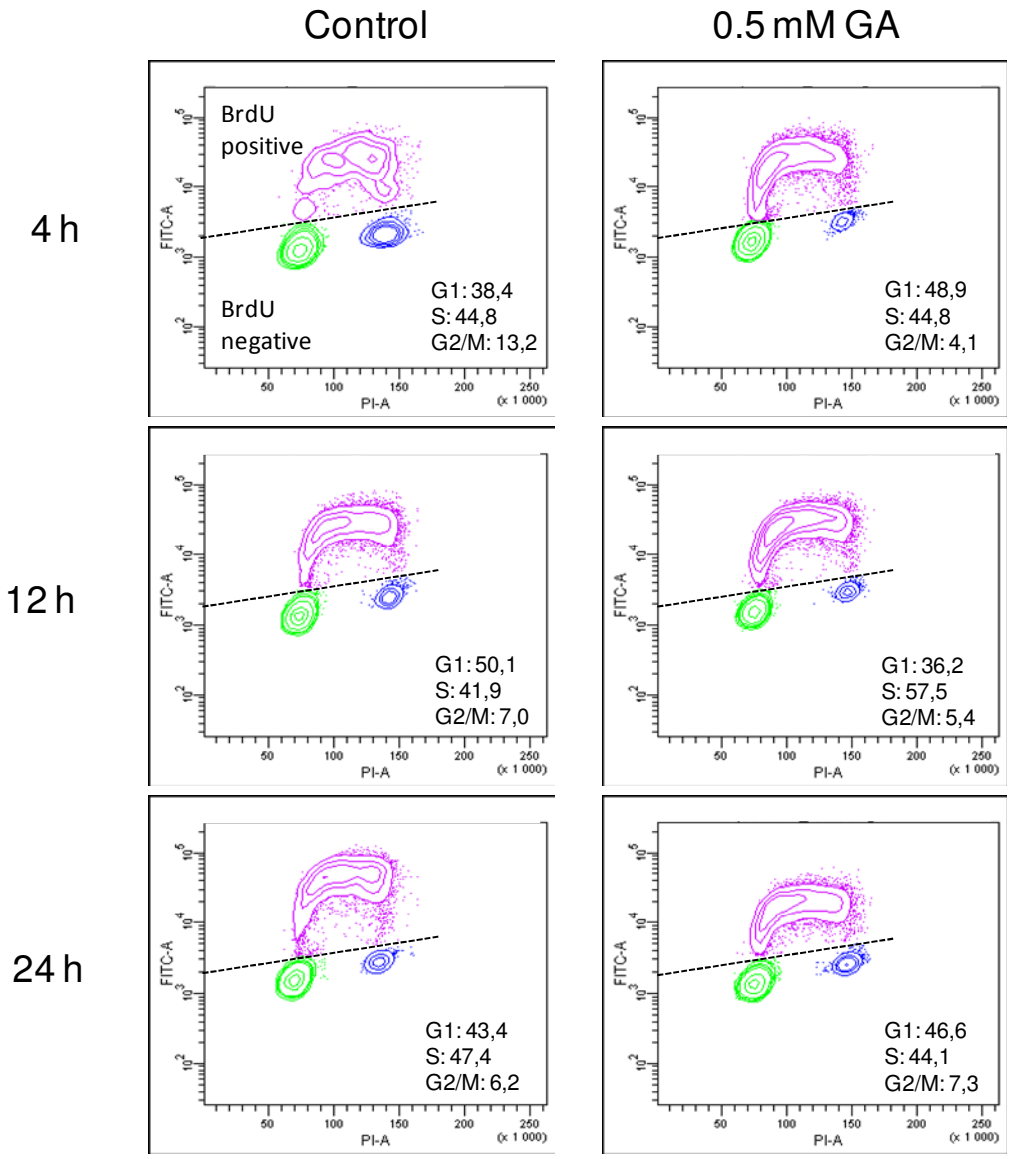

Figure 21: Level of BrdU incorporation following GA treatment.
GM00130C cells were treated with 0.5 mM GA and harvested at the respective time points following BrdU incorporation for 60 minutes. Cells were stained with FITC-coupled anti-BrdU antibody and PI and analyzed by flow cytometry as described in the method section. The figure shows contour plots with the log FITC anti-BrdU staining (FITC-A) versus PI staining (PI-A). The figure shows only gated populations for G_1 (green), S (purple) and G_2/M (blue). The area over the dotted line represents BrdU incorporated cells. The figure shows one experiment performed (n=1).

7.4 GA-induced phosphorylation and expression of p53

Genotoxic stress is shown to rapidly induce phosphorylation of serin 15 (ser 15) on p53 and also to increase protein expression of total p53 as described earlier (Shieh et al., 1997). GA induced changes in p53 level and activity was therefore explored.

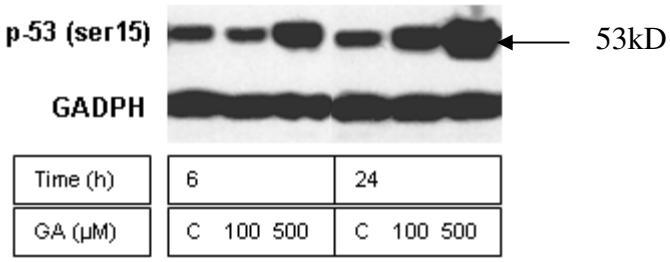

Figure 22: GA-induced phosphorylation on serin 15 of p53.
GM00130 cells were exposed to different concentrations of GA and cells were harvested at different time points. 25 µg of lysate was separated through an SDS-PAGE followed by immunoblotting (see Methods section) to detect phosphorylation of serin15 on p53. To check for equal loading of the samples, a GADPH antibody was used. One representative experiment out of three is shown (n = 3).

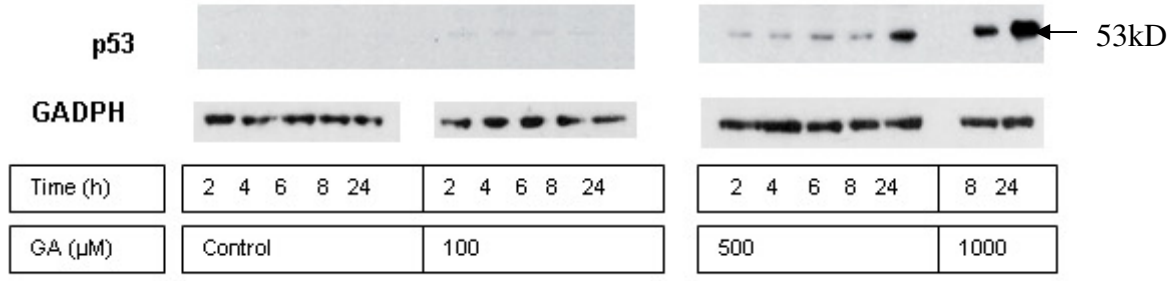

Figure 23: Upregulation of total p53 in response til GA exposure.
GM00130 cells were exposed to different concentrations of GA and cells were harvested at different time points. 25 µg of lysate was separated through an SDS-PAGE followed by immunoblotting (see Methods section) to detect the expression of p53. To check for equal loading of the samples, a GADPH antibody was used. One representative experiment is shown (n = 3).

Phosphorylation of p53 at Ser-15 was induced by GA exposure and was apparent after 6 hours exposure time with 0.5 mM GA (Figure 22, left). However after 24 hours a dose dependent increase in phosphorylation of p53 was seen starting from 0.1 mM GA (Figure 22, right). Total p53 was also increased after prolonged GA-exposure (Figure 23). Apparently, phosphorylation of p53 increases prior to total p53 upregulation, which appears in both a time- and dose dependent manner in response to GA exposure.

7.5 Protein expression of the CDK inhibitors, $p21^{CIP1}$ and $p27^{KIP1}$.

DNA damage very often leads to cell cycle arrest by inhibiting cell cycle dependent kinases (CDK) through the induction or translocation of the CDK inhibitors, $p21^{CIP1/WAF1}$ and $p27^{KIP1}$. We were particularly interested to see whether DNA damage induced by GA would lead to an upregulation of $p21^{CIP1/WAF1}$ as a consequence of the p53 activation and upregulation. We therefore studied the effect of GA on the protein expression of these inhibitors.

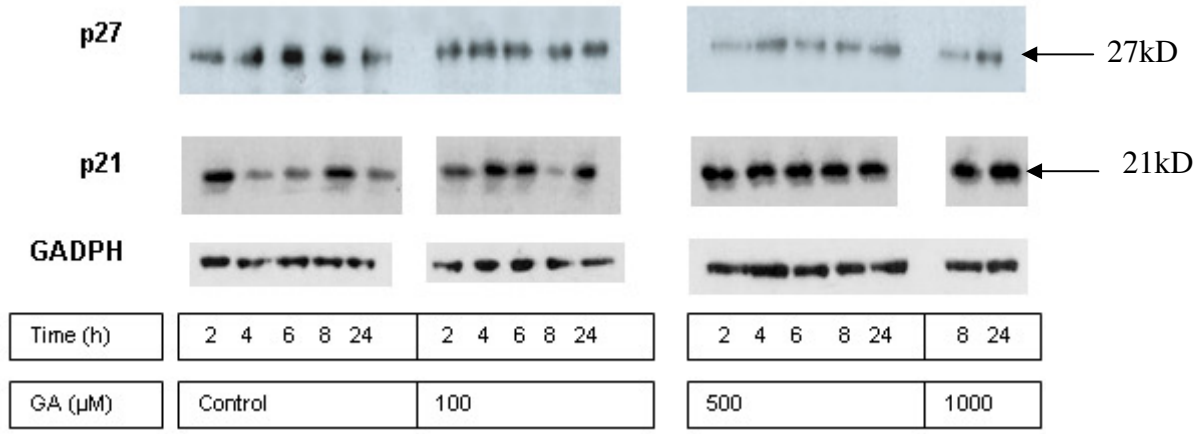

Figure 24: Protein expression of the CDK inhibitors $p21^{CIP1}$ or $p2^{KIP1}$ in response to GA exposure.
GM00130 cells were exposed to different concentrations of GA and cells were harvested at different time points. 45 µg of lysate was seperated through an SDS-PAGE followed by immunoblotting (see method section) to detect the expression of $p2^{KIP1}$ or $p21^{CIP1}$. To check for equal loading of the samples, a GADPH antibody was used. One representative experiment is shown (p21: n = 3, p27: n = 2)

The results show no upregulation of the $p27^{KIP1}$inhibitor at any exposure times or concentrations of GA, compared to the control. In the case of $p21^{CIP1/WAF1}$ a small induction of the protein was noted when a higher concentration of GA (0.5 mM and 1.0 mM) was used, although this expression did not increase in a clear time dependent manner (Figure 22). Due to the lack of a clear upregulation, we tested both a mono- and polyclonal antibody against $p21^{CIP1/WAF1}$ without any changes in the result. However, 0.5 mM GA treatment of PBL induced an upregulation of $p21^{CIP1/WAF1}$ at 2, 4 and 14 hours with 0.5 mM GA (data not shown).

7.5.1 Protein expression of cyclin A after GA-exposure

Cyclin D and E are important for the G1/S transition and cyclin A is especially needed for the passage through the S-phase (Maddika et al., 2007). Cyclins are the regulatory unit of the CDK enzymes and are rapidly up- or downregulated in response to mitogens. We therefore wanted to see whether the genotoxic stress after GA exposure leads to a change in protein expression of these cyclins. Cyclin A showed no downregulation after GA exposure, rather a small increase in protein expression occurred with higher concentrations of GA (Figure 25). However, no clear time dependent response was observed. Cyclin E and cyclin D was also tested, however the results were difficult to interpret due to high background with the Abs that we had in hand (data not shown).

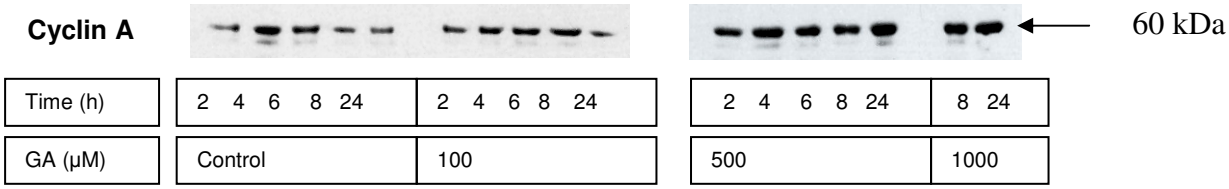

Figure 25: Protein expression of cyclin A in reponse to GA exposure. *GM00130 cells were exposed to different concentrations of GA and harvested at different time points. 25 µg of lysate was separated using SDS-PAGE followed by immunoblotting (see method section) to detect the expression of cyclin A. One representative experiment is shown (n = 2).*

7.5.2 Protein expression of the NER proteins, XPA and XPC, following GA-exposure

The NER-pathway is one of the most flexible DNA repair pathways, when looking at the diversity of DNA lesions it may act upon. The XPC protein is needed for DNA damage recognition in global genome repair of the NER pathway and XPA plays a crucial role in confirming correct assembly of the NER complex and in incision of the DNA damage. Previous results in our laboratory indicate a GA-induced upregulation of XPA, and to some extent XPC transcription by RT-PCR in the testicular germ cell tumor cell line 833K (data not shown). For this reason, using western blot analysis we examined wether GA induced any regulation of these repair proteins.

However, our preliminary data indicated that the GA concentrations used did not induce any noteworthy up- or down regulation of XPA (Figure 26) or XPC (Figure 27) proteins. However, only one experiment was performed. Even though it may look like an upregulation, this is caused by background on the film and the digitalization process. No notable increase in these proteins was noted, indicating that these NER proteins are not up- or downregulated in GM00130C cells in response to the GA concentrations and treatment periods used. Because of the limited experimental data, this interpretation should be taken with some caution.

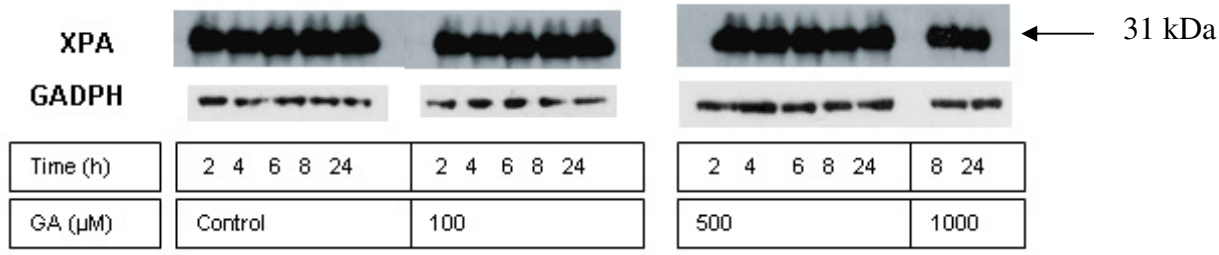

Figure 26: Protein expression of XPA in reponse to GA exposure
GM00130 cells were exposed to different concentrations of GA and harvested at different time points. 25 µg of lysate was separated through an SDS-PAGE followed by immunoblotting (see Methods section) to detect the level of expression of XPA. To check for equal loading of the samples, a GADPH antibody was used. Data from one experiment.

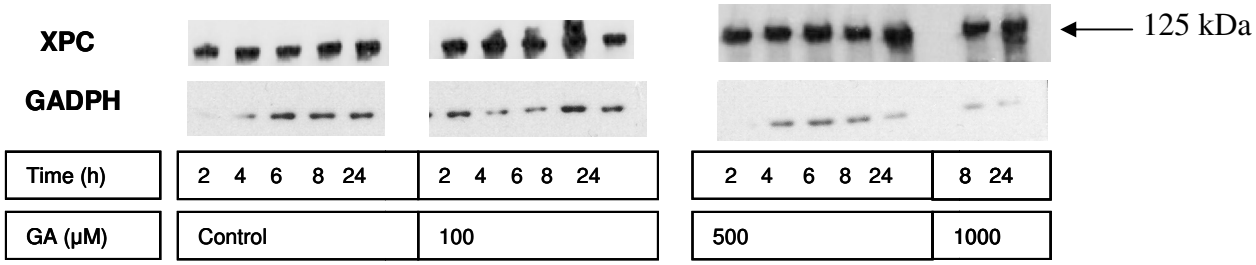

Figure 27: Protein expression of XPC in reponse to GA exposure
GM00130 cells were exposed to different concentrations of GA and harvested at different time points. 25 µg of lysate was separated through an SDS-PAGE followed by immunoblotting (see method section) to detect the level of expression of XPC. To check for equal loading of the samples, a GADPH antibody was used. Data from one experiment.Cell viability /Induction of Apoptosis

As observed by flow cytometry, an increase in apoptotic and/or necrotic cells was prominent after prolonged exposure to high concentrations of GA (Figure 18). Therefore a standard DNA staining assay of cells, visualized by fluorescent microscopy, was used to look for apoptotic and necrotic cells

7.6 Cell viability

Flow cytometric analysis of cell cycle revealed apoptotic behaviour, though apoptosis measurement with only PI staining does not give reliable results. Therefore, a cell viability assay based on morphological changes was conducted. As can be seen in Figure 28, GA concentrations of 0.5 mM and 1 mM induced apoptosis, but no necrosis, commencing already after 8 hours exposure. For exposure up to 6 hours, no significant induction of apoptosis was measured with this method. Figure 29 shows the typical morphology of apoptotic cells (bold arrow) and the red necrotic cells (thin arrow). Apoptotic cells include both regular apoptotic cells and apoptotic-necrotic cells (cells with condensed nuclei, and a compromised plasma membrane (PI positive) secondary to the apoptotic process)

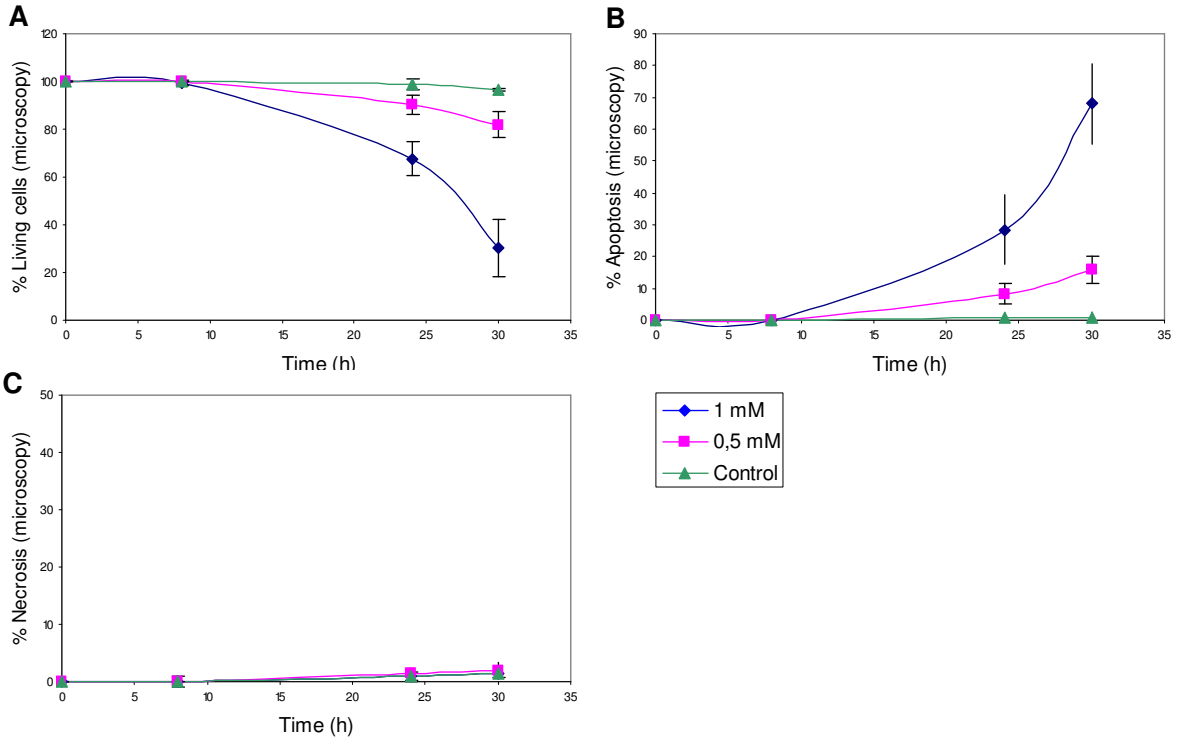

Figure 28: GA-induced cell death.
GM00130C cells were treated with 0.5, or 1 mM GA and harvested at the time points indicated. Cells were stained with Hoechst 33342 and PI and analyzed in a fluorescence microscope as described in the Methods section. Results are presented as % living cells (A), apoptotic cells (B) and necrotic cells (C). The data are means ± SD from 3 separate experiments (n=3).

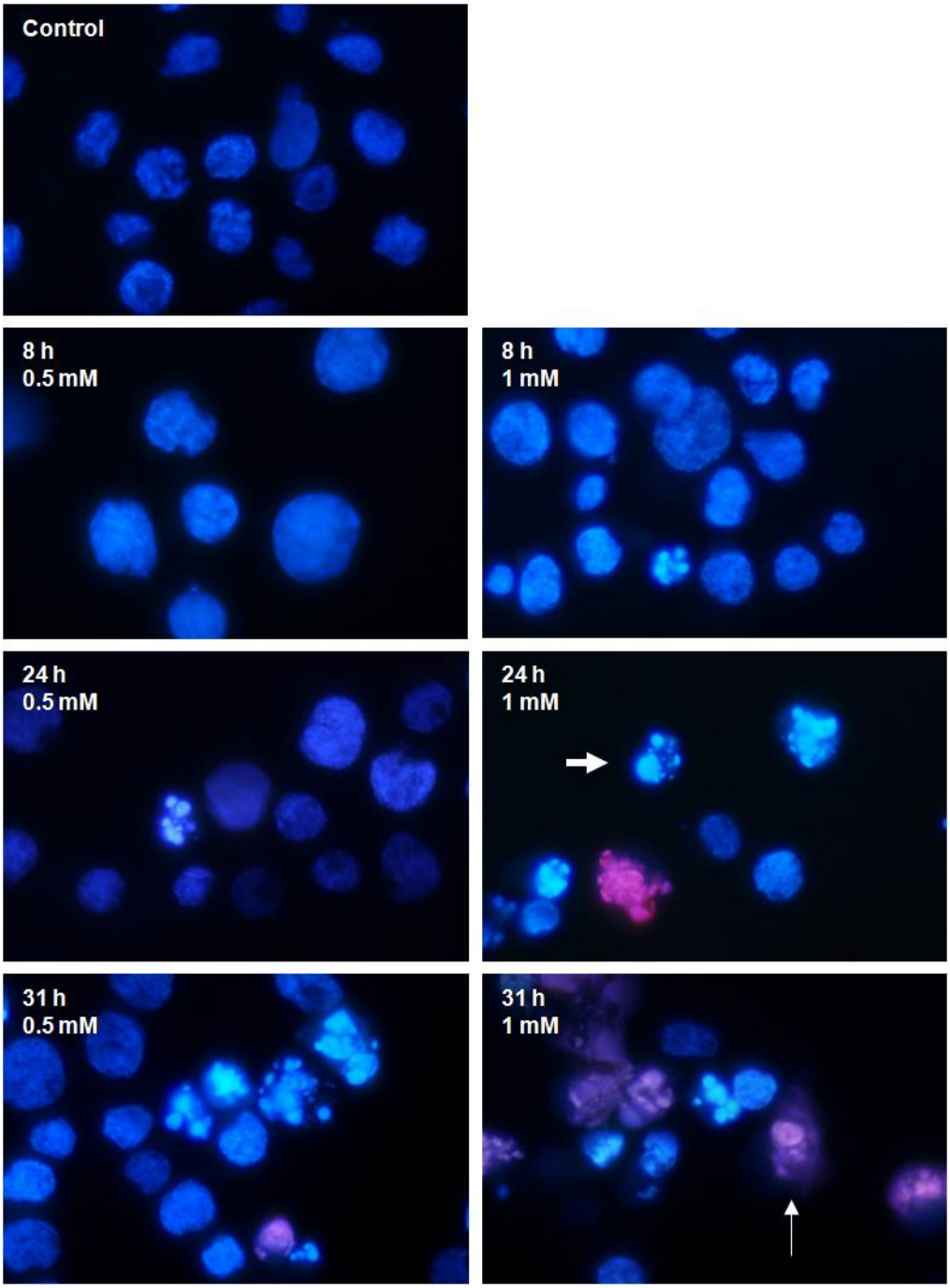

Figure 29: Effects of GA on cell morphology.
GM00130C cells treated with 0.5 mM and 1 mM GA for different hours as indicated. The cells are stained with Hoechst 33342 and PI and analyzed by fluroecense microscopy. Bold arrow indicate apoptotic cells, thin arrow indicate apoptotic-necrotic cells. The figure represent one representative experiment (n = 3). Magnification 400x with oil immersion.

8. Discussion:

8.1 Methodological considerations

8.1.1 An Epstein–Barr virus (EBV) immortilized B-cell, as a model system for stimulated normal human peripheral lymphocytes.

Lymphocytes are a convenient and easily available source for genotoxic studies, and as biomarkers. Though, they do possess limited lifetime, therefore are lymphoid cell lines convenient to use as a modelsystem. The EBV-transformed lymphoblastoid cell line, GM00130C, was chosen because of its availablility in the laboratory, and because of its apparent wild type (wt) features compared to stimulated lymphocytes. A further important reason for using this cell line was that our laboratory has previous experience with various types of lymphoblastoid cell lines, i.e. the same cell type but being isolated from patients with various types of deficiencies in the NER path for excision repair (XPA, XPC, CSB). As described in 5.5.2, we observed no clear indication that the NER pathway is involved in repair of GA-induced DNA damage. Furthermore, recently we obtained strong evidence that DNA glycosylases involved in BER are good candidates for repair of the DNA base changes that are induced by BER (Hansen, 2009). If this had not been so, and if the time frame of this thesis had allowed it, then the whole set of lymphoblastoid cell lines would have appeared to be highly useful for the study of effects of GA on cell-cycle.

Stimulation of PBL is a time consuming procedure and requires large amounts of donated blood, and the resulting cells can only be cultured for a limited time period. Working with cell lines has several advantages as described in the Methods section. However, since normal cell cycle regulation has been altered in immortalised cells, there are several important issues with this cell line that also need to be addressed and taken into consideration when interpreting the data. In addition, the cells are asynchronous in all experiments performed. The disadvantages of using asynchronous cells emerge when looking at discrete cell cycle alterations. Such alterations would have been more apparent if using synchronous cells, but they become masked due to the presences of cells in every cell cycle phase; this is particularly the case when studying weak responses in protein expression. Several of the common methods for cell

culture synchronization involve the use of pharmacological agents acting at various points throughout the cell cycle. This often leads to adverse cellular perturbations that may lead to false positive or negative results. Other methods for synchronizing cells involve less dramatic perturbations of the biological system, such as serum deprivation. However, due to time limitations, attempts to synchronize the cells were not performed.

Although the tumour virus EBV apparently drives cell proliferation by stimulation of B cell activation and growth programmes, rather than by subverting cell cycle regulatory mechanisms (Bornkamm and Hammerschmidt, 2001), there is some evidence that EBV latent proteins, such as EBNA3C and LMP1, can disrupt normal cell cycle control and even normal responsiveness to some DNA checkpoints, upon exposure to genotoxic drugs(Chen et al., 1998; Parker et al., 2000; Wade and Allday, 2000).

Apparently, EBNA3C is essential for growth transformation of primary B-lymphocytes *in vitro* and regulates a number of viral and cellular genes important for the immortalization process (Subramanian et al., 2002). The latent proteins have been suggested to facilitate cell survival by suppressing the apoptotic program in addition to continuous cell division (Chen et al., 1998). For instance, the EBV nuclear antigen, EBNA3C, has been shown to disrupt both G_1/S and G_2/M checkpoints (Allday et al., 1993; Allday and Farrell, 1994; Parker et al., 2000), enhance the kinase activity of the cyclin A/cdk2 complex, and regulate components of the SCF^{Skp2}E3 ubiquitin ligase complex (Knight et al., 2005; Knight and Robertson, 2004). EBNA3C have also been shown to complete the cell cycle in cells lacking mitogen signals from the external medium *in vitro*(Parker et al., 2000). Overall, it may indicate that these cells, to some extent, overcome or ignore normal DNA damage activated checkpoints, and that this may be the case in our studies as well. When discussing the results obtained from the GA-treated lymphoblastoid cell line these issues must be taken into consideration.

8.1.2 The Comet assay

The comet assay is a very sensitive and well established assay for genotoxic screening. In addition, it is an easy assay to run and can be performed at a low cost. However, there are a few shortcomings that need to be addressed, especially concerning scoring the comets and analysing the data. Especially one need to be certain that the DNA staining of the comets is

optimal and that the settings and configuration of the fluorescence microscope and programme to analyse the comets are optimized and not subject to change during scoring of one experiment. Even so, one may obtain both false positive and false negative results. False positive results, meaning too high DNA damage response in the comet assay, can be due to DNA degradation resulting from cell death, thereby reflecting secondary effect of a cytotoxic effects of a compound, and not genotoxicity *per se*. False negative results, meaning too low damage response, may be obtained if – which is particularly relevant for GA –the initial DNA lesion is not measurable in the traditional comet assay, i.e. does not lead to DNA strand breaks even at high pH. A negative result may also result if the GA-exposure is too short. Both cytotoxicity and induction of DNA damage may take some time to develop and may require prolonged exposure times. However, this situation was addressed by using a wide concentration range of GA and by exposing over a 24 hour time period. In general, false negative results may occur in *in* vitro toxicological experiments if the compound(s) involved are unstable under experimental conditions. With GA this was obviously not the case since the measured DNA damage was high all through the time course of the GA-exposure. To avoid degradation, GA was routinely prepared fresh and diluted in PBS shortly before being added to the cell cultures. In addition, loss of heavily damaged cells (apoptotic or necrotic) may occur during washing steps and therefore lead to less recorded damage or even false negative results.

8.1.3 Metabolizing AA with human S9 extract

In order to metabolise AA in our cell culture treatment we introduced a human liver S9-fraction during the exposure, which is standard procedure when using cell cultures with limited capacity for metabolic activation. However the results showed that the S9 fraction did not facilitate the DNA damaging effect of AA, instead it lead to a small decrease in the level of damage in the exposed samples. AA alone did not induce any significant increase in DNA damage compared the control even at 4 mM. The lack of DNA damaging effect of AA, even in combination with the S9 fraction for metabolic activation, is in accordance with previous experiments performed in our laboratory (Hansen, 2007; Sipinen, 2007).. The function of the S9 fraction was tested using human HPBL and benzo(a)pyrene (BaP) as a positive control, since the BaP- metabolite, benzo[*a*]pyrene -7,8-dihydrodiol-9,10-epoxide, has previously

been shown to induce DNA-damage detectable in the comet-assay in the presence of S9 (Speit et al., 1996), however no increased DNA-damaging effect was observed. The CYP2E1 activity is the main oxidative metabolic step of activation of AA into GA; however, the activity level of CYP2E1 in the commercial S9 preparation was unknown to us. A high GSH activity in S9 may also contribute to a rapid deactivation of GA.Segerbäck and coworkers tested AA together with an S-9 mix prepared from rats in the Ames test without any positive effect, which is in correspondence with our findings. They concluded that the amount of GA produced in microsomal suspensions with AA is insufficient to produce a statistically significant response (Segerback et al., 1995). Koyama et al (2006) tested AA together with rat liver S9 for cytotoxicity and genotoxicity without any influence on cytotoxicity or genotoxicity of AA, even up to 15 mM. On the other hand, an enhanced activity of N-*di*-N-butylnitrosamine (DBN), a positive control chemical, was seen with S9 (Koyama et al., 2006). In addition no GA-derived DNA adducts were found in cells treated with concentrations of 2-18 mM of AA and S9, consistent with a lack of metabolic conversion of AA to GA(Mei et al., 2008).

8.1.4 Cell cycle analysis by Flow cytometry

A major advantage of flow cytometry is that it offers the possibility of mulitparametric analysis of several cell attributes, including cell cycle position. In this way we were able to analyse whether GA-treatment lead to an accumulation of cells in a particular phase of the cell cycle by staining the DNA with PI/Hoechst in addition to a BrdU-staining in order to look at replicating cells in particular. In general one has to be aware of cell clumping during fixation of cells since doublets of G_1 cells may be falsely detected as a G_2/M, and cell aggregates in general may give high background noise during flow cytometric analysis.

The BrdU-staining procedure is a somewhat stringent procedure with many steps and incubations. Unfortunately we experienced problems with obtaining enough cells throughout the procedure. Different spinning procedures was attempted but without improvement. The source of error was sadly never revealed, therefore we had to continue only using PI staining.

In this study, GA-exposed cells seem to enter apoptosis or necrosis at high concentrations and long exposure times. The major drawback of flow cytometric methods is that the

identification of apoptotic or necrotic cells is not based on morphology and cannot be correlated with morphological characterization and therefore difficult to detect in a regular PI staining. Other methods must therefore be applied such as the TUNEL (Terminal Deoxynucleotide Transferase dUTP Nick End Labeling) assay where the amount of DNA fragmentation is detected. In addition, flow cytometric analysis of apoptosis, regardless of method used, is associated with selective loss of apoptotic cells during sample preparation. Morphological alterations were therefore examined with PI and Hoechst 342 staining in a fluorescent microscopy, which enables us to distinguish some of the different types of cell death as described it the method section.

Because of the difference between apoptotic and necrotic cells in plasma membrane integrity one can preincubate with a mixture of Dnase I and trypsin that results in total loss of necrotic and late apoptotic cells from the suspension due to lack of the ability to exclude these enzymes. Live and early apoptotic cells exclude these enzymes and remain in the suspension. Such treatment prior flow cytometry analysis ensures that only early apoptotic and live cells are analyzed (Darzynkiewicz et al., 1992). Hence, explaining whether the accumulation of cells in the S-phase area with 1 mM GA treatment for 24 or 31 hours is due to an arrest or perhaps an increase of apoptotic and even necrotic cells from late S or G_2/M.

8.1.5 Cell viability/Cell death

Many pathways leading to apoptosis exists, and DNA fragmentation and loss of DNA fragments is not a universal finding in apoptotic death. Necrotic cells may also display some degree of DNA degradation that may result in hypodiploid nuclei. The sub- G_1 peak can also represent nuclear fragments, chromosome clumps, micronuclei or nuclei with normal DNA (i.e., cells undergoing differentiation) (Darzynkiewicz et al., 2001). Therefore morphological analysis by microscopic observation of apoptotic bodies was performed. However, this method can be time consuming, lacking objectivity and reproducibility, and making it difficult to identify subtle changes in large populations. Thus, additional applications to detect apoptosis such as biochemical analysis by DNA ladder in agarose gel, or specific demonstration of DNA breaks such as in the TUNEL assay should be used to confirm apoptosis. One should also remember that apoptosis is a dynamic process and there is a short

”time window” during which apoptotic cells display their characteristic features. Therefore, different methods can produce different results depending on the time of the apoptotic process.

8.1.6 Western

Problems which may arise when detecting proteins on western blot include; fuzzy bands ,low signal, high background, spots on film, too many bands on the blot and weak signal.

We mainly experienced problems with too many non-specific bands on the film, making it difficult to analyse the protein of interest. This may be caused by old or poor primary antibody quality, or insufficient blocking. This can be optimised by testing different blocking procedures since dry non-fat milk or BSA may give different results, depending on the primary antibody. In addition to increase or decrease both incubation time and concentration of milk/BSA. Also, the recommended primary antibody concentration given by the datasheet is usually higher than necessary, resulting in unspecific binding, and therefore optimisation experiments need to be performed in order to determine the proper antibody dilutions.

Nonspecific signals due to weak antibody binding may be removed by increasing washing times and volumes. Using a stronger detergent in the washingbuffer than TBST may provide more stringent wash and reduce background. Though, only if the band is strong since washing also removes some of the band of interest.

Different protein/antibodies require different exposure time. Without experience with the protein of interest, and cell type one might overlook results due to lack of long enough exposure, since exposure time can be from seconds and up to a day (especially phosphor proteins). Low or weak signal may also be due to insufficient protein loaded on the gel, which often applies to small proteins. In order to concentrate the protein of interest, one might perform immunoprecipitation which concentrate a particular protein from the sample containing many different proteins.

8.2 Statistical analysis

All comet assay experiments were performed twice. To be able to perform proper statistical analysis, at least three independent experimental runs are necessary. Due to time constraints, this was not possible. Nonetheless, the data obtained in the two experimental runs are analyzed statistically to look for trends.

Comet data failed normality test and homogeneity of variance, which suggest the use of non-parametric tests. Duez *et al*. (2003) looked at the use of non-parametric test and found the tests to be overly sensitive, detecting significant, but objectively unimportant, differences. However this might be due to the erroneous use of the single comet to be the experimental unit which result in a very large n. Non-parametric tests of the comet data was attempted but, due to only two independent experiments statistical significance of obvious differences were not detected (data not shown). The 95% confidence intervals of the mean values were also examined and showed no overlap in the statistical significant exposures analyzed by ANOVA.

The experimental design is nested which can not be used in non-parametric tests. A possibility would have been to analyse the data with a parametric analysis of median values obtained in each gel, but this would lead to loss of information, as experiment and gel number can not be factors in this analysis. The power of this analysis would also be low. The distribution of the data is quite different in control and treatment groups with Fpg treatment and long exposure times and high concentrations of GA (0.5 mM) due to highly damaged cells which are left skewed while some damaged cells are right skewed. Non-parametric tests do not require normality, but similar distributions in all groups. Transformation of data using Log transformation could work on right skewed, but not left skewed, and might result in heterogeneity of variances (Lovell and Omori, 2008). ANOVA is thought to be robust enough to conduct with some differences in the variances, and with a minor violation of the normality (Lovell and Omori, 2008).

Effects size, using partial eta squared obtained from SPSS were evaluated with each ANOVA analysis, and gave a value above 0.8 at all cases. Partial eta squared effect size indicate the proportion of variance of the dependent variable that is explained by the independent variable, with values ranging from 0 to 1. Though, with a large enough sample, quite small differences

can become statistically significant, even if the difference between the groups is of little practical significance. The use of raw data in the comet analysis may have affected this value.

8.3 GA-induced DNA damage

We showed that AA exposure alone or together with the S9 extract did not lead to any increased DNA-damage even at high AA concentrations in the lymphoblastoid cell line as well as in normal human peripheral lymphocytes, when exposed for 2 hours. Apparently, Fpg-treatment did not detect any additional lesions either, indicating no induction of oxidative damage or ring opened structures recognised by Fpg after 2 hours AA exposure *in vitro*. The lack of damage response with AA in the comet assay is in contrast to studies by Blasiak and coworkers and Jiang and his group, who observed induced DNA damage with lower concentrations of AA in human lymphocytes and hepatoma cells, respectively (Blasiak et al., 2004; Jiang et al., 2007). Nevertheless, our results are in accordance with other studies where no or low observed DNA damaging effect of AA was observed (Baum et al., 2005; Koyama et al., 2006; Puppel et al., 2005). Therefore, AA seems to be only slightly genotoxic *in vitro* when analysed in the comet assay.

In addition, GA did not induce any significant increase in SSB or AP-sites at concentrations up to 0.5 mM GA following two hours exposure time as no increase in DNA damage was observed. Nevertheless, longer exposure periods with GA lead to an increase in GA-induced SSB and AP-sites. On the other hand, Fpg treatment induced high levels of DNA-damage even at very low GA concentrations (down to 0.05 mM GA) indicating either a high level of oxidative damage or ring opened structures, recognised by Fpg. Previous reports have shown that GA forms adducts directly with DNA and protein, making GA highly genotoxic (Gamboa da Costa et al., 2003; Ghanayem et al., 2005a; Segerback et al., 1995) Our results are in favour of previous *in vitro* observations that GA is the directly DNA reacting compound and that AA is rather inactive towards DNA (Baum et al., 2005; Koyama et al., 2006; Puppel et al., 2005).

8.3.1 GA induced DNA damage recognized by Fpg

Using Fpg highly increased the detection of GA-induced lesions as detected in the comet assay, both with the normal human lymphocytes and with the lymphoblastoid cell line. Fpg recognizes a variety of substrates, and excises preferentially 8-oxoG but also FaPy-G, FaPyA and methylated FaPyG (Me-FaPyG) (Asagoshi et al., 2000; Boiteux et al., 1984; Boiteux et al., 1992). This wide substrate affinity is in contrast to the more specific hOGG1 enzyme which has a high affinity for 8-oxoG although FaPy-G is also recognised (Asagoshi et al., 2000; Graves et al., 1992). Preliminary and very recent experiments in our laboratory comparing the Fpg enzyme with a commercial hOGG1-enzyme showed that hOGG1 gave nearly no GA-induced damage detection compared to Fpg (Hansen, 2009). This suggests that the Fpg-sensitive sites caused by GA exposure are not likely to represent oxidative damage. In these experiments, a photoactive compound (Ro 12-9786 plus visible light, inducing predominantly oxidated purines) was used as a positive control for the activity of the hOGG1 enzyme to recognise and cleave 8-oxoG. Nevertheless, based on the chemical properties of GA, it is not likely to cause significant levels of oxidative damage of the DNA. However, exposure to GA at high concentrations and for extended periods may lead to GSH depletion (Kurebayashi and Ohno, 2006)which in turn may lead to increased ROS formation and secondary oxidative effects.

Apparently, when exposing the cells to GA, the lysing procedure in the comet assay may affect the results when treating with the Fpg-enzyme. The standard procedure has previously been to lyse the cells for a minimum of 1.5 hours, to overnight. However, according to preliminary results in our laboratory when lysing GA-exposed cells overnight, a striking increase in Fpg-sensitive sites was noted (Hansen, 2009). This is believed to be caused by alkali catalyzed ring-opening of GA-adducts during lysis, (favoured during alkaline conditions, relative to depurination) (Gates et al., 2004) thereby increasing the number of ring-opened GA-lesions recognised by Fpg.

Since GA preferably forms N7-GA-Gua adducts (Gamboa da Costa et al., 2003) there may be a number of ring opened structures identified by Fpg. To address this problem, in each experiment the lysis conditions should be carefully controlled with respect to temperature,

duration and pH. Previous studies have also shown that Fpg detects DNA damage from other classical alkylated agents (Smith et al., 2006; Speit et al., 2004). Additionally, *in vivo* experiments with wild-type and the Ogg1-knockout mice showed minor differences in their repair capability of GA-induced damage (Hansen, 2009), further strengthening the hypothesis that the GA-induced DNA lesions are not oxidative. Rather, it seems that the DNA-damage caused by GA *in vitro* is mainly due to alkylated adducts and not oxidative lesions.

8.3.2 GA induced DNA adducts

It has been shown that the *in vitro* reaction of GA with DNA results in the formation of different adducts in the following order: N7-GA-Gua > N1-GA-dA > N3-GA-dA (Gamboa da Costa et al., 2003). Depurination of N7-alkyl-Gua and N3-alkyl-Ade, and the imidazole ring opening of N7-alkyl-Gua yielding Alkyl-Fapy-G are acid- and alkali-catalysed, respectively, but occur even at physiological conditions. Depurination is usually the predominant reaction observed for N7-alkylguanine residues in double stranded DNA under physiological conditions (Gates et al., 2004). Therefore, GA adducts may spontaneously depurinate in cells and form AP-sites which are converted into strand breaks. This may be the case when GA (0.5 mM) exposure was performed for 24 hours and high levels of DNA-damage without Fpg-treatment were observed. Otherwise they may transform into ring-opened GA-lesions, GA-FaPy-G during the alkaline lysis in the comet assay. Both AP sites and ring-opened lesions are recognised by the Fpg-enzyme and excised as previously described (Boiteux et al., 1984; Boiteux et al., 1987; Graves et al., 1992).

Both N7-GA-Gua and N3-GA-dA are promutagenic due to the spontaneous depurination (Gamboa da Costa et al., 2003; Segerback et al., 1995). The N7G and N3A adducts formed by binding of GA to DNA are not involved in the hydrogen bond basepairing region and therefore do not mispair during replication (as reviewed in Jenkins et al., 2005), but are prone to spontaneously formed AP sites (Besaratinia and Pfeifer, 2004). But the N3 atom is important in stabilising contact between the polymerase and the template (Engelward et al., 1998). N1-GA-dA adducts are also highly promutagenic because of the impaired base pairing potential (Gamboa da Costa et al., 2003; Segerback et al., 1995). The N3-alkylated adenine adducts are considerably more labile than those of the N7-guanines (Koskinen and Plna,

2000) Since AP sites and Alkyl-Fapy-G can persist in DNA for extended periods, they may have biological implications since these lesions are both mutagenic and cytotoxic (Chetsanga et al., 1982; Koskinen and Plna, 2000; O'Connor et al., 1988; Tudek, 2003).

The resulting GA-adduct density may influence the stability of adducts in dsDNA. Distortion of the DNA duplex in heavily adducted DNA may be responsible for the decreased stability as seen in the case of the Aflatoxin lesion (Gates et al., 2004). Thus in our case, the continuous exposure to GA over time (Figure 14), may lead to heavily adducted DNA which may further decrease the stability, since a large number of structures are excised by Fpg. For this reason, cells exposed to 1 mM GA for up to 31 hours are prone to exhibit apoptotic or necrotic behaviour as our results show.

The rate at which different N7-alkylguanine lesions undergo depurination from dsDNA varies widely, and is dependent of the structure of the substituent in the N7 position of guanine. The half-life of N7-GA-Gua in salmon testis DNA incubated with GA at 37˚C was determined to be 42 h, while the half-life of N3-GA-Ade was measured as 14 h, and increasing with lower temperatures (Gamboa da Costa et al., 2003). Even though N3-Ade adducts typically undergo spontaneous depurination of DNA at higher rates than N7-Gua adducts (Koskinen and Plna, 2000) they can also block transcription which can lead to sister chromatid exchange and S-phase arrest (Engelward et al., 1998). Therefore, a possible depurination of N3-Ade adducts due to the continuous GA-exposure may occur in great numbers and contribute to the apparent S-phase accumulation observed with 0.5 mM and 1 mM GA and 24 hours exposure time.

8.4 Repair of GA-induced DNA-damage

The GA-induced DNA damage detected by Fpg was apparently subjective to repair. The high level of damage obtained with Fpg treatment in the comet assay saturated the system and made it more difficult to measure and calculate the repair-kinetics of Fpg sensitive sites. However there was a marked reduction over time both with and without Fpg treatment implying a repair of strand breaks, ALS and the Fpg-sensitive sites in lymphoid cells. The repair of GA-lesions has according to Johansson et al 2005 been associated with the small

patch BER pathway (Johansson et al., 2005), although this has never been disproven or confirmed by others. However, the fact that Fpg recognises the GA-induced lesions supports this notion. Further, DNA glycosylases in the BER pathway, such as Fpg, are involved in repairing alkylated DNA by the removal and replacement of alkylated bases (Frosina et al., 1996; Petermann et al., 2003). This is especially important for the N7G and N3A adducts (Jenkins et al., 2005).

Previous results in our laboratory indicated a GA-induced upregulation of XPA, and to some extent XPC transcription by RT-PCR in the testicular germ cell tumor cell line 833K (data not shown). For this reason we examined whether GA induced any changes in the expression of these repair proteins by western blot analysis. However, neither XPA nor XPC, two of the enzymes responsible for damage detection and initiation of DNA damage repair in NER, showed any protein upregulation. This does not exclude the possibility that NER is involved in repair of GA-induced DNA damage. However, based on the Fpg-comet observations, we interprete our preliminary results as suggesting little or no contribution of NER in the repair of GA-induced DNA lesions. Taken together, our results support the involvement of a short patch BER-pathway in the repair of GA-induced DNA lesions. On the other hand, we can not exclude the possibility that other repair pathways are induced additionally, especially when higher GA-concentrations are used. For instance, HR may be involved when high numbers of SSB are induced by exposing to high GA-concentrations over time, which my lead to DSB.

Once BER is initiated, damage-specific glycosylases give rise to accumulation intermediates that can cause a partial or complete block to replication fork progression possibly inducing fork regression(Sobol et al., 2003). We observed an accumulation of cells in S-phase (high exposure <8 hours) and a seemingly reduced DNA-replication, and the former mechanism may be an explanation to these observations. Further, if the BER pathway is initiated during continuous GA-exposure, this might lead to an accumulation of BER intermediates that in combination with the adducts, AP sites and potentially Fapy lesions leads to cell death with high GA-exposures as observed.

8.5 Biological consequences of GA-induced lesions

Proliferating cells in G_1 or G_2 phases may respond to genotoxic stress by activating checkpoints that impose shorter or lasting arrest in G_1 or G_2 before they enter S phase or M phase, respectively. In contrast, cells that experience genotoxic stress during DNA replication will only delay their progression through S phase in a transient manner, and if damage is not repaired during this delay they exit S phase and should arrest later when reaching the G_2 checkpoint (Bartek et al., 2004). The mammalian S phase checkpoints are thought to only have a minor role, compared to the more robust G_1 and G_2 checkpoints. The S phase is the most vulnerable period of the cell cycle, and protecting the integrity of the genome during this critical phase is important. Though DNA damaging insult during this period have more repair opportunities than in the G_1-phase (Bartek et al., 2004).

It has been published that AA and GA can inhibit the microtubule-depolymerizing kinesin leading to failure of the migration of chromosomes from the metaphase plate and reduced mitotic activity (Adler et al., 1993; Gassner and Adler, 1996). However, our results did not indicate any accumulation in the G_2/M phase by GA which one might expect. We did not test AA effect on cell cycle, such an experiment might have revealed some more insight on this matter. It is probable that inhibition of kinesin involved in the mitotic/meotic spindle is related to blocks in cell division by AA and/or GA (Sickles et al., 2007) However we did not investigate direct effects on kinesins, but we observed transient arrest in S-phase rather than G_2/M and may only speculate if this effect might have be caused by kinesin-effects in our experiments.

8.5.1 GA-induced S-phase arrest and apoptosis

N1-GA-Ade and N3-GA-Ade may serve as a block to DNA synthesis (Boiteux et al., 1984; Engelward et al., 1998; Singer, 1975). Inhibition of DNA synthesis by Fapy-7MeG is stronger than that of 8-oxoG, but weaker than that of AP site (Tudek, 2003). The extensison step constitutes a major kinetic barrier to DNA synthesis, and thus DNA polymerase incorporates nucleotide opposite Fapy-7MeG and stops. FapyA and Fapy-7MeA also possesses miscoding potential. Though, Fapy lesions are actively eliminated by repair glycosylases, specific for oxidized purines and pyrimidines (Tudek, 2003). GA adducts and secondary lesions therefore

possess the potential to inhibit DNA replication, however we do not know the amount of adduct, Fapy lesions or AP sites that may be present. However, Fapy lesions are not likely the most prominent lesion since it is preferentially formed under alkali conditions. 8-oxo-G is also not likely to be present in high amounts due to low levels of oxidative damage detected with hOGG1 enzyme in the comet assay (Hansen, 2009). Therefore, due to the fact that it has been shown that the *in vitro* reaction of GA with DNA forms adduct in the following order: N7-GA-Gua > N1-GA-dA > N3-GA-dA (Gamboa da Costa et al., 2003) there might be a large number of adducts with long exposure duration, that has DNA synthesis block property due to possibly depurination of N7-GA-Gua and replication block by N1-GA-Gua and N3-GA-Gua. In addition to possible BER intermediates, leading to replication block that with high exposure becomes overwhelming for the cell and leads to apoptosis.

0.1 mM GA did not seem to induce any typical arrest behaviour at any of the cell cycle phases for up to 24 hours exposure time when analyzed with PI staining and flow cytometry. Though, preliminary results indicated a small accumulation between G_1 and early S phase with GA exposure of 0.3 mM after 72 hours (results not shown). Further, with BrdU incorporation, the major S-phase population of cells after GA-exposure indicated a reduction in both PI- and FITC-staining, shown in Figure 21. Thus, the reduced BrdU-incorporation at 24 hours and maybe even at 12 hours, indicates a lower replication rate induced by GA. The number of cells residing in S-phase increased prominently after 24 hours exposure time, while the number of cells in G_1 decreased, implying that the cells are arrested in early S- phase. However it is important to point out that this assumption is only based on one experiment, and variations may apply. Unfortunately we experienced difficulties with the BrdU-incorporation method, which is a more sensitive method to visualize more discrete alterations in the different cell cycle phases, especially the S-phase. Therefore, transient arrests may have occurred, which was not detectable with the PI-staining method used. Therefore, BrdU-incorporation with both low and high GA-concentrations and with different exposure times up to 24 hours would maybe reveal new insight into the actions of GA on cell cycle.

However, at 24 hours the 0.5 mM and 1 mM GA exposure with PI staining had induced significant amounts of apoptosis. This was markedly increased after 31 hours exposure time, implying that the DNA damage caused by GA at these concentrations is lethal. No time points

between 8 and 24 hours in the cell viability assay were tested (Figure 28), making it difficult to state the onset of apoptosis in our assay. However, after 30 hours, a large amount of apoptotic-necrotic cells appeared when high GA concentrations were used, implying that a large number of cells become apoptotic at an earlier stage. It is noteworthy that we did not see a more prominent arrest in any of the cell cycle phases after cells were exposed to low GA concentrations, in order to attempt DNA repair. For instance, no arrest in the G_1-phase after GA-exposure was detected. Rather, the cells were able to continue cell cycle even with high numbers of Fpg-sensitive lesions. The cells may be able to rapidly repair these lesions without disturbing the cell cycle, for instance with short-patch BER. In addition, since the cell line used may have malfunctional checkpoints and may override the GA-induced lesions, the next step would therefore be to test GA-exposure on normal stimulated human lymphocytes.

The comet assay shows a sustained saturation in Fpg sensitive sites when exposing the lymphoid cells to 0.1 mM GA starting at 6 hours exposure time. This does not seem to affect cell cycle regulation but induces phosphorylation of p53 at serine 15, and an up-regulation of total p53. Activation of p53 is normally associated with DNA repair, cell cycle arrest and apoptosis (Vazquez et al., 2008). The lack of cell cycle responses to the high levels of Fpg-sensitive sites seen at lower GA concentrations may imply that these lesions are repaired without the need for cell cycle arrest or ignored by the cell system used, as already mentioned.

The high levels of DNA damage seen with 0.5 mM GA after 24 hours exposure time without Fpg-treatment implies high levels of SSB and AP-sites. These high levels of Fpg-independent lesions may be responsible for the apoptosis observed. It has been shown that chromosomal SSBs can, if not repaired rapidly, block DNA replication forks during the S-phase of the cell cycle, possibly leading to the formation of DSB (Kuzminov, 2001). Even though this type of DSB is rapidly repaired by homologous recombination (HR), an acute increase in cellular SSB levels might saturate this pathway, leading to genetic instability and/or cell death (Kuzminov, 2001).

8.5.2 Regulation of cyclin A following GA-exposure

Since cyclin A is especially needed for the passage through S-phase (S. Maddika et al., 2007) we would expect a decrease in cyclin A level after GA-exposure and the observed S-phase

arrest. Nevertheless, cyclin A showed no down regulation after GA exposure at any time points, rather a small increase in protein expression with higher concentrations of GA. We can of course not exclude the fact that the kinase activity of the cyclinA/cdk2 complex was reduced by i.e. binding of a CDK inhibitor, or modified by phosphorylation/dephosphorylation events. The slight induction of $p21^{CIP1}$ observed after GA-treatment might be sufficient to inhibit CDK2/cyclin A activity. In addition, $p21^{CIP1}$ may be translocated from the cytoplasm to the nucleus and thereby able to inhibit CDK2 without any observed up regulation of the inhibitor protein, $p21^{CIP1}$, on the western blot. A CDK2/cyclin A kinase activity assay or a co-precipitation experiment with $p21^{CIP1}$ -CDK2/cyclinA would be an appropriate assay to perform to evaluate this. On the other hand, the overexpression of the EBV-protein EBNA3C may result in constitutive cyclin A-overexpression and kinase activity (Knight and Robertson, 2004) which may mask any effect of GA on cyclin A and might explain why we do not see any down regulation. Cyclin E and cyclin D was also tested, however the results were difficult to interpret due to high background on the immunoblot with the Abs that we had in hand (data not shown).

8.5.3 Regulation of p53 and $p21^{CIP1}$ following GA-exposure

While cell-cycle arrest depends on the ability of p53 to induce the transcription of target genes such as the CDK inhibitor $p21^{CIP1}$ (W. S. El-Deiry et al., 1993), apoptosis depends on induction of a distinct class of target genes.

We observed that GA induced a stress response leading to a phosphorylation on serine15 of p53. The ser15-phosphorylation increased in a both time and dose dependent manner. This phosphorylation stabilizes p53 (Lavin and Gueven, 2006). When detecting the protein level of total p53 an increase following phosphorylation was observed which is in accordance with the literature. Increased p53 levels have several downstream effects such as cell cycle arrest, repair or apoptosis. In our case, increased p53 as a result of GA-exposure may have resulted in the induction of $p21^{CIP1}$ protein expression. This pathway has been described in several other genotoxic studies (M. Mahyar-Roemer et al., 2001,D. L. Persons et al., 2000). A small induction of $p21^{CIP1}$ protein in GM00130C was noted with higher concentrations of GA (0.5 mM and 1.0 mM) used. We expected a much more prominent induction of $p21^{CIP1}$ and also a

time dependent induction of $p21^{CIP1}$ following p53-phosphorylation and expression. In general, upon DNA damage induction, the protein ATM is recruited to DSBs, and phosphorylate proteins such as p53 leading to the stabilization of p53 and further $p21^{CIP1}$ induction (as reviewed in Kurz and Lees-Miller, 2004). Due to the lack of a clear upregulation of $p21^{CIP1}$, we tested both a mono- and polyclonal antibody against $p21^{CIP1}$ without any changes in the result. However, preliminary results using normal PBL showed that 0.5 mM GA exposure induced a more pronounced upregulation of $p21^{CIP1}$ already at 2, 4 and 14 hours (data not shown). The different $p21^{CIP1}$ responses in PBL and GM00130C may be caused by actions of latent EBV in GM00130 which have been reported to inhibit $p21^{CIP1}$ accumulation (J. O'Nions et al., 2003,L. S. Young et al., 2003). Further, several studies have established that EBNA3C have potential inhibitory effects on p53 functional activities (Yi et al., 2009). According to the authors, this include repression of p53 mediated transactivation, due to binding of EBNA3C to p53 (Yi et al., 2009). This could, for example, have an effect on $p21^{CIP1}$ expression since we do not see any clear upregulation of $p21^{CIP1}$ or a G_1 arrest in GM00130C.

The genotoxic drug cisplatin, which generates DNA adducts and triggers the ATM-p53-$p21^{CIP1}$ response (S. L. Colton et al., 2006), was used to trigger checkpoints on proliferating B-blast infected with EBV. Latent EBV did not appear to affect the activity of p53 but rather downstream of p53 and interfered with the regulation $p21^{CIP1}$. By preventing the accumulation of $p21^{CIP1}$ it appears to prevent the inactivation of CDK2, and therefore DNA replication continued instead of being inhibited (O'Nions and Allday, 2003). p53 does not seem to be affected by EBV in our case either, but a downstream effect is highly likely since $p21^{CIP1}$ and $p27^{KIP1}$does not appear to be significantly regulated despite the high level of GA-induced DNA damage. How EBV actually may prevent the accumulation of $p21^{CIP1}$ is not fully clear. Never the less, since there is an observed increase in the level of $p21^{CIP1}$ mRNAs, it is possible that there is a block to its translation (O'Nions and Allday, 2003). Another explanation to the lack of accumulation could be that EBV direct the degradation of this newly synthesized by acting on either $p21^{CIP1}$ or CDK2 in a way that prevents $p21^{CIP1}$ from forming complexes with CDK2 and therefore exposing it for degradation by the proteasome. Alternatively, EBV may increase the access to or affinity of $p21^{CIP1}$ for proteasomes (J. O'Nions et al., 2003,L. S. Young et al., 2003) which leads to degradation. Cells with

insufficient $p21^{ClP1}$ to exert an antiproliferative effect are highly prone to apoptosis when their genome is severely damaged. This could be related to altered repair capacity, since $p21^{CIP1}$ have been reported to be involved in different forms of repair (Gartel and Tyner, 2002).

A dose and time dependent apoptotic response was observed, but no G_1 arrest. However we did see an accumulation in S-phase together with apoptosis when cells were exposed to high concentrations of GA over time. Reports have shown that $p21^{CIP1}$ can inhibit as well as induce apoptosis. The anti- or pro-apoptotic character of $p21^{CIP1}$ partly depends on its subcellular localization (Gartel and Tyner, 2002). Nuclear localized $p21^{CIP1}$ have shown to be pro-apoptotic, whereas cytosolic localized $p21^{CIP1}$ has anti-apoptotic properties (Coqueret, 2003). $p21^{CIP1}$ may therefore have performed apoptotic actions which are not visible to us without checking the subcellular localization of $p21^{CIP1}$ i.e. using immuno fluorescence microscopy techniques. Another possibility may be EBV latent genes affecting $p21^{CIP1}$. These genes, if affecting $p21^{CIP1}$ actions, may disrupt the G_1 checkpoint that otherwise might have been triggered by GA, which make the cells prone for apoptosis. This could have been examined by exposing our cells to genotoxic drugs known to initiate a G_1 arrest, but was not performed due to time limitations.

8.5.4 Regulation of p27 following GA exposure

As already mentioned in the introduction, anti-mitogenic signals result in an increased $p27^{KIP1}$level (J. Vervoorts et al., 2008,Z. Wang et al., 2003) and that $p27^{KIP1}$ is involved in the induction of apoptosis when overexpressed (Vervoorts and Luscher, 2008). However, no upregulation in the protein content of $p27^{KIP1}$ was observed at any exposure times or concentrations of GA used, when compared to the control. This may again be due to the EBV latent gene EBNA3C shown to inhibit accumulation of $p27^{KIP1}$ similar to $p21^{CIP1}$ inhibition (Knight and Robertson, 2004). This inhibition might be achieved through the reqruitment of SCF^{Skp2} E3 ligase complex activity to cyclin A complexes by EBNA3C which results in ubiquitination and SCF^{Skp2} dependent degradation of $p27^{KIP1}$or destabilisation (as reviewed in J. S. Knight et al., 2004,J. S. Knight et al., 2005). Also, EBNA3C have shown to overcome the restriction checkpoint that causes cells to arrest in G_1 of the cell cycle in reduced serum. This failure to respond to normal anti-proliferative signals is consistent with the

demonstration of failed $p27^{KIP1}$accumulation when mitogens are withdrawn (G. A. Parker et al., 2000).

To exert its CDK inhibitory functions, $p27^{KIP1}$ is required to be localized to the nucleus by phosorylation events of its nuclear localization signal (NLS) (as reviewed in Denicourt and Dowdy, 2004). In quiescent normal cells, $p27^{KIP1}$ is nuclear. Then in early G_1, $p27^{KIP1}$ export may be required to support assembly and nuclear import of newly translated D-type cyclins and Cdks. Both $p27^{KIP1}$ and $p21^{CIP1}$ facilitate assembly of D-type cyclin complexes *in vitro* and *in vivo* and direct nuclear import (Chu et al., 2008). Since the activated form of CDK2 is located in the nucleus (Dietrich et al., 1997), only the nuclear forms of Cip/Kip proteins could be considered as CDK inhibitors. However $p21^{CIP1}$ and $p27^{KIP1}$ are also located in the cytoplasm where they even activate D-type complexes through an enhanced association and nuclear accumulation (as reviewed in Coqueret, 2003). Therefore, a study of the sub cellular localization of $p21^{WAF1}$ and $p27^{KIP1}$in accordance with cell cycle arrest and apoptosis would be of great interest in order to clarify their roles in cell cycle arrest, repair and apoptosis. In addition we could maybe exclude or verify if in fact the EBV latent genes have affected a normal response of $p21^{WAF1}$ and $p27^{KIP1}$ to GA exposure of GM00130.

9. Conclusions and future work

In summary, we found GA to be highly genotoxic at relatively low levels. However, although we were able to measure high levels of Fpg-sensitive sites after exposure to low concentration of GA *in vitro,* no effect on the cell cycle of the lymphoblastoid cell line was observed. Nevertheless, genotoxic stress response such as phosphorylation of p53 and a small induction of $p21^{CIP1}$ was observed. On the other hand, higher concentration of GA (0.5 mM – 1 mM) resulted in a putative halt in the DNA-replication and an accumulation of cells in S-phase together with an increased apoptotic progression. Therefore, it seems that the EBV-transformed cells are able to overcome or ignore the initial Fpg-recognised lesions induced by GA. When higher levels of strand breaks are introduced with increasing GA-concentrations, the cells eventually undergo apoptosis.

Since several studies indicate an EBV-mediated interference with regular stress responses as already discussed, it may be that the latent EBV in our cell system affects the B-blasts from GA-induced stress responses. Therefore, further studies using stimulated normal PBL are highly relevant in order to confirm or compare the responses observed with GA-induced genotoxic stress on GM00130C cell cycle. In this way we may able to explore whether the EBV latent viral genes are affecting important DNA damage checkpoints in our system. In addition, it will be important to establish how normal lymphoid cell cycle responds to low levels of GA. If lymphoid cells in general are able to ignore low levels of GA-induced lesions without triggering a sufficient repair process, it may eventually lead to an accumulation of mutations in the cell and eventually lead to cancerous development over time.

In addition, further studies to reveal what type of lesions GA induces will be important to explore in order to understand the mechanisms by which these lesions are repaired and dealt with by the cell. There are already good indications in our laboratory that the hOGG1 does not recognise GA-induced lesions and thus no induced oxidative damage such as 8-oxo-G. Therefore, further analysis to reveal the amount of the different GA-adducts introduced will be important, especially in connection with cell cycle arrest.

Additionally we may take advantage of the different NER defective cell lines available in our laboratory in order to reveal whether this repair pathway is involved or not. If GA-induced lesions are repaired less efficient in these defective cell lines, the NER-pathway may well be involved and vice versa.

The GA concentrations used in this thesis is much higher than what an average person is exposed to on a daily basis. The general belief regarding toxicity of AA dietary intake is not alarmingly, though there is an increasing awareness regarding genotoxic compounds in food, which in the case of AA, is quite popular; coffee, chicken, crisp bread and chips. GA-induced adducts has shown to have a relative long half-life, and may therefore lead to accumulation with continuous dietary exposure. With the observed cell DNA damage, cycle alterations and the induction of p53 there is potentially risk of carcinogenesis and therefore more knowledge is important.

References

Adler, I.D., Zouh, R., and Schmid, E. (1993). Perturbation of cell division by acrylamide in vitro and in vivo. Mutat. Res 301, 249-254.

Allday, M.J., Crawford, D.H., and Thomas, J.A. (1993). Epstein-Barr virus (EBV) nuclear antigen 6 induces expression of the EBV latent membrane protein and an activated phenotype in Raji cells. J Gen. Virol. 74 (Pt 3), 361-369.

Allday, M.J., and Farrell, P.J. (1994). Epstein-Barr virus nuclear antigen EBNA3C/6 expression maintains the level of latent membrane protein 1 in G1-arrested cells. J Virol. 68, 3491-3498.

Asagoshi, K., Yamada, T., Terato, H., Ohyama, Y., Monden, Y., Arai, T., Nishimura, S., Aburatani, H., Lindahl, T., and Ide, H. (2000). Distinct repair activities of human 7,8-dihydro-8-oxoguanine DNA glycosylase and formamidopyrimidine DNA glycosylase for formamidopyrimidine and 7,8-dihydro-8-oxoguanine. J Biol Chem. 275, 4956-4964.

Azqueta, A., Shaposhnikov, S., and Collins, A.R. (2008). DNA oxidation: Investigating its key role in environmental mutagenesis with the comet assay. Mutat. Res.

Bartek, J., Lukas, C., and Lukas, J. (2004). Checking on DNA damage in S phase. Nat Rev. Mol. Cell Biol 5, 792-804.

Baum, M., Fauth, E., Fritzen, S., Herrmann, A., Mertes, P., Merz, K., Rudolphi, M., Zankl, H., and Eisenbrand, G. (2005). Acrylamide and glycidamide: genotoxic effects in V79-cells and human blood. Mutat. Res 580, 61-69.

Besaratinia, A., and Pfeifer, G.P. (2004). Genotoxicity of acrylamide and glycidamide. J Natl. Cancer Inst. 96, 1023-1029.

Blasiak, J., Gloc, E., Wozniak, K., and Czechowska, A. (2004). Genotoxicity of acrylamide in human lymphocytes. Chem. Biol Interact. 149, 137-149.

Boiteux, S., Belleney, J., Roques, B.P., and Laval, J. (1984). Two rotameric forms of open ring 7-methylguanine are present in alkylated polynucleotides. Nucleic Acids Res 12, 5429-5439.

Boiteux, S., Gajewski, E., Laval, J., and Dizdaroglu, M. (1992). Substrate specificity of the Escherichia coli Fpg protein (formamidopyrimidine-DNA glycosylase): excision of purine lesions in DNA produced by ionizing radiation or photosensitization. Biochemistry 31, 106-110.

Boiteux, S., O'Connor, T.R., and Laval, J. (1987). Formamidopyrimidine-DNA glycosylase of Escherichia coli: cloning and sequencing of the fpg structural gene and overproduction of the protein. EMBO J 6, 3177-3183.

Bornkamm, G.W., and Hammerschmidt, W. (2001). Molecular virology of Epstein-Barr virus. Philos. Trans. R. Soc. Lond B Biol Sci. 356, 437-459.

Cann, K.L., and Hicks, G.G. (2007). Regulation of the cellular DNA double-strand break response. Biochem. Cell Biol. 85, 663-674.

Cavalieri, E., Frenkel, K., Liehr, J.G., Rogan, E., and Roy, D. (2000). Estrogens as endogenous genotoxic agents--DNA adducts and mutations. J Natl. Cancer Inst. Monogr, 75-93.

Chen, W., Huang, S., and Cooper, N.R. (1998). Levels of p53 in Epstein-Barr virus-infected cells determine cell fate: apoptosis, cell cycle arrest at the G1/S boundary without apoptosis, cell cycle arrest at the G2/M boundary without apoptosis, or unrestricted proliferation. Virology 251, 217-226.

Chetsanga, C.J., Bearie, B., and Makaroff, C. (1982). Alkaline opening of imidazole ring of 7-methylguanosine. 1. Analysis of the resulting pyrimidine derivatives. Chem. Biol Interact. 41, 217-233.

Chu, I.M., Hengst, L., and Slingerland, J.M. (2008). The Cdk inhibitor p27 in human cancer: prognostic potential and relevance to anticancer therapy. Nat Rev. Cancer 8, 253-267.

Coller, H.A., Grandori, C., Tamayo, P., Colbert, T., Lander, E.S., Eisenman, R.N., and Golub, T.R. (2000). Expression analysis with oligonucleotide microarrays reveals that MYC regulates genes involved in growth, cell cycle, signaling, and adhesion. Proc. Natl. Acad. Sci. U. S. A 97, 3260-3265.

Collins, A.R., Dobson, V.L., Dusinska, M., Kennedy, G., and Stetina, R. (1997). The comet assay: what can it really tell us? Mutat. Res 375, 183-193.

Collins, A.R., Duthie, S.J., and Dobson, V.L. (1993). Direct enzymic detection of endogenous oxidative base damage in human lymphocyte DNA. Carcinogenesis 14, 1733-1735.

Collins, J.J., Swaen, G.M., Marsh, G.M., Utidjian, H.M., Caporossi, J.C., and Lucas, L.J. (1989). Mortality patterns among workers exposed to acrylamide. J. Occup. Med. 31, 614-617.

Coqueret, O. (2003). New roles for p21 and p27 cell-cycle inhibitors: a function for each cell compartment? Trends Cell Biol 13, 65-70.

Darzynkiewicz, Z., Bedner, E., and Smolewski, P. (2001). Flow cytometry in analysis of cell cycle and apoptosis. Semin. Hematol. 38, 179-193.

Darzynkiewicz, Z., Bruno, S., Del, B.G., Gorczyca, W., Hotz, M.A., Lassota, P., and Traganos, F. (1992). Features of apoptotic cells measured by flow cytometry. Cytometry 13, 795-808.

Deng, C., Zhang, P., Harper, J.W., Elledge, S.J., and Leder, P. (1995). Mice lacking p21CIP1/WAF1 undergo normal development, but are defective in G1 checkpoint control. Cell 82, 675-684.

Deng, H., He, F., Zhang, S., Calleman, C.J., and Costa, L.G. (1993). Quantitative measurements of vibration threshold in healthy adults and acrylamide workers. Int. Arch. Occup. Environ. Health 65, 53-56.

Denicourt, C., and Dowdy, S.F. (2004). Cip/Kip proteins: more than just CDKs inhibitors. Genes Dev. 18, 851-855.

Dietrich, C., Wallenfang, K., Oesch, F., and Wieser, R. (1997). Translocation of cdk2 to the nucleus during G1-phase in PDGF-stimulated human fibroblasts. Exp Cell Res 232, 72-78.

Duez, P., Dehon, G., Kumps, A., and Dubois, J. (2003). Statistics of the Comet assay: a key to discriminate between genotoxic effects. Mutagenesis 18, 159-166.

Dulic, V., Kaufmann, W.K., Wilson, S.J., Tlsty, T.D., Lees, E., Harper, J.W., Elledge, S.J., and Reed, S.I. (1994). p53-dependent inhibition of cyclin-dependent kinase activities in human fibroblasts during radiation-induced G1 arrest. Cell 76, 1013-1023.

Engelward, B.P., Allan, J.M., Dreslin, A.J., Kelly, J.D., Wu, M.M., Gold, B., and Samson, L.D. (1998). A chemical and genetic approach together define the biological consequences of 3-methyladenine lesions in the mammalian genome. J Biol Chem. 273, 5412-5418.

Fennell, T.R., Sumner, S.C., Snyder, R.W., Burgess, J., Spicer, R., Bridson, W.E., and Friedman, M.A. (2005). Metabolism and hemoglobin adduct formation of acrylamide in humans. Toxicol. Sci. 85, 447-459.

Fousteri, M., and Mullenders, L.H. (2008). Transcription-coupled nucleotide excision repair in mammalian cells: molecular mechanisms and biological effects. Cell Res 18, 73-84.

Friedberg, E.C. (2001). How nucleotide excision repair protects against cancer. Nat. Rev. Cancer 1, 22-33.

Friedman, M.A., Dulak, L.H., and Stedham, M.A. (1995). A lifetime oncogenicity study in rats with acrylamide. Fundam. Appl. Toxicol. 27, 95-105.

Frosina, G., Fortini, P., Rossi, O., Carrozzino, F., Raspaglio, G., Cox, L.S., Lane, D.P., Abbondandolo, A., and Dogliotti, E. (1996). Two pathways for base excision repair in mammalian cells. J Biol Chem. 271, 9573-9578.

Gamboa da Costa, G., Churchwell, M.I., Hamilton, L.P., Von Tungeln, L.S., Beland, F.A., Marques, M.M., and Doerge, D.R. (2003). DNA adduct formation from acrylamide via conversion to glycidamide in adult and neonatal mice. Chem. Res Toxicol. 16, 1328-1337.

Gartel, A.L., and Tyner, A.L. (2002). The role of the cyclin-dependent kinase inhibitor p21 in apoptosis. Mol. Cancer Ther. 1, 639-649.

Gassner, P., and Adler, I.D. (1996). Induction of hypoploidy and cell cycle delay by acrylamide in somatic and germinal cells of male mice. Mutat. Res 367, 195-202.

Gates, K.S., Nooner, T., and Dutta, S. (2004). Biologically relevant chemical reactions of N7-alkylguanine residues in DNA. Chem. Res Toxicol. 17, 839-856.

Ghanayem, B.I., McDaniel, L.P., Churchwell, M.I., Twaddle, N.C., Snyder, R., Fennell, T.R., and Doerge, D.R. (2005a). Role of CYP2E1 in the epoxidation of acrylamide to glycidamide and formation of DNA and hemoglobin adducts. Toxicol. Sci. 88, 311-318.

Ghanayem, B.I., Wang, H., and Sumner, S. (2000). Using cytochrome P-450 gene knock-out mice to study chemical metabolism, toxicity, and carcinogenicity. Toxicol. Pathol. 28, 839-850.

Ghanayem, B.I., Witt, K.L., Kissling, G.E., Tice, R.R., and Recio, L. (2005b). Absence of acrylamide-induced genotoxicity in CYP2E1-null mice: evidence consistent with a glycidamide-mediated effect. Mutat. Res 578, 284-297.

Gorczyca, W. (1999). Cytometric analyses to distinguish death processes. Endocr. Relat Cancer 6, 17-19.

Graves, R., Laval, J., and Pegg, A.E. (1992). Sequence specificity of DNA repair by Escherichia coli Fpg protein. Carcinogenesis 13, 1455-1459.

Guttinger, S., Laurell, E., and Kutay, U. (2009). Orchestrating nuclear envelope disassembly and reassembly during mitosis. Nat Rev. Mol. Cell Biol 10, 178-191.

Hansen, S.H. (01.08.2007). The Norwegian Institute of Public health.

Hansen, S.H. (01.05.2009). The Norwegian Institute of Public health.

He, F.S., Zhang, S.L., Wang, H.L., Li, G., Zhang, Z.M., Li, F.L., Dong, X.M., and Hu, F.R. (1989). Neurological and electroneuromyographic assessment of the

adverse effects of acrylamide on occupationally exposed workers. Scand. J. Work Environ. Health 15, 125-129.

Hegde, M.L., Hazra, T.K., and Mitra, S. (2008). Early steps in the DNA base excision/single-strand interruption repair pathway in mammalian cells. Cell Res 18, 27-47.

Hoeijmakers, J.H. (2001). Genome maintenance mechanisms for preventing cancer. Nature 411, 366-374.

IARC. (1994). IARC working group on the evaluation of carcinogenic risks to humans: some industrial chemicals. Lyon, 15-22 February 1994. IARC Monogr Eval. Carcinog. Risks Hum. 60, 1-560.

Jeffrey, P.D., Tong, L., and Pavletich, N.P. (2000). Structural basis of inhibition of CDK-cyclin complexes by INK4 inhibitors. Genes Dev. 14, 3115-3125.

Jeggo, P.A., and Lobrich, M. (2006). Contribution of DNA repair and cell cycle checkpoint arrest to the maintenance of genomic stability. DNA Repair (Amst) 5, 1192-1198.

Jenkins, G.J., Doak, S.H., Johnson, G.E., Quick, E., Waters, E.M., and Parry, J.M. (2005). Do dose response thresholds exist for genotoxic alkylating agents? Mutagenesis 20, 389-398.

Jiang, L., Cao, J., An, Y., Geng, C., Qu, S., Jiang, L., and Zhong, L. (2007). Genotoxicity of acrylamide in human hepatoma G2 (HepG2) cells. Toxicol. In Vitro 21, 1486-1492.

Johansson, F., Lundell, T., Rydberg, P., Erixon, K., and Jenssen, D. (2005). Mutagenicity and DNA repair of glycidamide-induced adducts in mammalian cells. Mutat. Res 580, 81-89.

Johnson, K.A., Gorzinski, S.J., Bodner, K.M., Campbell, R.A., Wolf, C.H., Friedman, M.A., and Mast, R.W. (1986). Chronic toxicity and oncogenicity study on acrylamide incorporated in the drinking water of Fischer 344 rats. Toxicol. Appl. Pharmacol. 85, 154-168.

Knaap, A.G., Kramers, P.G., Voogd, C.E., Bergkamp, W.G., Groot, M.G., Langebroek, P.G., Mout, H.C., van der Stel, J.J., and Verharen, H.W. (1988). Mutagenic activity of acrylamide in eukaryotic systems but not in bacteria. Mutagenesis 3, 263-268.

Knight, J.S., and Robertson, E.S. (2004). Epstein-Barr virus nuclear antigen 3C regulates cyclin A/p27 complexes and enhances cyclin A-dependent kinase activity. J Virol. 78, 1981-1991.

Knight, J.S., Sharma, N., and Robertson, E.S. (2005). SCFSkp2 complex targeted by Epstein-Barr virus essential nuclear antigen. Mol. Cell Biol 25, 1749-1763.

Koskinen, M., and Plna, K. (2000). Specific DNA adducts induced by some mono-substituted epoxides in vitro and in vivo. Chem. Biol Interact. 129, 209-229.

Koyama, N., Sakamoto, H., Sakuraba, M., Koizumi, T., Takashima, Y., Hayashi, M., Matsufuji, H., Yamagata, K., Masuda, S., Kinae, N., and Honma, M. (2006). Genotoxicity of acrylamide and glycidamide in human lymphoblastoid TK6 cells. Mutat. Res 603, 151-158.

Krishnamurthy, N., Haraguchi, K., Greenberg, M.M., and David, S.S. (2008). Efficient removal of formamidopyrimidines by 8-oxoguanine glycosylases. Biochemistry 47, 1043-1050.

Kroemer, G., Galluzzi, L., Vandenabeele, P., Abrams, J., Alnemri, E.S., Baehrecke, E.H., Blagosklonny, M.V., El-Deiry, W.S., Golstein, P., Green, D.R., Hengartner, M., Knight, R.A., Kumar, S., Lipton, S.A., Malorni, W., Nunez, G., Peter, M.E., Tschopp, J., Yuan, J., Piacentini, M., Zhivotovsky, B., and Melino, G. (2009). Classification of cell death: recommendations of the Nomenclature Committee on Cell Death 2009. Cell Death Differ. 16, 3-11.

Krokan, H.E., Standal, R., and Slupphaug, G. (1997). DNA glycosylases in the base excision repair of DNA. Biochem. J. 325 (Pt 1), 1-16.

Kurebayashi, H., and Ohno, Y. (2006). Metabolism of acrylamide to glycidamide and their cytotoxicity in isolated rat hepatocytes: protective effects of GSH precursors. Arch. Toxicol. 80, 820-828.

Kurz, E.U., and Lees-Miller, S.P. (2004). DNA damage-induced activation of ATM and ATM-dependent signaling pathways. DNA Repair (Amst) 3, 889-900.

Kuzminov, A. (2001). Single-strand interruptions in replicating chromosomes cause double-strand breaks. Proc. Natl. Acad. Sci. U. S. A 98, 8241-8246.

Lavin, M.F., and Gueven, N. (2006). The complexity of p53 stabilization and activation. Cell Death. Differ. 13, 941-950.

Leibeling, D., Laspe, P., and Emmert, S. (2006). Nucleotide excision repair and cancer. J Mol. Histol. 37, 225-238.

Loeb, L.A., and Preston, B.D. (1986). Mutagenesis by apurinic/apyrimidinic sites. Annu. Rev. Genet. 20, 201-230.

LoPachin, R.M. (2004). The changing view of acrylamide neurotoxicity. Neurotoxicology 25, 617-630.

Lovell, D.P., and Omori, T. (2008). Statistical issues in the use of the comet assay. Mutagenesis 23, 171-182.

Lukas, J., Lukas, C., and Bartek, J. (2004). Mammalian cell cycle checkpoints: signalling pathways and their organization in space and time. DNA Repair (Amst) 3, 997-1007.

Maddika, S., Ande, S.R., Panigrahi, S., Paranjothy, T., Weglarczyk, K., Zuse, A., Eshraghi, M., Manda, K.D., Wiechec, E., and Los, M. (2007). Cell survival, cell death and cell cycle pathways are interconnected: implications for cancer therapy. Drug Resist. Updat. 10, 13-29.

Maniere, I., Godard, T., Doerge, D.R., Churchwell, M.I., Guffroy, M., Laurentie, M., and Poul, J.M. (2005). DNA damage and DNA adduct formation in rat tissues following oral administration of acrylamide. Mutat. Res 580, 119-129.

Marsh, G.M., Lucas, L.J., Youk, A.O., and Schall, L.C. (1999). Mortality patterns among workers exposed to acrylamide: 1994 follow up. Occup. Environ. Med. 56, 181-190.

Martins, C., Oliveira, N.G., Pingarilho, M., Gamboa da, C.G., Martins, V., Marques, M.M., Beland, F.A., Churchwell, M.I., Doerge, D.R., Rueff, J., and Gaspar, J.F. (2007). Cytogenetic damage induced by acrylamide and glycidamide in mammalian cells: correlation with specific glycidamide-DNA adducts. Toxicol. Sci. 95, 383-390.

Matsumoto, Y., Kim, K., and Bogenhagen, D.F. (1994). Proliferating cell nuclear antigen-dependent abasic site repair in Xenopus laevis oocytes: an alternative pathway of base excision DNA repair. Mol. Cell Biol 14, 6187-6197.

Mei, N., Hu, J., Churchwell, M.I., Guo, L., Moore, M.M., Doerge, D.R., and Chen, T. (2008). Genotoxic effects of acrylamide and glycidamide in mouse lymphoma cells. Food Chem. Toxicol. 46, 628-636.

Mottram, D.S., Wedzicha, B.L., and Dodson, A.T. (2002). Acrylamide is formed in the Maillard reaction. Nature 419, 448-449.

Nunez, R. (2001). DNA measurement and cell cycle analysis by flow cytometry. Curr. Issues Mol. Biol 3, 67-70.

O'Connor, T.R., Boiteux, S., and Laval, J. (1988). Ring-opened 7-methylguanine residues in DNA are a block to in vitro DNA synthesis. Nucleic Acids Res 16, 5879-5894.

O'Nions, J., and Allday, M.J. (2003). Epstein-Barr virus can inhibit genotoxin-induced G1 arrest downstream of p53 by preventing the inactivation of CDK2. Oncogene 22, 7181-7191.

Parker, G.A., Touitou, R., and Allday, M.J. (2000). Epstein-Barr virus EBNA3C can disrupt multiple cell cycle checkpoints and induce nuclear division divorced from cytokinesis. Oncogene 19, 700-709.

Petermann, E., Ziegler, M., and Oei, S.L. (2003). ATP-dependent selection between single nucleotide and long patch base excision repair. DNA Repair (Amst) 2, 1101-1114.

Puppel, N., Tjaden, Z., Fueller, F., and Marko, D. (2005). DNA strand breaking capacity of acrylamide and glycidamide in mammalian cells. Mutat. Res 580, 71-80.

Riccardi, C., and Nicoletti, I. (2006). Analysis of apoptosis by propidium iodide staining and flow cytometry. Nat Protoc. 1, 1458-1461.

Roos, W.P., and Kaina, B. (2006a). DNA damage-induced cell death by apoptosis. Trends Mol. Med 12, 440-450.

Roos, W.P., and Kaina, B. (2006b). DNA damage-induced cell death by apoptosis. Trends Mol. Med. 12, 440-450.

Sanchez-Beato, M., Saez, A.I., Martinez-Montero, J.C., Sol, M.M., Sanchez-Verde, L., Villuendas, R., Troncone, G., and Piris, M.A. (1997). Cyclin-dependent kinase inhibitor p27KIP1 in lymphoid tissue: p27KIP1 expression is inversely proportional to the proliferative index. Am. J Pathol. 151, 151-160.

Schwartz, G.K., and Shah, M.A. (2005). Targeting the cell cycle: a new approach to cancer therapy. J. Clin. Oncol. 23, 9408-9421.

Sedgwick, B. (1997). Nitrosated peptides and polyamines as endogenous mutagens in O6-alkylguanine-DNA alkyltransferase deficient cells. Carcinogenesis 18, 1561-1567.

Segerback, D., Calleman, C.J., Schroeder, J.L., Costa, L.G., and Faustman, E.M. (1995). Formation of N-7-(2-carbamoyl-2-hydroxyethyl)guanine in DNA of the mouse and the rat following intraperitoneal administration of [14C]acrylamide. Carcinogenesis 16, 1161-1165.

Settels, E., Bernauer, U., Palavinskas, R., Klaffke, H.S., Gundert-Remy, U., and Appel, K.E. (2008). Human CYP2E1 mediates the formation of glycidamide from acrylamide. Arch. Toxicol. 82, 717-727.

Shapiro, H.M. (2003). Practical Flow Cytometry ().

Shieh, S.Y., Ikeda, M., Taya, Y., and Prives, C. (1997). DNA damage-induced phosphorylation of p53 alleviates inhibition by MDM2. Cell 91, 325-334.

Shimada, M., and Nakanishi, M. (2006). DNA damage checkpoints and cancer. J. Mol. Histol. 37, 253-260.

Shuck, S.C., Short, E.A., and Turchi, J.J. (2008). Eukaryotic nucleotide excision repair: from understanding mechanisms to influencing biology. Cell Res 18, 64-72.

Sickles, D.W., Brady, S.T., Testino, A., Friedman, M.A., and Wrenn, R.W. (1996). Direct effect of the neurotoxicant acrylamide on kinesin-based microtubule motility. J Neurosci. Res 46, 7-17.

Sickles, D.W., Sperry, A.O., Testino, A., and Friedman, M. (2007). Acrylamide effects on kinesin-related proteins of the mitotic/meiotic spindle. Toxicol. Appl. Pharmacol. 222, 111-121.

Singer, B. (1975). The chemical effects of nucleic acid alkylation and their relation to mutagenesis and carcinogenesis. Prog. Nucleic Acid Res Mol. Biol 15, 219-284.

Sipinen, V.E. (01.08.2007). The Norwegian Institute of Public health.

Smith, C.C., O'Donovan, M.R., and Martin, E.A. (2006). hOGG1 recognizes oxidative damage using the comet assay with greater specificity than FPG or ENDOIII. Mutagenesis 21, 185-190.

Smith, M.L., and Seo, Y.R. (2002). p53 regulation of DNA excision repair pathways. Mutagenesis 17, 149-156.

Smith, S.A., and Engelward, B.P. (2000). In vivo repair of methylation damage in Aag 3-methyladenine DNA glycosylase null mouse cells. Nucleic Acids Res. 28, 3294-3300.

Sobel, W., Bond, G.G., Parsons, T.W., and Brenner, F.E. (1986). Acrylamide cohort mortality study. Br. J Ind. Med 43, 785-788.

Sobol, R.W., Kartalou, M., Almeida, K.H., Joyce, D.F., Engelward, B.P., Horton, J.K., Prasad, R., Samson, L.D., and Wilson, S.H. (2003). Base excision repair intermediates induce p53-independent cytotoxic and genotoxic responses. J. Biol. Chem. 278, 39951-39959.

Solomon, J.J., Fedyk, J., Mukai, F., and Segal, A. (1985). Direct alkylation of 2'-deoxynucleosides and DNA following in vitro reaction with acrylamide. Cancer Res 45, 3465-3470.

Somasundaram, K., Zhang, H., Zeng, Y.X., Houvras, Y., Peng, Y., Zhang, H., Wu, G.S., Licht, J.D., Weber, B.L., and El-Deiry, W.S. (1997). Arrest of the cell cycle by the tumour-suppressor BRCA1 requires the CDK-inhibitor p21WAF1/CiP1. Nature 389, 187-190.

Speit, G., Hanelt, S., Helbig, R., Seidel, A., and Hartmann, A. (1996). Detection of DNA effects in human cells with the comet assay and their relevance for mutagenesis. Toxicol. Lett. 88, 91-98.

Speit, G., Schutz, P., Bonzheim, I., Trenz, K., and Hoffmann, H. (2004). Sensitivity of the FPG protein towards alkylation damage in the comet assay. Toxicol. Lett. 146, 151-158.

Stadler, R.H., Blank, I., Varga, N., Robert, F., Hau, J., Guy, P.A., Robert, M.C., and Riediker, S. (2002). Acrylamide from Maillard reaction products. Nature 419, 449-450.

Strickland, P.T., and Groopman, J.D. (1995). Biomarkers for assessing environmental exposure to carcinogens in the diet. Am. J. Clin. Nutr. 61, 710S-720S.

Su, T.T. (2006). Cellular responses to DNA damage: one signal, multiple choices. Annu. Rev. Genet. 40, 187-208.

Subramanian, C., Knight, J.S., and Robertson, E.S. (2002). The Epstein Barr nuclear antigen EBNA3C regulates transcription, cell transformation and cell migration. Front Biosci. 7, d704-d716.

Sumner, S.C., MacNeela, J.P., and Fennell, T.R. (1992). Characterization and quantitation of urinary metabolites of [1,2,3-13C]acrylamide in rats and mice using 13C nuclear magnetic resonance spectroscopy. Chem. Res Toxicol. 5, 81-89.

Svensson, K., Abramsson, L., Becker, W., Glynn, A., Hellenas, K.E., Lind, Y., and Rosen, J. (2003). Dietary intake of acrylamide in Sweden. Food Chem. Toxicol. 41, 1581-1586.

Tareke, E., Rydberg, P., Karlsson, P., Eriksson, S., and Tornqvist, M. (2000). Acrylamide: a cooking carcinogen? Chem. Res Toxicol. 13, 517-522.

Tsuda, H., Shimizu, C.S., Taketomi, M.K., Hasegawa, M.M., Hamada, A., Kawata, K.M., and Inui, N. (1993). Acrylamide; induction of DNA damage, chromosomal aberrations and cell transformation without gene mutations. Mutagenesis 8, 23-29.

Tsuiki, H., Nitta, M., Tada, M., Inagaki, M., Ushio, Y., and Saya, H. (2001). Mechanism of hyperploid cell formation induced by microtubule inhibiting drug in glioma cell lines. Oncogene 20, 420-429.

Tudek, B. (2003). Imidazole ring-opened DNA purines and their biological significance. J Biochem. Mol. Biol 36, 12-19.

Vazquez, A., Bond, E.E., Levine, A.J., and Bond, G.L. (2008). The genetics of the p53 pathway, apoptosis and cancer therapy. Nat. Rev. Drug Discov. 7, 979-987.

Vervoorts, J., and Luscher, B. (2008). Post-translational regulation of the tumor suppressor p27(KIP1). Cell Mol. Life Sci. 65, 3255-3264.

Vogel, C., Kienitz, A., Hofmann, I., Muller, R., and Bastians, H. (2004). Crosstalk of the mitotic spindle assembly checkpoint with p53 to prevent polyploidy. Oncogene 23, 6845-6853.

Wade, M., and Allday, M.J. (2000). Epstein-Barr virus suppresses a G(2)/M checkpoint activated by genotoxins. Mol. Cell Biol 20, 1344-1360.

Wyatt, M.D., and Pittman, D.L. (2006). Methylating agents and DNA repair responses: Methylated bases and sources of strand breaks. Chem. Res. Toxicol. 19, 1580-1594.

Yi, F., Saha, A., Murakami, M., Kumar, P., Knight, J.S., Cai, Q., Choudhuri, T., and Robertson, E.S. (2009). Epstein-Barr virus nuclear antigen 3C targets p53 and modulates its transcriptional and apoptotic activities. Virology 388, 236-247.

Yousef, M.I., and El-Demerdash, F.M. (2006). Acrylamide-induced oxidative stress and biochemical perturbations in rats. Toxicology 219, 133-141.

Zhang, H., Xiong, Y., and Beach, D. (1993). Proliferating cell nuclear antigen and p21 are components of multiple cell cycle kinase complexes. Mol. Biol Cell 4, 897-906.

Zhou, B.P., Liao, Y., Xia, W., Spohn, B., Lee, M.H., and Hung, M.C. (2001). Cytoplasmic localization of p21Cip1/WAF1 by Akt-induced phosphorylation in HER-2/neu-overexpressing cells. Nat Cell Biol 3, 245-252.

Zurer, I., Hofseth, L.J., Cohen, Y., Xu-Welliver, M., Hussain, S.P., Harris, C.C., and Rotter, V. (2004). The role of p53 in base excision repair following genotoxic stress. Carcinogenesis 25, 11-19.

10. Appendix

Chemicals	Producer
8-16% Precise Protein Gels (15-well)	Thermo Fischer Scientific
β-Mercaptoethanol	Sigma-Aldrich
Absolute alcohol prima	Arcus Kjemi, Norway
Anti-mouse HRP-conjugate	Jackson Laboratories
Anti-rabbit HRP-conjugate	Jackson Laboratories
Bio-Rad CD Protein Assay Kit	BioRad
BrdU	Sigma-Aldrich
Bromophenol Blue	Sigma-Aldrich
Bovine serum, albumin (BSA)	Sigma, USA
Bio Whittaker® RPMI 1640 medium with and L-Gluthamine	Lonza, Belgium
Bio-Rad DC (detergent compatible) protein assay	Bio-Rad, USA
Complete	Roche
Cyclin A (rabbit)	BD Bioscience, USA
Developer (LX 24)	Kodak
Dubeccos`s Phosphate Buffer solution (PBS)	Locally produced
Dimetyhylsulfoxide (DMSO)	Merck, Germany
EDTA	Sigma-Aldrich
Ethanol (Absolute)	Arcus Kjemi, Norway
Ethylenediaminetetraacetic acid disodium salt dihydrate (EDTA)	Sigma, USA
Fetal calve serum (FCS)	Gibco, NY, USA
Fpg crude enzyme extract	Locally produced
FITC antibody	BD Bioscience, USA
Fixer (AL 4)	Kodak
GAPDH ab (mouse)	Biogenesis
GelBond® Film	Cambrex, USA
Glycerol	Sigma-Aldrich , USA
Glycine	Sigma-Aldrich , USA

Hydrogen chloride (HCl)	Merck, Germany
Hepes	Sigma, USA
Hoechst 33342	Calbiochem
Lymphoprep Tube	Axis-Shield, Norway
Medical X-ray film, Super RX	FUJI
Methanol	Merck
NuSieve GTG Low melting agarose	Cambrex, USA
P21 (mouse)	Santa Cruz, USA
P27 (mouse)	Santa Cruz, USA
p-53 serin 15 (mouse)	Cell Signalling, USA
p-53 (rabbit)	Cell Signalling, USA
Potassium hydroxide (KOH)	Merck, Germany
Potassium chloride (KCl)	Merck, Germany
Penicillin/Streptomycin (P/S)	Sigma, Norway
PBS	Dulbecco
Pierce Supersignal West Dura Extended Duration substrate	Thermo Fisher Scientific
Precision Plus ProteinTM Standards, Kaleidoscope	BioRad
Protran BA 85 Nitrocellulose	Whatman
S9-mix	In Vitro Technologies
Sodium chloride (NaCl)	Merck, Germany
Sodium Hydroxide (NaOH)	Merck, Germany
Sodium lauryl sarcocinate	Sigma, UK
SYBR Gold	Invitrogen, USA
Starting block™ blocking buffer	Thermo Fisher Scientifc
Trizma® base (Tris (hydroxymethyl)-aminomethane, Tris-base)	Sigma, USA
Triton-X	Sigma, USA
Thimerosal	Sigma, USA
Trypan Blue Stain	Cambrex, USA
Tween 20	BioRad, USA
XPC (mouse)	Pharmingen
XPA (rabbit)	Santa Cruz, USA

10.1 Solutions and media

Medium:
RPMI 1640 added 10% FCS and 1% P/S

Lysis stock solution:
2,5 M NaCl, 100 mM EDTA, 10mM Trizma base, 12g/l NaOH. Adjust pH to 10. Add 1% Sodium lauryl sarcocinate.

Lysis solution:
Dilute stock solution 10 times, add 10% DMSO and 1% Triton-X

Fpg-enzyme reaction buffer:
40mM Hepes, 0,1 M KCl, 0,5mM EDTA. pH adjusted to 7,6.

Unwinding and electrophoresis stock solution:
10N NaOH, 200mM EDTA

Unwinding and electrophoresis buffer:
Dilute electrophoresis stock solution 10 times, adjust pH to 13,2

Neutralization solution:
0,4 M Trizma base, pH adjusted to 7,5.

TE-buffer:
1mM EDTA, 10mM Tris HCl, pH adjusted to 8,0.

1X Loading buffer (for preparation of protein extract):

SDS-buffer:

60 mM Tris-HCL (50 ml 0.5 M Tris-HCL pH 6.8)

10 % glycerol (40 ml 100 % glycerol)

2 % SDS (80 ml 10 % SDS)

1 mM EDTA (4 ml 0.1 M EDTA)

pH is adjusted to 6.8 with NaOH and dH2O is added up to 400ml.

2 ml of loading buffer were made using:

SDS-buffer: 1.79 ml

Protease inhibitor, Complete (25X): 80 µl

Phosphatase inhibitors: Sodium fluoride (NaF) (50 mM stock): 100 µl

B-glycerolphosphate (Stock 100X): 20 µl Na3VO4 (stock 200mM): 10 µl

10X Running buffer
2000 ml:
60g TRIS Base (Tris-hydroxsymethyl-aminomethane)
88g Glycine
20g SDS (Sodium Dodecyl Sulphate)
Distilled water up to 2000 ml

1X Running buffer
1000 ml:
100 ml of 10X Electrophoresis buffer
900 ml distilled water

10X Transfer buffer
2000 ml:
TRIS base 60 g
288 g Glycine
Distilled water up to 2000 ml

1X Transfer buffer
1000 ml:
100 ml of 10X Transfer buffer
700 ml distilled water 200 ml methanol
The methanol was added just before use to avoid evaporation.

10X TBS-T (Tris buffer with Tween 20) – wash buffer:
5000 ml:
10 mM Trizma base (60,5g)
137 mM NaCl (400g)
0.1%Tween 20 (50ml)
350 ml of 1M HCl

Distilled water was added up to 5000 ml and pH adjusted to 7.6.
The solution was then diluted 1:10 before use.

10X TBS (Tris buffer):
5000 ml:
10 mM Trizma base (60,5g)
137 mM NaCl (400g)
350 ml of 1M HCl
Distilled water was added up to 5000 ml and pH adjusted to 7.6.
The solution was then diluted 1 : 10 before use.

IFA buffer:
10 mM HEPES [pH 7.4]
25 mM NaCl
4% fetal calf serum